Title
ATG12 Conjugation to ATG3 Modulates Mitochondrial Homeostasis and Cell Death

Author
Radoshevich, Lilliana C.

Publication Date
2011

Peer reviewed|Thesis/dissertation

ATG12 Conjugation to ATG3 Modulates Mitochondrial Homeostasis and Cell Death

by

Lilliana C. Radoshevich

DISSERTATION

Submitted in partial satisfaction of the requirements for the degree of

DOCTOR OF PHILOSOPHY

in

Biomedical Sciences

in the

GRADUATE DIVISION

of the

UNIVERSITY OF CALIFORNIA, SAN FRANCISCO

Acknowledgements

First and foremost, I would like to thank my thesis advisor, Dr. Jay Debnath, who had enough faith in me to encourage me to tackle a risky project and helped me every step of the way to make it succeed. He offered consistent encouragement and sometimes even technical help at the bench and I am certain that without his intellectual support and guidance that my project would not have borne fruit. I am grateful to Dr. Phil Coffino for his excellent biochemical advice and for offering me a bench in his lab to learn the basics of yeast biology. I would like to thank Dr. Don Ganem, my thesis committee chair, for the invaluable role he has played in my scientific development over the past five years. He always makes astute and timely observations scientifically and was quick to offer sage advice during our paper submission process and during my post-doctoral search for which I am exceedingly grateful. I have noticed that Don perceives when someone needs an encouraging word both at hockey and in science. During the struggles and frustrations of my thesis, there were many times that I benefited from his wisdom. If I ever have a lab of my own, I aspire to emulate this aspect of his mentorship, as well as his vast scientific acumen.

I would like to thank all of the members of the Debnath lab for their help and support during my tenure in the lab. In particular, I would like to thank Ed Salas for keeping everything running and in order (and for keeping everyone happy). I would also like to thank Srirupa Roy for her friendship and advice. I am also grateful to Lyndsay Murrow who put up with my idiosyncrasies during the

revision process and who I am certain will do great things with the continuation of the project. The UCSF community is extremely collaborative and friendly and my project has benefited dramatically from it. I would like to thank Eric Johansen from the Sandler-Moore Mass-Spectrometry Core for help with the identification of ATG3 as a conjugate of ATG12. I am grateful for early help with ubl biochemistry from Dr. Feroz Papa, for help with cloning and purification from Dr. Scott Oakes and Katie Austgen, and later for help on the yeast project from Drs. Phil Merksamer, Martin Hoyt and Allen Henderson.

Many of my classmates at UCSF have become my close friends. I am particularly grateful to Mary Mohrin, Alana Lerner and Shuyi Zhang for their friendship and support. It was a comfort to have them by my side to weather the ups and downs of graduate school. I would also like to thank my best friend, Amy Rice-Jones, for encouraging me and getting me out of lab every once and a while. I thank Lisa Magargal and Monique Piazza for everything that they do for us. Monique was also always a great listener during the most difficult challenges of my thesis.

I have an incredibly supportive and wonderful family. I thank my mother and father, Ruth Kolarik and Zhivoin Radoshevich, for their love and limitless support and pride in my achievements. I am grateful to my brother Nik and my sister Dani for their frequent visits, their companionship and their help with everything and to my grandfather Rolland Kolarik, who always encouraged me when no one else had time to listen.

Chapters II and III are an expanded version of my published paper (see permissions below). The authors are: Lilliana Radoshevich, Lyndsay Murrow, Nan Chen, Estefania Fernandez, Srirupa Roy, Christopher Fung and Jayanta Debnath. Lyndsay Murrow contributed the mitochondrial fusion experiments. Dr. Nan Chen helped with the cis/trans experiments and cloned some of the constructs for the 293T experiments. Estefania Fernandez, an undergraduate summer student, worked with me on the cell death experiments. Dr. Srirupa Roy performed the BHMT assay. Chris Fung made the ATG12 stop mutant and some of the retrovirus used. Dr. Jay Debnath supervised and guided the entire project as my thesis advisor. I initiated the project and completed all of the experiments not listed above.

Statement from Dr. Jay Debnath

"I directed and supervised the work presented in this dissertation. Lilliana Radoshevich completed ninety percent of the work included. This dissertation is an original contribution to scientific knowledge and meets the standards for a doctoral dissertation in the Biomedical Sciences Program at the University of California, San Francisco."

Reprinted from *Cell*, 142, Radoshevich, L., Murrow, L., Chen, N., Fernandez, E., Roy, S., Fung, C. & Debnath, J. ATG12 conjugation to ATG3 regulates mitochondrial homeostasis and cell death, 590-600. (2010), with permission from Elsevier.

ATG12 modification of ATG3 Modulates Mitochondrial Homeostasis and Cell Death

Lilliana C. Radoshevich

Autophagy is an intracellular response to starvation, which is conserved in eukaryotes from unicellular to metazoan organisms. While autophagy sustains an individual cell from death by a variety of cellular stresses, evidence suggests that it is also critically important on an organismal level for the prevention of cancer, neurodegenerative and autoimmune diseases. In light of the therapeutic implications of autophagy, much remains to be understood about the function of individual autophagy genes.

Many of the autophagy genes participate in two ubiquitin-like conjugation systems. The first mediates conjugation of ATG12 to ATG5 and the second mediates lipidation of LC3/ATG8 by phosphatidylethanolamine. We hypothesized that ATG12 conjugates to other substrates in addition to ATG5, as is the case for most ubiquitin-like proteins (ubls). By increasing the cellular pool of ATG12, we were able to identify and characterize a novel covalent complex between ATG12 and ATG3.

A small subset of the cellular pool of ATG3 is in complex with ATG12 at baseline conditions in mammalian cells. Formation of the ATG12-ATG3 complex requires activation by ATG7, the autophagy E1-like enzyme. ATG12 subsequently becomes auto-conjugated *in cis* by ATG3. Unlike ATG12-ATG5 complex formation, ATG12-ATG3 conjugation does not require the E2-like

enzyme ATG10. The c-terminal glycine of ATG12 specifically binds to K243 of ATG3.

The ATG12-ATG5 complex and ATG3 each modulate steps in early autophagosome expansion and closure. Therefore, we initially expected that the ATG12-ATG3 complex would affect autophagy. To our surprise, disruption of the ATG12-ATG3 complex had no effect on autophagy induced by starvation, rapamycin or chemical uncoupling of the mitochondria. Instead disruption of the ATG12-ATG3 complex leads to a highly fragmented mitochondrial network that is incapable of fusion, increased in mass and defective in mitochondrial autophagy. These phenotypes also correlate with resistance to mitochondrial cell death.

In summary, we have demonstrated evidence for a previously unknown conjugate between ATG12 and ATG3. Conjugation between ATG12 and ATG3 endows each protein with an entirely separate function from either protein's known role in autophagosome biogenesis. Our work suggests that ATG12 may be a more broad-based protein modification than previously anticipated.

Table of Contents

Table of Figures

CHAPTER I:

AUTOPHAGY: HISTORICAL PERSPECTIVES, MOLECULAR MECHANISMS AND IMPLICATIONS FOR DISEASE

Introduction

In 1963 at a meeting on the lysosome, Christian de Duve first described autophagy as a self-digestive process in which organelles and cytosolic material became encapsulated in double membrane vesicles and are degraded over time[1]. Nearly three decades later, three groups discovered the genetic basis for the process that de Duve observed in electron micrographs through large-scale screens in yeast [2-4]. Gene deletion studies in model organisms from yeast to mice suggest that the fundamentally conserved function of autophagy is a cellular response to starvation or other energy deprivation. Additionally tissue-specific gene deletion in metazoans and genome wide association studies have highlighted the role of autophagy in organelle homeostasis and its potential therapeutically for many hard to treat human diseases such as cancer, neurodegenerative and autoimmune diseases.

Since the *A*u*T*opha*G*y (*atg*) genes were initially cloned, our grasp of what induces the process, what happens during autophagy induction and how the *atg* genes mediate it has grown exponentially but there still remains much to uncover about individual ATG protein function. To date there are thirty-two known autophagy genes in yeast, many of which have mammalian homologues. A number of these genes are dedicated to two ubiquitin-like (ubl) protein modification systems. Covalent protein modification can alter protein fate, localization, function and transcriptional activity. As such, most ubl proteins have many, diverse substrates, however it was long believed that one of the

autophagy ubl proteins, ATG12, solely modified the autophagy modulator ATG5. During the course of my thesis work, I tested whether ATG12 modifies other substrates and identified another modulator of early autophagy, ATG3, as a novel conjugate of ATG12. The ATG12-ATG3 complex profoundly affects the mitochondrial network and mitochondrial cell death. Ultimately, this work posits that ATG12 acts as a more broad-based ubl than previously appreciated and furthermore suggests that ATG12 has pleiotropic roles in cell biology beyond canonical starvation-induced autophagy.

This chapter will begin with an exposition of the types of autophagy and an account of early seminal discoveries in the field, followed by an explanation of the current understanding of the molecular mechanisms of autophagy in yeast and in metazoans, and will culminate with a description of covalent protein modification with specific emphasis on the autophagy ubiquitin-like conjugation cascades.

History and Types of Autophagy

Macroautophagy is a process of self-catabolism in response to energetic crisis within a cell, in which double-membranes sequester portions of cytosol, including proteins and organelles. The membranes then further expand and close through hemifusion to form an autophagosome[5]. The autophagosome can subsequently fuse with the lysosome, whose hydrolases then gain access to the contents of the autophagosome. The autophagosome's cargo subsequently

becomes rapidly degraded and thus can rescue the energetic deficiency of the cell. There are several other cellular autophagy-related processes in addition to macroautophagy: chaperone-mediated autophagy, microautophagy and selective autophagy of organelles. Chaperone-mediated autophagy describes a process in which specific chaperones unfold their client molecules directly into the lysosome, through docking with the lysosomal receptor LAMP2A[6]. Microautophagy is the direct delivery of cytosolic constituents to the lysosome through invagination of the lysosomal membrane. Selective autophagy of organelles in metazoans seems to make use of the macroautophagy machinery, with the exception that specific targeting molecules connect the nascent autophagosome with the damaged or surplus organelle[7]. The linker molecules for this process have only recently been identified and characterized, thus many mechanistic questions remain to be answered. These autophagy-related processes, however, are not as well understood as macroautophagy, which will hereafter be referred to as autophagy.

Since the initial characterization of autophagy occurred in mammalian cells, it was difficult to determine how the process was regulated genetically. Ohsumi and colleagues made a major advance in the field by discovering evidence of autophagy in yeast[8]. By using yeast deficient in vacuolar proteolysis, they were able to observe accumulated cytoplasmic constituents in the vacuole during carbon or nitrogen starvation. Once the authors could observe and block the process either genetically or chemically, it paved the way for their group and two others to mutagenize yeast to isolate and identify genetic modulators of

autophagy[2-4]. Around the same time the genes for another yeast-specific catabolic process called cytoplasm-to-vacuole targeting (CVT) were cloned[9]. In yeast, these two processes require related machinery and shared many of the same complementation groups in one of the autophagy screens, though some of the genes are unique to each process. CVT is a homeostatic targeting pathway, which delivers two hydrolases: α-mannosidase and pre-aminopeptidase I (pre-AP1) into the vacuole, where pre-AP1 then becomes processed into AP1 by specific hydrolases[10]. During vegetative growth conditions, initial targeting and bundling of AP1 requires a specific set of CVT proteins but subsequently the autophagy proteins wrap the bundles in membrane, enclose them and deliver them to the vacuole for processing. During starvation however, the cytoplasmic localization of pre-AP1 renders it susceptible to stochastic delivery to the vacuole by bulk autophagy[11]. Though interesting biologically in its own right, the differential homeostatic and starvation processing of AP1 led to a better biochemical marker for autophagy; thus expediting structure function studies of the newly identified genes[12].

Mechanisms of Yeast Autophagy

Autophagy in yeast serves the same fundamental purpose as in metazoans but in yeast the pathway, as with many conserved processes, proceeds more linearly with fewer instances of complementary gene duplications or redundant signaling pathways than in mammalian cells. As such, we

understand much more about how autophagy initiation and completion occurs in yeast than in mammalian cells. Furthermore, though many of the autophagy genes have identified mammalian homologues, some still remain to be discovered. The autophagy genes participate downstream of nutrient sensing in four discrete steps which in sum form an autophagosome: 1) initiation 2) nucleation 3) expansion and completion and 4) fusion with the lysosome.

During vegetative growth in yeast, autophagy is repressed by the target of rapamycin (TOR), which when active directly phosphorylates ATG13. This baseline hyper-phosphorylation precludes the formation of an autophagy-induction complex between ATG13 and ATG1. Autophagy initiation occurs when cells are starved for nutrients. TOR becomes inactive and as a result ATG13 is dephosphorylated over time. ATG13 can then bind to ATG1, which is a serine/threonine kinase whose activity depends on complex formation with ATG13[13]. The ATG1/ATG13 complex subsequently interacts with ATG17, ATG29, ATG31, ATG20 and ATG24[14, 15]. Together these proteins recruit a second autophagy complex, which then nucleates the pre-autophagosomal structure (PAS).

Nucleation of the PAS is mediated by ATG6 in complex with the Type III PI3 kinase, Vps34, Vps15 and ATG14[16]. The complex shifts the phosphoinositide content of the PAS towards a PI3P rich membrane. As a consequence, a number of PI3P binding ATG proteins descend on the PAS, including ATG18, ATG21, ATG20, ATG24 and ATG27[17-19]. Though some of

these proteins were initially thought to be CVT specific, the early nucleation steps require common proteins so bulk autophagy can proceed efficiently.

The presence of these key proteins at the PAS leads to a dynamic and rapid relocalization of an autophagy ubiquitin-like complex between ATG12 and ATG5 from the cytoplasm to the PAS[20]. This relocalization requires the integral membrane protein ATG9 and the coiled-coil domain protein ATG16[21]. Furthermore, the ATG12-ATG5 complex interacts with ATG16 in a large multi-protein oligomer, whose formation is mediated by a homotypic interaction of several ATG16 molecules[22]. Ultimately, this supramolecular complex tightly associates with early autophagic membranes on the outer side of the growing membrane, functioning as a protein scaffold. Autophagy is blocked at early PAS formation when cells lack any of the components of the complex[23, 24]. Temporally, the ATG12-ATG5·ATG16 complex mediates early expansion of the PAS into the autophagosomal membrane, which is evident from electron micrographs of nascent, abortive autophagosomes in mammalian cells lacking ATG5[25].

Further autophagosome expansion and completion requires the second autophagy ubl complex between ATG8/LC3 and the lipid phosphatidylethanolamine (PE). This second ubl becomes covalently conjugated to the growing PAS through the amino-terminus of PE[26]. Unlike the ATG12-ATG5 complex this modification is induced by autophagy stimulators and only occurs on autophagosomes, therefore ATG8/LC3 conjugation to PE (visualized as a faster migrating band on western blot) serves as a useful tool to monitor and

quantify levels of autophagy[27]. Mechanistically, ATG8/LC3 conjugation to PE follows ATG12-ATG5·ATG16 relocalization and depends on the ATG12-ATG5 complex for an E3-like function for efficient lipidation[28]. ATG8/LC3 becomes intimately associated with the autophagosomal membrane on both surfaces of the PAS and is responsible for its rapid expansion and cargo enclosure through hemifusion[5].

Upon fusion of the termini of the growing membrane, the autophagosome is formed and competent to fuse with either multi-vesicular bodies or directly with the lysosome. In yeast, this requires the homotypic fusion machinery including certain specific SNARE, NSF and Sec proteins as well as the RAB protein Ypt7 (similar to mammalian Rab7)[29]. Finally, ATG22 completes the last step in autophagy by acting as a permease to transport recycled leucine (delivered as protein cargo to the lysosome by autophagy and degraded by lysosomal hydrolases) from the vacuole to the cytoplasm to sustain the starving cell[30, 31].

Mechanisms of Metazoan Autophagy

In metazoans, autophagy proceeds in a largely analogous fashion, with the exception that both upstream signaling and ATG signaling networks are more complex (Figure 1A). Over the past decade there have been many seminal papers, which identified and characterized the mammalian homologues of *atg* genes and how they function either similar to or slightly divergent from their yeast counterparts. Initially upstream signaling proteins, such as AMPK, REDD1, AKT

Figure 1: Diagram of Critical Steps in Mammalian Autophagy Initiation

Autophagosome biogenesis begins with a pre-autophagosomal structure that is nucleated and expands into an autophagosome, which subsequently fuses with an autolysosome to degrade the initial cellular cargo as a source of nutrients.

A) Upstream sensors of cellular nutrients, growth factor signaling, ATP levels and DNA damage all impinge on the mammalian target of rapamycin or mTOR, which when active exerts a repressive effect on autophagy induction.

B) A subset of mTOR is in complex with ULK1/2, mATG13 and FIP200. While active it directly phosphorylates mATG13 and ULK1/2. After a drop in cellular nutrient availability, mTOR rapidly disassociates from the mATG13 complex. ULK1/2 phosphorylates mATG13 and FIP200 and the complex leads to the nucleation of the pre-autophagosomal structure (PAS).

C) Nucleation of the PAS occurs through a number of different Beclin 1 complexes, which together prepare the PAS for expansion. Beclin 1 disassociates with Bcl-X_L upon nutrient starvation and can subsequently interact with hVps34 and p150, which increase PI3P levels at the PAS. Beclin 1 also binds UVRAG. UVRAG interacts with the N-BAR domain protein Bif-1, which could help deform the PAS into an early autophagosome.

(Figure adapted from Mizushima *et al*, 2001 and Yang and Klionsky, 2010)[25, 32]

Figure 1

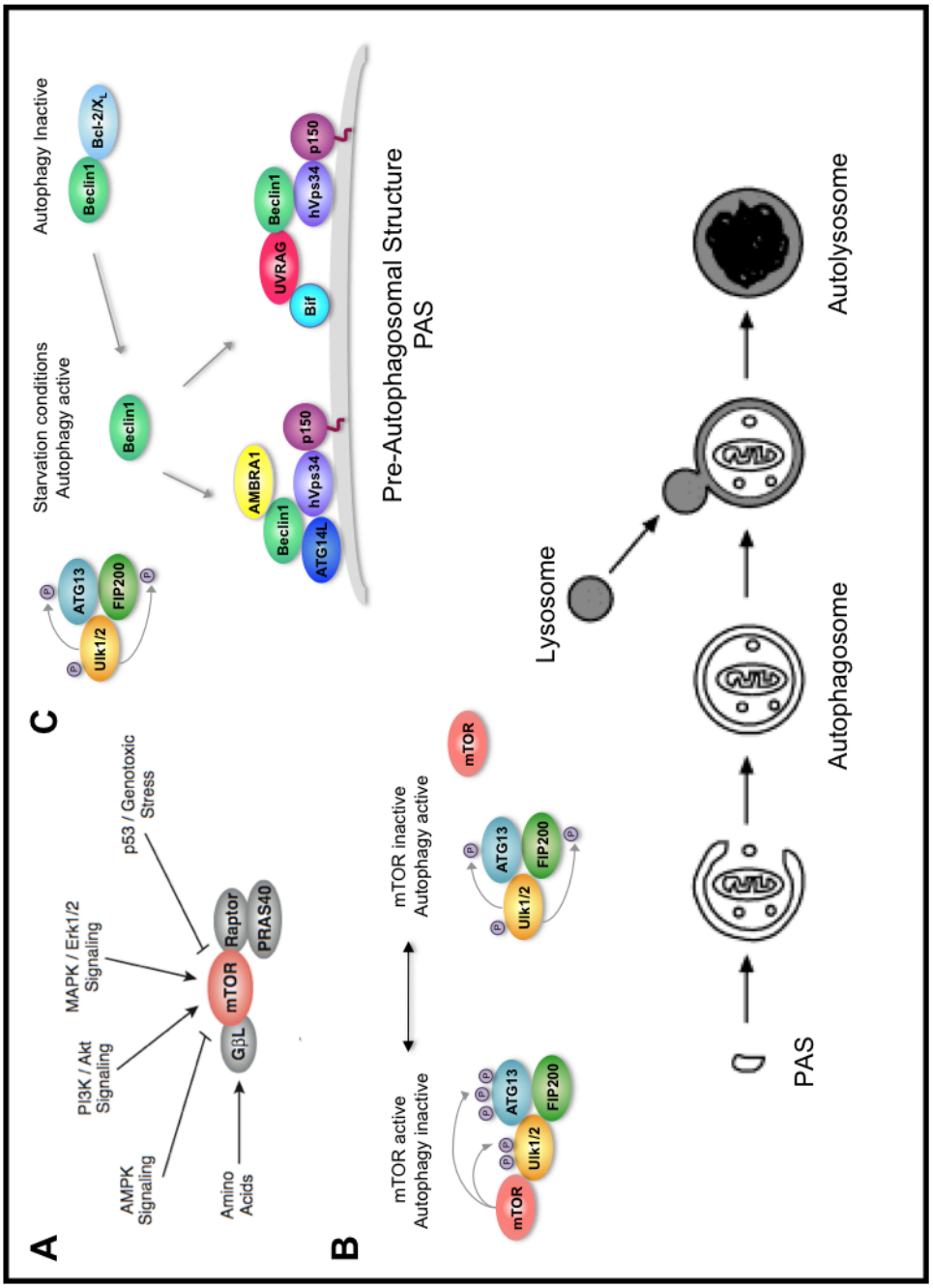
A
MAPK / Erk1/2 Signaling
p53 / Genotoxic Stress
PI3K / Akt Signaling
AMPK Signaling
Amino Acids
mTOR
Raptor
PRAS40
GβL
B
mTOR active
Autophagy inactive
mTOR inactive
Autophagy active
mTOR
ATG13
FIP200
Ulk1/2
C
Starvation conditions
Autophagy active
Autophagy Inactive
Beclin1
Bcl-2/XL
AMBRA1
Beclin1
p150
hVps34
ATG14L
UVRAG
Bif
Pre-Autophagosomal Structure
PAS
Lysosome
Autophagosome
Autolysosome
PAS

and VPS34, on the plasma membrane or within the cytoplasm assess levels of various essential cellular building blocks, energy, growth factors and stress. If levels of growth factors outside the cell or ATP or amino acids within the cell become limited autophagy is induced[33]. In addition, cellular stress from protein misfolding, increased reactive oxygen species (ROS), DNA damage or detachment from the extracellular matrix can also lead to autophagy induction[34].

Autophagy induction in response to a change in energy homeostasis is controlled by the nutrient-signaling node, the mammalian target of rapamycin complex 1 (mTORC1)[35]. Though recently, there is mounting evidence that some of the aforementioned sensors can directly interact with the autophagy initiating complexes as well[36]. As with yeast, mTOR exerts a repressive effect on autophagy through direct phosphorylation of mammalian ATG13 (mATG13) and mammalian ATG1, called ULK1, which was first identified for its homology to the unc-51 like kinase[37]. ULK1 shares homology with ULK2 and ULK3 and these proteins can complement each other's function when deleted. Essentially, animals that lack ULK1 remain autophagy competent, though they cannot effectively clear their mitochondria during reticulocyte maturation[38]. On the other hand, deleting either mammalian ATG13 or a functional orthologue of ATG17, FIP200, ablates autophagosome formation[39, 40]. Unlike in yeast, the ATG1 homologues do not preferentially associate with ATG13 based on its phosphorylation state. If nutrients are abundant, ULK1, ULK2, ATG13 and FIP200, are in complex with mTORC1[41, 42]. As nutrients become limited, mTORC1 rapidly disassociates from the complex, ATG13 becomes

dephosphorylated and ULK1/ULK2 phosphorylate key residues on ATG13 and FIP200 (Figure 1B). In an as yet unknown mechanism, this differential phosphorylation pattern leads to or correlates with autophagy initiation.

Nucleation of the preautophagosomal structure (PAS) in mammalian cells also requires several Vps34 complexes. As with yeast, hVps34 interacts with a homologue of ATG6 (Beclin1), a homologue of Vps15 (p150), mammalian ATG14 (ATG14L or Barkor) and a homologue of Vps38 called ultraviolet irradiation associated-resistance gene (UVRAG)[43-45]. In addition, this complex can interact with the activating molecule in Beclin1-related autophagy (Ambra1), though it is still unclear how Ambra1 exerts its effects mechanistically[46]. Proper localization of Beclin1, hVps34 and p150 depends largely on the complex's interacting partners, some of which are mutually exclusive (Figure 1C).

In nutrient-rich conditions Beclin1 interacts with the anti-apoptotic protein, Bcl-2 and this interaction represses autophagosome formation. Under starvation conditions, this interaction ceases and Beclin1 is free to interact with hVps34 and p150[47]. ATG14L plays a critical role in specifying the site of the hVps34 complex relocalization and therefore PAS nucleation[48]. Depletion of ATG14L restricts autophagic puncta formation, whereas overexpression of the protein leads to increased PI3P production and increased autophagosome formation. Interestingly, ATG14L and UVRAG cannot simultaneously bind Beclin1[49]. UVRAG also interacts with both Bif-1 (an N-BAR domain protein), which potentially leads to phagophore membrane curvature, and the Class C Vps/HOPS complex, which expedites autophagosome-lysosome fusion[50, 51].

UVRAG can also bind to RUN domain and cysteine-rich domain containing, Beclin1-interacting protein (Rubicon), which is a negative regulator of autophagy, thus contributing an additional level of regulation so that a cell does not succumb to excessive autophagy[48, 52]. Ultimately, these hVps34 complexes can exist concurrently in the same cell and can potentially simultaneously mediate their specific functions at different stages of autophagosome formation. A future challenge will be to dissect how the complexes are interrelated and regulated and whether the same common proteins sequentially shift complexes as autophagy proceeds.

One notable difference between yeast and mammalian PAS formation, is that in mammalian cells the structure can be trapped in association with the endoplasmic reticulum (ER) whereas in yeast, the structure is often isolated from organelles and as such was hypothesized to form de novo[53]. Several recent studies suggest that PAS nucleation in mammalian cells occurs at sites that emanate from the ER. A novel marker of this PAS site, termed the omegasome, is a non-ATG, double FYVE domain protein called DFCP1, whose depletion does not block autophagy[54, 55]. Nucleation at this site depends on a subset of ATG14L that localizes to the ER, furthermore an ATG14L mutant that cannot localize to the ER, abrogates proper autophagosome formation[56]. As additional support for this concept, artificially localizing the mutant protein to the ER is sufficient to restore effective nucleation. The omegasome subsequently acts as a scaffold for the nucleation complexes and eventually localizes with ATG18 homologues (WIPI2 and WIPI1-4), ULK1, ATG16 and LC3[57, 58]. In contrast, another group

traced the membrane origins of the starvation-induced autophagosome to the outer leaflet of the mitochondria, a known source of phosphatidylethanolamine (PE, the lipid target of ATG8/LC3)[59]. This study also featured colocalization experiments with ATG16 and ATG5. While seemingly contradictory, it is probable that additional experimental evidence will reveal that both sources could play a role depending on the specific cellular context or alternatively one source could precede the other temporally.

The two ubiquitin-like systems, which mediate early autophagosome expansion and completion, are the most highly conserved between yeast and metazoans at the level of protein networks and individual amino acid conservation. As in yeast, ATG12 modifies ATG5 and LC3 (the homologue of ATG8) modifies the lipid PE. Several critical observations in mammalian systems suggest that the LC3-PE conjugation system is functionally downstream of the ATG12-ATG5 conjugation system. Firstly, in genetic deletions of ATG5 in mice, LC3 conversion does not occur. In complementation experiments using wild type ATG5 or conjugation deficient ATG5 K130R, the mutant does not rescue LC3 conversion. This illustrates that ATG12-ATG5 conjugation rather than free ATG5 is necessary for LC3 lipidation to proceed. Secondly, LC3 remains cytoplasmic in ATG5-deficient ES cells complemented with the K130R mutant rather than colocalizing with ATG5 or the few aberrant isolation membranes that form[25]. Finally, as discussed previously the ATG12-ATG5 complex seems to expedite lipidation of PE by LC3 in *in vitro* reconstitution experiments with the yeast proteins; acting as an E3-like enzyme for LC3-PE

formation[28]. Given the yeast study it is somewhat paradoxical that ectopic overexpression of mammalian ATG12 or the ATG12-ATG5 complex in HEK293 cells instead increases or dampens basal LC3 conversion, respectively[60]. However, it is possible that the presence of wild type proteins confounds the analysis or that under starvation conditions the ATG12-ATG5 complex may have a different effect.

In metazoans there are three other homologues of Microtubule-associated protein light chain 3 (MAP-LC3) that have been identified: GABA-receptor associated protein (GABARAP), Golgi-associated ATPase enhancer of 16 kiloDaltons (GATE-16) and ATG8-like protein (ATG8L)[61-64]. All of these proteins are capable of modifying PE as LC3 does[65], however an early paper suggested that during nutrient starvation in various rat tissues all of the LC3-PE fractionates with the pellet as opposed to part of the lipidated protein being associated with the supernatant (as is the case with GABARAP and GATE-16)[63, 66]. This suggested that LC3 was the primary ATG8 homologue responsible for starvation-induced autophagy, as it was the primary homologue associated with autophagosomal membranes. Furthermore, lipidated LC3 (LC3-II) is the only ATG8 homologue, which solely associates with the autophagosomal compartment, and does not simultaneously lipidate other vesicles. As such, LC3 remains the most-studied mammalian ATG8 homologue and the primary molecule followed as an indicator to quantify autophagy (either endogenously through western blotting or through relocalization of an ectopic GFP-LC3 fusion protein). Recent insight based on the specificity of cysteine proteases ATG4A

and ATG4B for GABARAP and all ATG8 homologues, respectively implies that GABARAP family ATG8 homologues contribute to autophagosome completion[53, 67]. An elegant study from Weidberg and colleagues further specifies that LC3 family and GABARAP family (GAPARAP1, GATE-16 and GAPARAP3) ATG8 homologues are both essential to autophagy but that LC3 family homologues expand the autophagosomal membranes and that GABARAP family homologues help to complete cargo enclosure[68]. Interestingly, knockdown of GABARAP with concomitant overexpression of LC3 leads to large isolation membranes and the reverse experiment leads to small, under-formed isolation membranes, highlighting the complementary functions of the ATG8 homologues. As mentioned previously, lipidated LC3 or LC3-II leads to autophagosome expansion and hemifusion (yeast ATG8) of the pre-autophagosomal membranes, it remains to be determined whether mammalian LC3, GABARAP or GATE-16 also function as fusases. Autophagosome-lysosome fusion in mammalian cells also requires Rab7 and a Rab7 effector called FYCO1, which pulls the vesicle in the direction of the microtubules' plus end and as a result towards the lysosome[69-71]. Finally, two of the hVps34 complexes, the UVRAG complex and the UVRAG/Rubicon complex, expedite and block autolysosome formation, respectively.

Animal Models of Autophagy Deficiency

Many essential autophagy genes have been deleted acutely or in specific tissues in mice. Autophagy is essential to survival in mice and in most cases acute *atg* deletion results in death on the first day after the animal's birth presumably during a period of massive nutrient starvation precipitated by the interruption of maternal-placental nutrient supply. The animals have a suckling defect but when force-fed are still unable to survive more than twenty-four hours after birth. Autophagy-incompetent animals have significantly lower plasma amino acids levels and they eventually succumb to what appears to be cardiac arrest[72]. As a correlation of the requirement for autophagy during the neonatal period, the GFP-LC3 transgenic mouse reports increased autophagic activity in many critical tissues at this time, namely in the heart, lung, diaphragm, skin and liver. The first autophagy gene to be acutely deleted (from the previous study) was *atg5*, however *atg7, atg3* and *atg12* (unpublished observation from Debnath lab) have all been acutely deleted as well, and exhibit similar phenotypes (albeit with subtle differences at the cell biological level)[73, 74]. Acute deletion of one of the autophagy genes *beclin1* (mammalian homologue of ATG6) results in a dramatically distinct phenotype. Animals that completely lack Beclin1 do not survive embryonic development past embryonic day 7.5, whereas the other ATG deficient animals seem to develop normally[75]. On the other hand, Beclin1 can act as a haploinsufficient tumor suppressor as heterozygous animals develop a number of spontaneous lymphoid, lung and liver tumors, despite an intact DNA

damage response[75, 76]. Ultimately, it remains to be determined whether the more severe phenotype observed in Beclin1-deficient animals represents a level of subtlety between autophagy proteins or whether Beclin1 has pleiotropic autophagy-independent roles, which when non-functional contribute to the relatively exacerbated phenotype.

Tissue-specific autophagy deletion highlights the potential for modulating autophagy as a therapeutic avenue for a number of human diseases. Conditional ATG7-deletion in neurons leads to spontaneous neurodegenerative disease, with protein aggregation, neuronal cell death and phenotypic consequences of neuronal degeneration (clasping phenotype)[77]. Significantly, this occurs in the absence of the ectopic expression of a pathogenic protein and strongly suggests that autophagy plays a critical role in maintaining neuronal health, potentially through clearance of protein aggregates or damaged organelles. Additionally, autophagy is essential for maintenance of healthy pancreatic beta cells, presumably due to clearance of protein aggregates amassed from insulin secretion[78]. ATG7 has also been deleted in the liver, which leads to hepatomegaly in combination with a buildup of ubiquitin-positive protein aggregates and damaged mitochondria[73]. Interestingly, both adaptive and innate immunity require functional autophagic degradation. Autophagy deficiency leads to impaired T-lymphocyte viability, antigen presentation and self-tolerance in the thymus. In innate immunity, autophagy affects cytokine production and the Type I interferon response; it can also mediate degradation of invading intracellular pathogens, which can be targeted for lysosomal destruction in a process called

xenophagy[79]. ATG16L has recently emerged as a disease-susceptibility locus in genome-wide association studies for Crohn's disease[80]. In support of this finding, ATG16 deletion or hypomorphophic alleles in the Paneth cells of the intestine, recapitulate a Crohn's-like phenotype in mice, following viral infection[81-83]. Finally, the Beclin1 haploinsufficient phenotype led to speculation on the role of autophagy in cancer. On the one hand, intact autophagy allows the cell to cull damaged mitochondria thereby avoiding ROS that could result in DNA damage leading to genomic instability and cancer[84, 85]. On the other hand, autophagy gene expression is rarely lost in human cancers and the pathway's conserved role as a stress response implies that tumor cells could monopolize on nutrients, amino acids and ATP garnered from autophagy to survive starvation, hypoxia and anchorage-independent growth[86-89]. To date most of the key evidence for each hypothesis has been *in vitro* or in xenograft studies of nude mice. A future challenge will be to dissect the stage specific-contribution of autophagy to tumor growth and metastasis in a bona fide animal model of tumor progression (Debnath lab in progress). Ultimately, tissue-specific deletion of autophagy in mice indicates that manipulating autophagy could be a viable therapeutic strategy for a number of hard to treat human diseases such as neurodegenerative, autoimmune and various cancers.

Ubiquitin-like protein modification and Autophagy UBLs

Post-translational modification of proteins greatly diversifies the functional repertoire of many cellular proteins. For example, proteins can be phosphorylated, acetylated, methylated and transiently or permanently bound to small protein tags like ubiquitin. Ubiquitin-like protein conjugations (UBLs), such as ubiquitination and sumoylation, are known to alter protein fate, localization, function and transcriptional activity[90]. Ubiquitin and UBLs covalently modify substrates through a series of chemical reactions mediated by specific enzymes[91]. Most UBLs have one E1 enzyme, several E2 enzymes and many E3 enzymes to efficiently target what can be several or hundreds of substrates, depending on the system. Before most UBLs can be adenylated, a cysteine protease exposes the c-terminal glycine of the protein. These proteases also perform the regulatory function of deubiquitinating UBLs once the protein complex has fulfilled its cellular function[92]. As a first step in the reaction, an E1 enzyme utilizes an ATP molecule to adenylate ubiquitin, thereby activating it. An active-site cysteine from the E1 activating enzyme subsequently attacks the adenylated ubiquitin to form a transient thioester intermediate[93]. By virtue of protein-protein interactions between the ubiquitin or E1 and the E2 conjugating enzyme as well as the charging of a second ubiquitin molecule, a transthiolation occurs and thereby transfers the ubiquitin between E1 and E2 to a distinct cysteine residue on the E2. An E3 ligase either analogously transfers the ubiquitin to its final substrate through transthiolation (HECT domain E3) or it

catalyzes the reaction by bringing the E2 and substrate into close proximity so that the E2 can pass the ubiquitin molecule to its cellular substrate (RING domain E3)[94]. The final linkage between ubiquitin and its substrate is typically an amide bond between the c-terminal glycine of ubiquitin and the ε-amino group of a lysine molecule on the target protein. However, under specific conditions ubiquitin or the UBL can also modify the amino group of the n-terminus of a protein or cysteine, serine or threonine residues[91].

Ubiquitin adopts a β-grasp fold conformation, which is the structural feature that identifies a ubiquitin-like protein. To date, there are nine identified UBLs out of which the small ubiquitin-like modifier (SUMO) is the best understood. Early characterization of ubiquitin focused on its role in targeting proteins for degradation by the 26S proteasome. Later reports, however, identified that ubiquitination can also lead to internalization of surface transmembrane proteins or to changes in signaling depending on the number of ubiquitin molecules attached to the substrate and in the case of polyubiquitination the location of the specific modified lysine residue on the ubiquitin chain. Generally, polyubiquitination with ubiquitin linkage on lysine 48 results in proteasomal degradation or in some cases changes in transcription. Whereas, polyubiquitination with ubiquitin linkage on lysine 63 results in changes in signal transduction, DNA repair, trafficking of membrane-proteins or endocytosis. Monoubiquitination of transmembrane proteins also results in endocytosis of the receptor or other molecule[90]. SUMO, like ubiquitin, can also modify thousands of substrates. SUMO modification can lead to a number of functional outcomes

including nuclear translocation, transcriptional repression through nuclear relocalization into PML bodies, competitive inhibition of degradation by ubiquitin and altering substrate affinity for various protein-protein interactions[95].

As previously mentioned, early autophagosome expansion and completion is modulated by two ubiquitin-like systems that covalently attach: 1) ATG12 to ATG5, and 2) ATG8/LC3 to the lipid (PE, Figure 3). ATG12 bears no primary sequence similarity to ubiquitin, however, based on its crystal structure, which includes a β-grasp fold, it is classified as a ubiquitin-like molecule[96]. In addition, ATG12 is activated by the E1-like enzyme ATG7, a step which requires ATP, and it is subsequently conjugated to ATG5 by ATG10, an E2-like enzyme.[97, 98] The conjugate is constitutively made and is required for membrane elongation and ATG localization to the PAS[21]. The second ubiquitin-like autophagic system mediates the lipidation of LC3 by PE. This conjugation shares ATG7 as an E1-like activating enzyme but has a distinct E2-like conjugating enzyme, ATG3. LC3 conjugation mediates further elongation of the isolation membrane and cargo enclosure[5, 26]. Both conjugation steps are necessary for early autophagosome formation and deletions of *atg*s that are essential to either conjugation system functionally block autophagic responses to starvation and clearance of protein aggregates[72, 73].

Since its initial characterization, ATG5 was proposed to be the sole substrate of ATG12. However, several papers demonstrated increased ATG12 expression during mitochondrial outer membrane permeabilization (MOMP), chloramphenicol-induced mitochondrial dysfunction and ER-stress without

Figure 2: Two ubiquitin-like protein modification systems are required for early autophagosome expansion and closure.

ATG12 is an autophagic ubiquitin-like molecule that is activated by ATG7 and conjugated by ATG10 to its only known substrate ATG5. The ATG12-ATG5 complex is temporally upstream of the second UBL modification required for autophagy and acts as an E3-like protein for LC3 lipidation of PE. LC3 (ATG8 homologue) shares ATG7 as an E1 enzyme and has a distinct E2-like enzyme, ATG3. LC3 conjugation to PE further expands the autophagosomal membrane and mediates hemifusion and cargo enclosure.

Figure 2

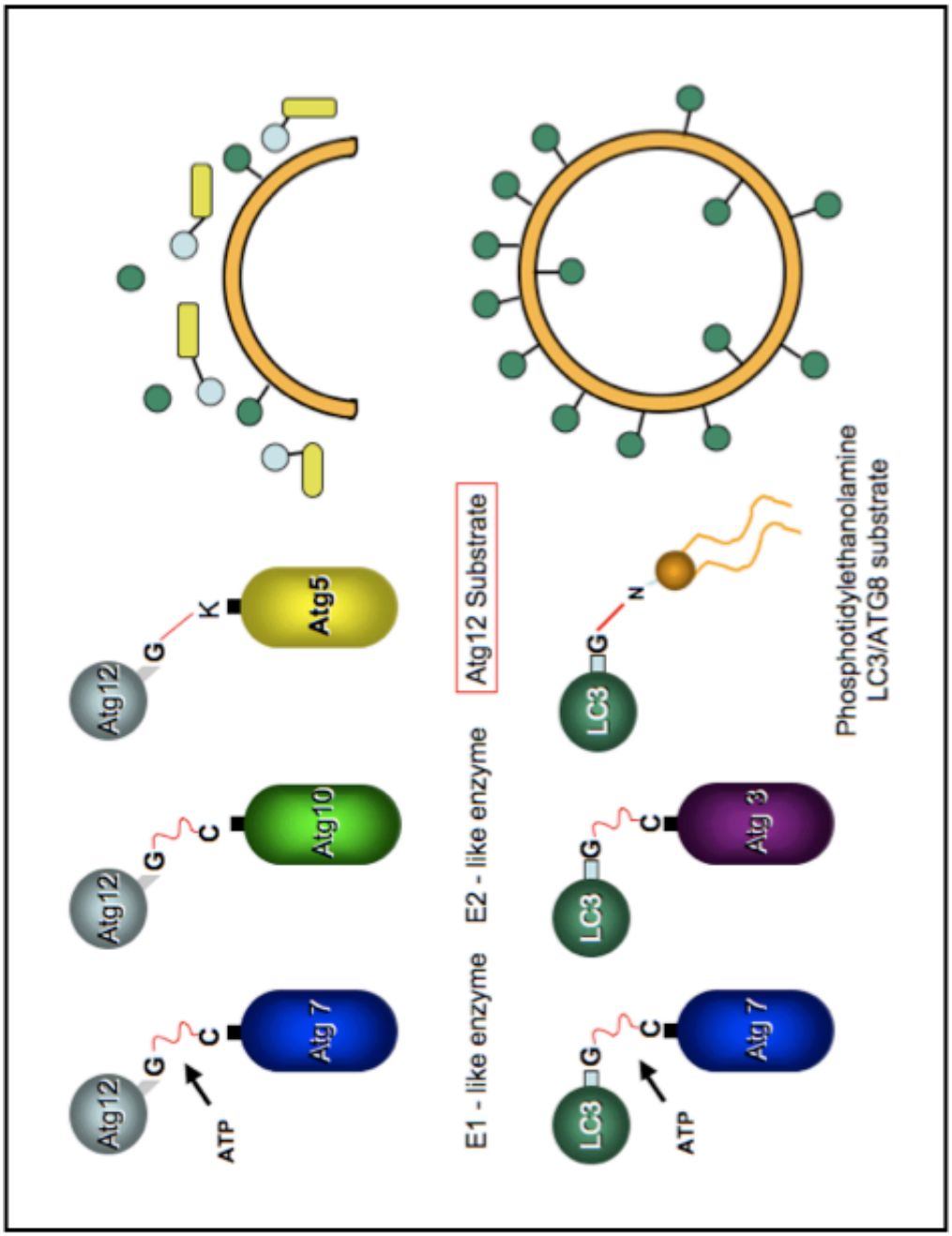
Atg12
G
C
ATP
Atg 7
Atg12
G
C
Atg10
Atg12
G
K
Atg5
E1 - like enzyme
E2 - like enzyme
Atg12 Substrate
LC3
G
C
ATP
Atg 7
LC3
G
C
Atg 3
LC3
G
N
Phosphotidylethanolamine
LC3/ATG8 substrate

measurable increases in ATG12-ATG5 complex formation[99-101]. In the first paper, the authors induce caspase-independent cell death (CICD) through the intrinsic pathway in concert with pan-caspase inhibitors. Through an unbiased approach, the authors found that overexpression of GAPDH could protect cells from CICD. GAPDH functions in glycolysis and also translocates to the nucleus during certain cellular stresses[102, 103]. Both of these functions were essential to protection from CICD and cellular survival of CICD required autophagy. Interestingly, the authors note that ATG12 is upregulated by GAPDH (perhaps indirectly) and that overexpression of ATG12 can substitute for the nuclear function of GAPDH, whereas ATG5 and LC3 did not confer the same effect. This was particularly compelling because it indicated that ATG12 might have additional functions outside of autophagy that could potentially be mediated by its conjugation to as yet unknown substrates. The second instance of upregulation of ATG12 occurred in cybrids of cells lacking mitochondria and diseased cells from patients with mitochondrial dysfunction. These cells have upregulated the ATG12 transcript following deletion of mitochondrial genes. The authors found that ATG12 upregulation is triggered by impaired mitochondrial protein synthesis as chloramphenicol treatment recapitulated the phenotype. Yet again, ATG12 is upregulated independently of ATG5, highlighting potential alternative roles of the protein. Finally, overexpression of eGFP fused to 72 glutamine repeats induces ER-stress and autophagy in several cell lines. The authors suggest that this induction is via PERK and eIF2α. Notably, ATG12 transcript levels are upregulated along with CHOP, a transcription factor downstream of PERK

activation. As in the other studies, ATG12 is the only autophagy gene that becomes transcribed, independently of ATG5, ATG16 and ATG7. The authors verified this result using thapsigargin, an agent that depletes ER calcium levels, and saw a parallel independent-upregulation of Atg12 mRNA.

We suspected that ATG12, like other UBLs, might modify additional proteins because the induction of autophagy rarely requires transcriptional upregulation and all three studies observed an ATG5-independent increase in ATG12 message or protein. Furthermore, it seemed unlikely that an energetically costly enzymatic cascade had evolved to modify a sole substrate. We hypothesized that multiple substrates for ATG12 existed. During my thesis work, we tested this hypothesis, found that ATG12 does indeed modify several additional substrates and identified ATG3 as a novel substrate of ATG12. Notably, ATG3 is the E2-like enzyme responsible for LC3 lipidation. Though it seemed logical that ATG12 modification of ATG3 would serve as a regulatory link between the two ubiquitin-like systems required for early autophagosome formation, abrogating ATG12 conjugation to ATG3 had little effect on starvation-induced autophagy. Instead, mitochondrial homeostasis and mitochondrial cell death were profoundly affected in cells that were unable to conjugate ATG12 and ATG3. Chapter II describes the biochemical mechanisms of ATG12-ATG3 conjugation and Chapter III discusses the biological consequences of ATG12-ATG3 conjugation.

CHAPTER II:

ATG12 CONJUGATES TO MULTIPLE NOVEL SUBSTRATES IN ADDITION TO ATG5

Abstract:

Ubiquitin-like protein (UBL) modification is a rapid and reversible covalent post-translational modification of a cellular substrate, which can alter its fate, function, localization or transcriptional activity. Ubiquitin and the small ubiquitin-like modifier (SUMO) can each bind to hundreds of substrates. However, ATG12, a ubiquitin-like modifier required for macroautophagy, has a single known conjugation target, another autophagy regulator called ATG5. Here we demonstrate that ATG12, like other UBLs, can modify a number of additional substrates independent of ATG5. Furthermore, we identify ATG3 as a novel substrate for ATG12 conjugation. ATG3 is the E2-like enzyme necessary for ATG8/LC3 lipidation during autophagy. ATG12-ATG3 complex formation requires ATG7 as the E1 enzyme and ATG3 autocatalytic activity as the E2, resulting in the covalent linkage of ATG12 onto a single lysine on ATG3. This autocatalytic conjugation occurs *in cis*, in a process that does not require ATG10. The identification of a novel covalent conjugate between ATG12 and ATG3 reveals that additional ATG12 targets (other than ATG5) exist and implies that ATG12 potentially functions as a more broad-based UBL than previously appreciated.

Introduction:

Ubiquitin-like (UBL) protein conjugations, such as ubiquitination and sumoylation, influence diverse cell biological processes, including protein targeting, organelle trafficking, cell division, signal transduction, and transcription [104]. These post-translational modifications, which typically result in the covalent attachment of the UBL tag to the e-amine group of lysine residues in target substrates, are highly dynamic, reversible, and tightly regulated by well-established biochemical cascades. First, the UBL is activated in an ATP dependent manner by an E1 activating enzyme in which the C-terminal glycine residue of the UBL moiety forms a high-energy thioester bond with a cysteine residue in the active site of the E1. Second, the activated UBL is transferred to an E2 conjugating enzyme via a trans-esterification reaction. Finally, the UBL is transferred onto a lysine of a target substrate; in many cases, this final transfer requires an E3 ligase enzyme [90]. To date, two family members, ubiquitin and small ubiquitin-like modifier (SUMO), have received the greatest attention; nonetheless, other UBLs undoubtedly have undiscovered functions in biology and disease [104].

Two UBLs, ATG12 and ATG8 (ATG stands for AuTophaGy gene), play critical roles in macroautophagy (hereafter called autophagy), a tightly controlled lysosomal degradation process in which a cell digests its own cytoplasmic proteins and organelles during starvation or stress [105, 106]. Although ATG12 and ATG8 possess little primary sequence homology to ubiquitin, both contain an

"ubiquitin superfold" and the C-terminal glycine required for isopeptide linkage [96, 107, 108]. Importantly, the early steps of autophagosome formation require these two ubiquitin-like conjugation processes, which covalently attach ATG12 to the target protein ATG5 [97, 98] and ATG8 (for which, microtubule associated protein light chain 3 or LC3 is a chief orthologue in mammals) to the lipid phosphotidylethanolamine (PE) [26, 109]. Both ATG8 and ATG12 are activated in an ATP-dependent process by a ubiquitin-like E1 activating enzyme, called ATG7 [110]. Subsequently, ATG12 is conjugated to ATG5 by ATG10, an E2-like conjugating enzyme [111], whereas ATG8/LC3 is conjugated to PE via another E2-like molecule, ATG3 [62, 112]. Furthermore, recent biochemical evidence supports a model in which the ATG12-ATG5 complex possesses an E3-like activity that mediates efficient PE-lipidation of ATG8 [28, 113].

Unlike other UBLs, ATG12 is proposed to modify a single target, ATG5. However, it remains unclear why a complex energy-consuming enzymatic cascade has evolved to conjugate a single substrate. Furthermore, certain stimuli, namely mitochondrial outer membrane permeabilization (MOMP) and endoplasmic reticulum (ER) stress, produce an increase in ATG12 transcript or protein levels, but no concomitant rise in ATG5; such discordant regulation is enigmatic given that ATG12 is solely proposed to function as part of an 1:1 stoichiometric complex with ATG5 [99, 101]. One potential explanation for these previous findings is that, similar to other UBLs, ATG12 modifies additional substrates that regulate autophagy or other cellular functions.

Hence, we sought to test the hypothesis that ATG12 is not an isolated UBL modification confined to a single target. Here, we identify ATG3, the E2 enzyme necessary for ATG8/LC3 lipidation during autophagy, as a novel substrate for ATG12 conjugation. ATG12-ATG3 complex formation requires ATG7 as the E1-activating enzyme and an autocatalytic function of ATG3 as the E2, resulting in the covalent attachment of ATG12 onto a single lysine on ATG3.

Results:

ATG12 covalently modifies multiple protein targets in addition to ATG5 in mammalian cells. To test whether ATG12 covalently modifies novel protein targets in addition to ATG5, we created a retroviral construct encoding epitope-tagged mouse ATG12 (FHA-ATG12); as a negative control, we generated a conjugation incompetent version in which the C-terminal glycine in ATG12, required for the isopeptide linkage to target lysine residues, was replaced with a stop codon (FHA-Stop) (Figure 1A) [98]. Upon stable expression in MCF10A human mammary epithelial cells, we observed a slower migrating ATG12-ATG5 complex, consistent with epitope tag addition, as well as additional higher molecular weight conjugates in FHA-ATG12 expressing cells but not in FHA-Stop cells (Figure 1B). Importantly, these higher molecular weight proteins were observed using denaturing and reducing conditions, suggesting that ATG12 was covalently attached to multiple novel protein targets. Furthermore, upon α-FLAG immunoprecipitation, we observed numerous additional ATG12-X species that

were unique to cells expressing conjugatable ATG12 (Figure 1C). Similar results were obtained upon stable FHA-ATG12 expression in HeLa cervical carcinoma cells, indicating that the ATG12-X proteins are present in multiple human cell types (Figure 1D).

We next asked whether the E1-like enzyme ATG7 is required for the activation of ATG12 and its subsequent conjugation to these novel targets [61, 110]. We stably infected ATG7 deficient fibroblasts with FHA-ATG12 or FHA-Stop and found that all ATG12 conjugations were eliminated in the absence of ATG7 (Figure 1E). Thus, ATG12 requires ATG7 as an E1-activating enzyme to be conjugated to any of its multiple protein targets. Since ATG5 is the only known substrate of ATG12, we tested if the additional higher molecular weight ATG12-X proteins were unique ATG12-modified proteins versus multiple ATG12 conjugations onto the ATG12-ATG5 complex [97, 98]. To distinguish among these possibilities, we stably expressed FHA-ATG12 and FHA-Stop in both wild type (*atg5*+/+) and ATG5 null (*atg5*-/-) mouse embryonic fibroblasts (MEFs). Similar to our results in human cells, we observed numerous ATG12 conjugates in both *atg5*+/+ and -/- mouse fibroblasts. In *atg5*-/- cells, only the band corresponding to the ATG12-ATG5 protein complex disappeared; the remaining ATG12-X proteins continued to be produced, supporting that these species are unique conjugation targets that can be formed in the absence of ATG5 (Figure 1F).

Figure 1: ATG12 covalently modifies multiple protein targets in mammalian cells.

(A) Schematic of ATG12 constructs: Mouse ATG12 was tagged at the N-terminus with tandem FLAG and HA epitopes to create FHA-ATG12. In FHA-Stop, the C-terminal glycine in ATG12 required for conjugation is replaced with a Stop codon.

(B) MCF10A human mammary cells stably expressing a control empty vector (MSCV), FHA-ATG12 and FHA-Stop were lysed and immunoblotted with α-ATG12 and α-HA antibodies. Asterisk (*) indicates a non-specific band observed during α-HA immunoblotting.

(C) MCF10A mammary epithelial cells stably expressing the indicated constructs were lysed and immunoprecipitated with α-FLAG; immune complexes were resolved using SDS-PAGE and subject to α-ATG12 immunoblotting.

(D) HeLa cells stably expressing the indicated constructs were lysed and immunoblotted with α-HA.

(E) *atg7+/+* (WT) and *atg7-/-* mouse embryonic fibroblasts (MEFs) stably expressing the indicated constructs were lysed and subject to α-HA immunoblotting. Asterisk (*) indicates non-specific band.

(F) Left: *atg5+/+* (WT) and *atg5-/-* stably expressing the indicated constructs were lysed and immunoblotted with α-HA or α-ATG5. Right: WT and *atg5-/-* MEFs expressing FHA-ATG12 were lysed and immunoprecipitated with α-FLAG; immune complexes were resolved and immunoblotted with α-HA.

Figure 1

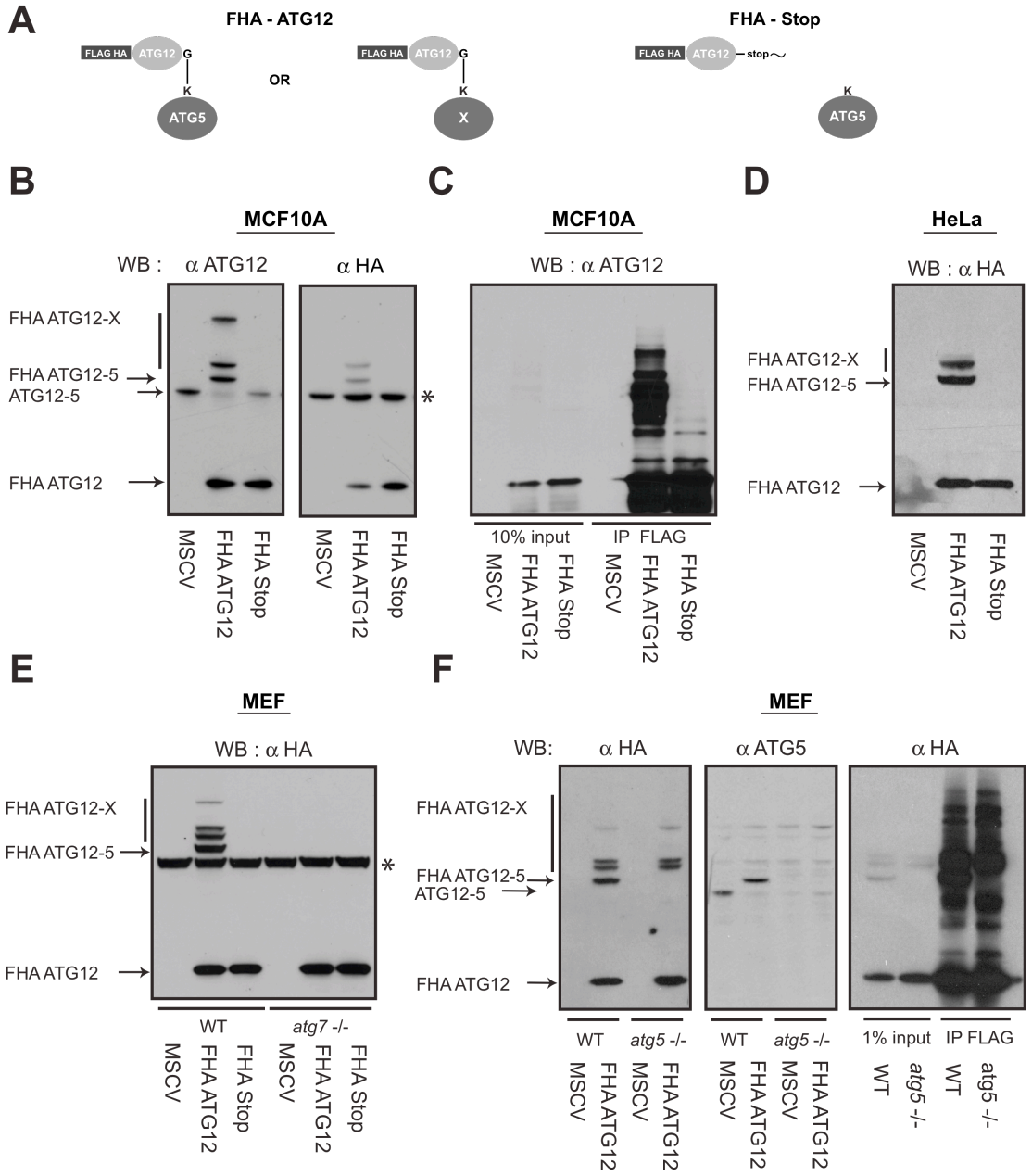
A
FHA - ATG12
FLAG HA
ATG12
G
K
ATG5
OR
X
FHA - Stop
stop
B
MCF10A
WB : α ATG12
α HA
FHA ATG12-X
FHA ATG12-5
ATG12-5
FHA ATG12
MSCV
FHA ATG12
FHA Stop
C
MCF10A
WB : α ATG12
10% input
IP FLAG
D
HeLa
WB : α HA
E
MEF
WB : α HA
WT
atg7 -/-
F
MEF
WB: α HA
α ATG5
α HA
atg5 -/-
1% input
IP FLAG

ATG12 and ATG3 form a covalent complex. To identify novel ATG12-X proteins, lysates from *atg5*-/- fibroblasts stably expressing either FHA-ATG12 or FHA-Stop were subject to large-scale tandem affinity purification with a-FLAG and a-HA antibodies. Upon resolving the eluted proteins, each protein in the predominant doublet on a Coomassie Brilliant Blue stained gel (Figure 2A, asterisk) was trypsin-digested and subject to tandem mass spectrometry (MS/MS). Both proteins in this doublet were identified as ATG12 conjugated to ATG3, with 33% sequence coverage and at least three peptides from each band with an ion score > 45 (Figure 2A). ATG3 is the E2-like enzyme responsible for ATG8/LC3 lipidation and has previously been demonstrated to interact with ATG12 [60, 62]. To our knowledge, we are the first to identify the formation of a covalent complex between ATG12 and ATG3.

In α-FLAG immunoprecipitates prepared from MEFs expressing FHA-ATG12, we detected the 65kD doublet using antibodies against either ATG12 or ATG3, confirming that this protein corresponded to ectopic FHA-ATG12 conjugated to endogenous ATG3 (Figure 2B). Remarkably, this doublet collapsed to a single protein when treated with calf intestinal phosphatase, suggesting that the ATG12-ATG3 complex undergoes phosphorylation (Figure 3). Furthermore, MCF10A cells stably expressing shRNA against ATG3 exhibited specific depletion of the ATG12-ATG3 complex, relative to a non-targeting shRNA control, whereas the ATG12-ATG5 complex continued to be produced (Figure 2C). Finally, the ATG12-ATG3 complex was not observed in *atg3*-/-

Figure 2: ATG12 and ATG3 form a covalent complex.

(A) Lysates from *atg5-/-* MEFs stably expressing FHA-ATG12 or FHA-Stop were subject to affinity purification with α-FLAG followed by α-HA antibodies. Eluted proteins at each stage were resolved using SDS-PAGE and immunoblotted with α-HA (left) or stained with Coomassie (middle). Each protein in the indicated doublet (arrows) was individually subject to MS/MS analysis and both were identified as ATG3. Right: Amino acid sequence of mouse ATG3; underlined sequences correspond to independent peptides identified by mass spectrometry.

(B) Lysates from wild type MEFs expressing the indicated constructs were immunoprecipitated with α-FLAG; immune complexes (FLAG IP) were resolved using SDS-PAGE and subject to α-ATG12 or α-ATG3 immunoblotting.

(C) MCF10A cells stably expressing FHA-ATG12 were infected with lentiviruses encoding non-targeting control shRNA or shRNA targeted to ATG3 (shATG3). Lysates were immunoblotted as indicated.

(D) Wild type and *atg3-/-* MEFs stably expressing the indicated constructs were lysed and subject to α-HA immunoblotting.

(E) Wild type and *atg3-/-* MEFs stably expressing FHA-ATG12 were lysed and subject to α-FLAG immunoprecipitation; immune complexes were resolved and immunoblotted with α-HA.

(F) Lysates from wild type and *atg3*-/- MEFs were immunoprecipated with α-ATG3; immune complexes were resolved using SDS-PAGE and subject to α-ATG3 or α-ATG12 immunoblotting. Asterisk (*) indicates immunoglobulin heavy chain.

Figure 2

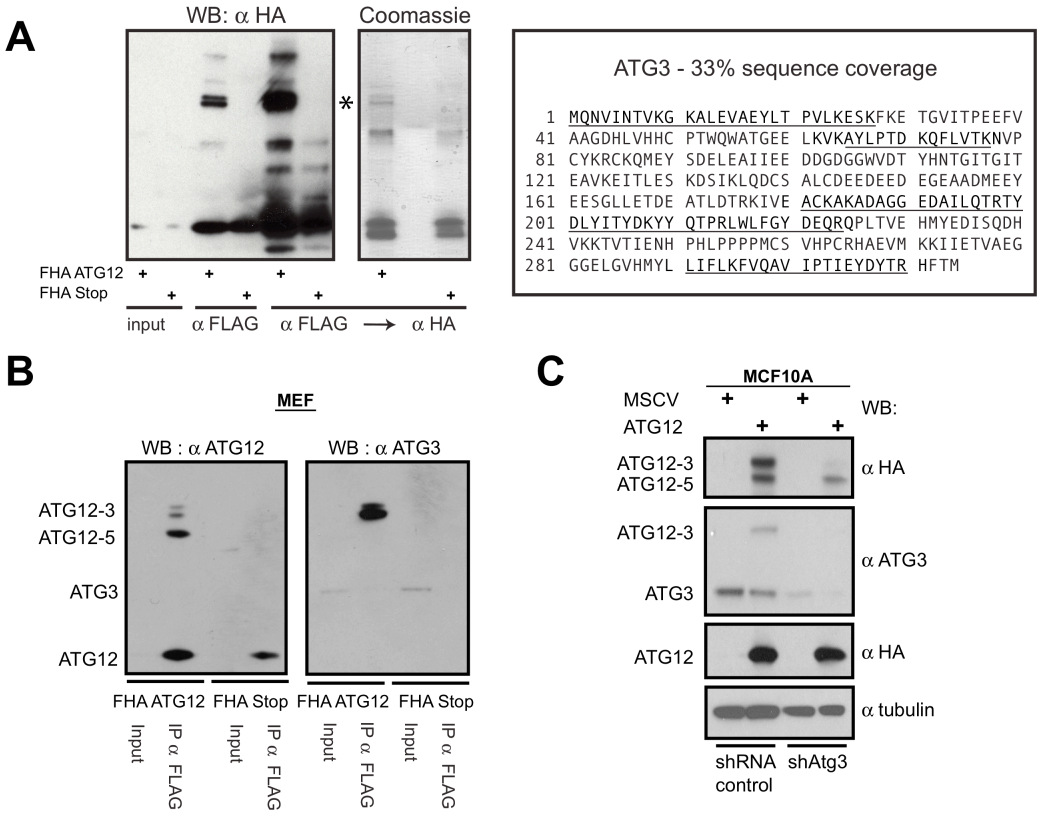
A
WB: α HA
Coomassie
*
FHA ATG12
FHA Stop
input
α FLAG
α FLAG → α HA
ATG3 - 33% sequence coverage
1 MQNVINTVKG KALEVAEYLT PVLKESKFKE TGVITPEEFV
41 AAGDHLVHHC PTWQWATGEE LKVKAYLPTD KQFLVTKNVP
81 CYKRCKQMEY SDELEAIIEE DDGDGGWVDT YHNTGITGIT
121 EAVKEITLES KDSIKLQDCS ALCDEEDEED EGEAADMEEY
161 EESGLLETDE ATLDTRKIVE ACKAKADAGG EDAILQTRTY
201 DLYITYDKYY QTPRLWLFGY DEQRQPLTVE HMYEDISQDH
241 VKKTVTIENH PHLPPPPMCS VHPCRHAEVM KKIIETVAEG
281 GGELGVHMYL LIFLKFVQAV IPTIEYDYTR HFTM
B
MEF
WB : α ATG12
WB : α ATG3
ATG12-3
ATG12-5
ATG3
ATG12
FHA ATG12
FHA Stop
FHA ATG12
FHA Stop
Input
IP α FLAG
Input
IP α FLAG
Input
IP α FLAG
Input
IP α FLAG
C
MCF10A
MSCV
ATG12
WB:
ATG12-3
ATG12-5
α HA
ATG12-3
ATG3
α ATG3
ATG12
α HA
α tubulin
shRNA control
shAtg3
D
MEF
WB : α HA
ATG12-3
ATG12-5
ATG12
WT
atg3 -/-
MSCV
FHA ATG12
FHA Stop
MSCV
FHA ATG12
FHA Stop
E
MEF
WB : α HA
ATG12-X
ATG12-3
ATG12-5
ATG12
input
α FLAG
WT
atg3 -/-
WT
atg3 -/-
F
MEF
WB : α ATG3
ATG12-3
ATG3
*
WB : α ATG12
ATG12-3
*
IP : α ATG3
WT
atg3 -/-

Figure 3: Phosphatase treatment of doublet corresponding to ATG12-ATG3 complex. MCF10A mammary cells expressing FHA-ATG12 were lysed as described and immunoprecipitated (IP-ed) with α-FLAG coupled agarose. One IP was treated with 50 units calf alkaline phosphatase (CIP, New England Biolabs) in a 300 mL reaction for 20 min at 37C, while the control IP was mock treated. Samples were resolved by SDS-PAGE and immunoblotted with α-ATG12 antibody. Arrow indicates the 65kD doublet corresponding to ATG12-ATG3, which collapses to a single protein band upon CIP treatment.

Figure 3

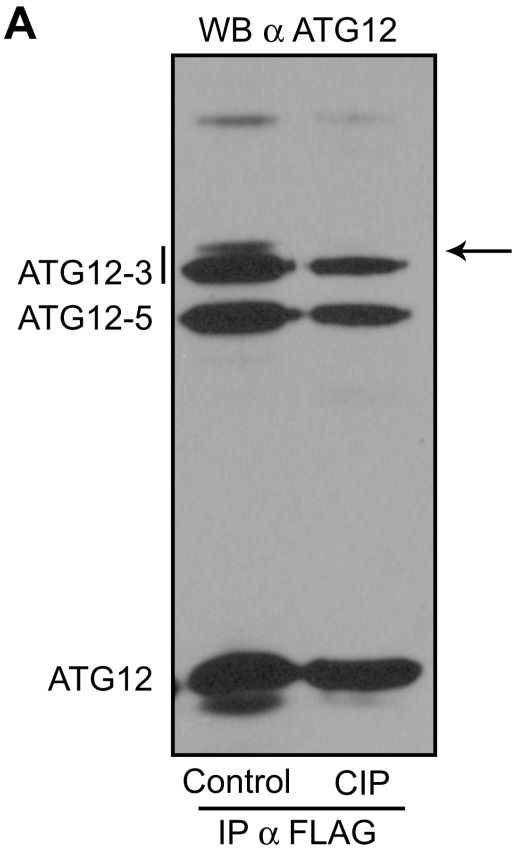

MEFs expressing FHA-ATG12, in contrast to wild type controls (Figure 2D), whereas ATG12-ATG5 and other higher molecular weight species, corresponding to other ATG12-X conjugates, persisted in *atg3*-/- cells (Figure 2E) [74]. Finally, to assess if the ATG12-ATG3 complex was present at endogenous expression levels, protein extracts were immunoprecipitated with α-ATG3 antibodies. We detected a 51kd protein complex in wild type fibroblasts that immunoblotted with both α-ATG3 and α-ATG12 antibodies; this complex was not present in protein lysates prepared from *atg3-/-* MEFs (Figure 2F). Overall, these data support that ATG12 forms a covalent complex with ATG3 and that this complex represents the second (with ATG12-ATG5 being the first) of several potential ATG12 conjugation targets.

Auto-conjugation of ATG12 onto a single lysine on ATG3. Similar to other UBLs, ATG12 is covalently attached to the e-amine group of a lysine residue of its target [90, 97]. To elucidate potential functions of the ATG12-ATG3 complex, we sought to identify the target lysine(s) in ATG3 required for ATG12 conjugation. First, we compared the amino acid sequence of ATG3 from multiple species and found five lysines to be highly conserved (Figure 4A). We used site-directed mutagenesis to systematically eliminate each of these lysines, or groups of lysines, and transiently co-expressed each mutant version of ATG3 along with ATG12 and ATG7 in HEK293T cells (Figure 5A and Figure 4B). Using this strategy, we reconstituted ATG12-ATG3 complex formation and identified lysine 243 (K243) as the primary lysine required for ATG12 conjugation. Upon mutation

Figure 4: Comparison of Primary Amino Acid Sequence of ATG3 from Seven Species and Mutational Analysis of Conserved Lysines in ATG3 for ATG12-ATG3 Complex Formation

(A) Comparison of ATG3 amino acid sequences from *Mus musculus* (MOUSE); *Homo sapiens* (HUMAN); *Xenopus laevis* (XENLA); *Danio rerio* (DANRE); *Arabidopsis thaliana* (ARATH); *Schizosaccharomyces pombe* (SCHPO); and *Saccharomyces cerevesiae* (YEAST). The conserved catalytic cysteine (green) and the conserved lysines (yellow) in ATG3 are highlighted. Alignment performed using ClustalW (Larkin et al., 2007).

(B) Mutational analysis of conserved lysines in ATG3 for ATG12-ATG3 complex formation. HEK293T cells were triply transfected as described with YFP-ATG12, Myc-tagged ATG7, and V5-tagged ATG3 constructs encoding the indicated lysine mutant. Cells were lysed and immunoblotted with α-V5 antibody to detect the ATG12-ATG3 complex.

(C) HEK293T cells transfected with Myc-tagged ATG7, YFP-ATG12, and either HA-tagged WTATG3 or ATG3 C264A (catalytically inactive) and either V5-tagged WTATG10 or ATG10 C165A (catalytically inactive). Cells were lysed and immunoblotted with the indicated antibodies.

Figure 4

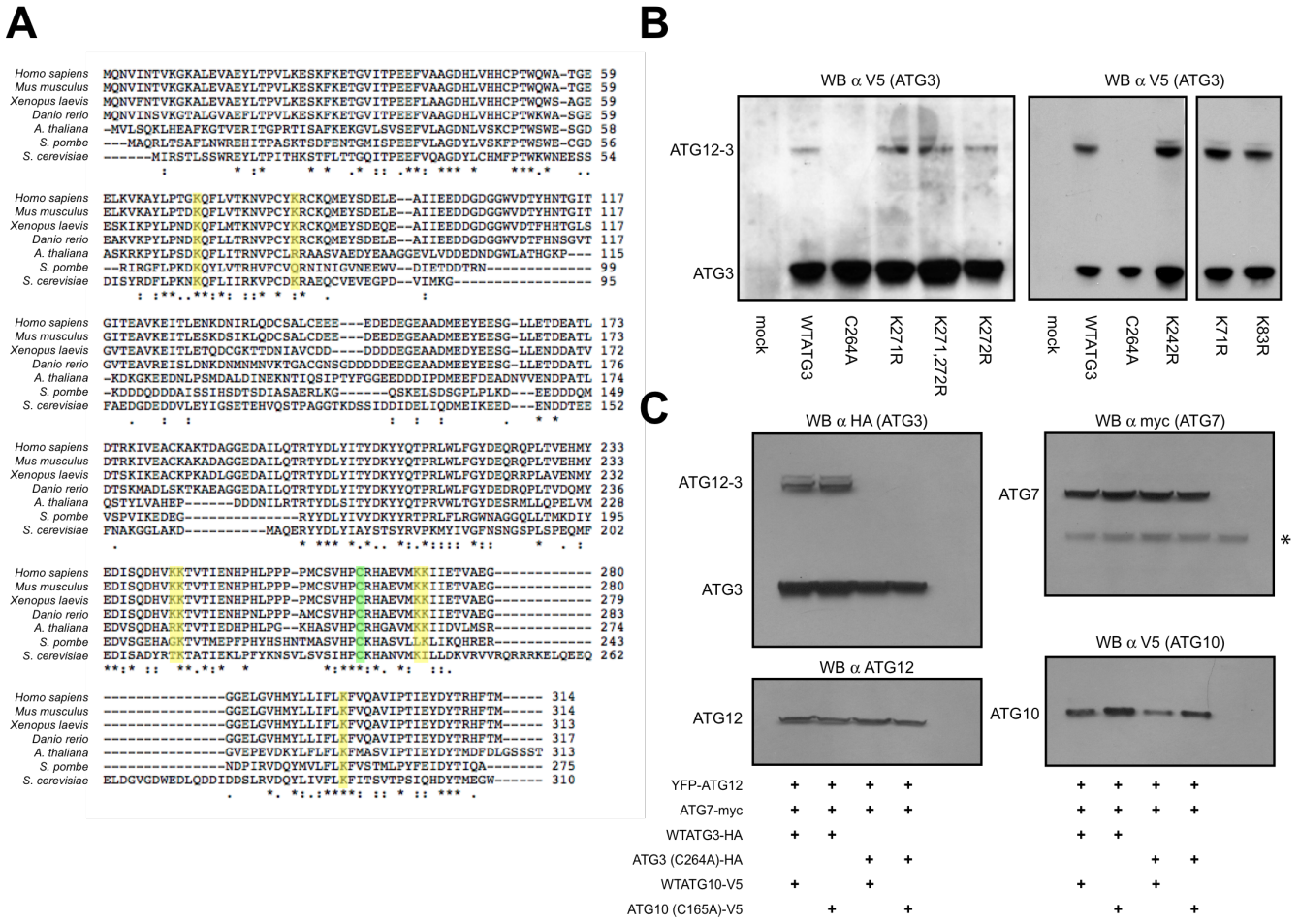
A
Homo sapiens MQNVINTVKGKALEVAEYLTPVLKESKFKETGVITPEEFVAAGDHLVHHCPTWQWA-TGE 59
Mus musculus MQNVINTVKGKALEVAEYLTPVLKESKFKETGVITPEEFVAAGDHLVHHCPTWQWA-TGE 59
Xenopus laevis MQNVFNTVKGKALEVAEYLTPVLKESKFKETGVITPEEFLAAGDHLVHHCPTWQWS-AGE 59
Danio rerio MQNVINSVKGTALGVAEFLTPVLKESKFKETGVITPEEFVAAGDHLVHHCPTWKWA-SGE 59
A. thaliana -MVLSQKLHEAFKGTVERITGPRTISAFKEKGVLSVSEFVLAGDNLVSKCPTWSWE-SGD 58
S. pombe ---MAQRLTSAFLNWREHITPASKTSDFENTGMISPEEFVLAGDYLVSKFPTWSWE-CGD 56
S. cerevisiae ------MIRSTLSSWREYLTPITHKSTFLTTGQITPEEFVQAGDYLCHMFPTWKWNEESS 54
ELKVKAYLPTGKQFLVTKNVPCYKRCKQMEYSDELE--AIIEEDDGDGGWVDTYHNTGIT 117
ELKVKAYLPTDKQFLVTKNVPCYKRCKQMEYSDELE--AIIEEDDGDGGWVDTYHNTGIT 117
ESKIKPYLPNDKQFLMTKNVPCYKRCKQMEYSDEQE--AIIEEDDGDGGWVDTFHHTGLS 117
EAKVKPYLPNDKQFLLTRNVPCYKRCKQMEYSDELE--AIIEEDDGDGGWVDTFHNSGVT 117
ASKRKPYLPSDKQFLITRNVPCLRRAASVAEDYEAAGGEVLVDDEDNDGWLATHGKP--- 115
--RIRGFLPKDKQYLVTRHVFCVQRNINIGVNEEWV--DIETDDTRN------------- 99
DISYRDFLPKNKQFLIIRKVPCDKRAEQCVEVEGPD--VIMKG----------------- 95
DTRKIVEACKAKTDAGGEDAILQTRTYDLYITYDKYYQTPRLWLFGYDEQRQPLTVEHMY 233
DTRKIVEACKAKADAGGEDAILQTRTYDLYITYDKYYQTPRLWLFGYDEQRQPLTVEHMY 233
DTSKIKEACKPKADLGGEDAILQTRTYDLYITYDKYYQTPRLWLFGYDEQRRPLAVENMY 232
DTSKMADLSKTKAEAGGEDAILQTRTYDLYITYDKYYQTPRLWLFGYDEDRQPLTVDQMY 236
QSTYLVAHEP------DDDNILRTRTYDLSITYDKYYQTPRVWLTGYDESRMLLQPELVM 228
VSPVIKEDEG--------------RYYDLYIVYDKYYRTPRLFLRGWNAGGQLLTMKDIY 195
FNAKGGLAKD----------MAQERYYDLYIAYSTSYRVPKMYIVGFNSNGSPLSPEQMF 202
EDISQDHVKKTVTIENHPHLPPP-PMCSVHPCRHAEVMKKIIETVAEG------------ 280
EDISQDHVKKTVTIENHPHLPPP-PMCSVHPCRHAEVMKKIIETVAEG------------ 280
EDISQDHVKKTVTIENHPHLPPP-PMCSVHPCRHAEVMKKIIETVAEG------------ 279
EDISQDHVKKTVTIENHPNLPPP-AMCSVHPCRHAEVMKKIIETVAEG------------ 283
EDVSQDHARKTVTIEDHPHLPG--KHASVHPCRHGAVMKKIIDVLMSR------------ 274
EDVSGEHAGKTVTMEPFPHYHSHNTMASVHPCKHASVLLKLIKQHRER------------ 243
EDISADYRTKTATIEKLPFYKNSVLSVSIHPCKHANVMKILLDKVRVVRQRRRKELQEEQ 262
----------GGELGVHMYLLIFLKFVQAVIPTIEYDYTRHFTM----- 314
----------GGELGVHMYLLIFLKFVQAVIPTIEYDYTRHFTM----- 314
----------GGELGVHMYLLIFLKFVQAVIPTIEYDYTRHFTM----- 313
----------GGELGVHMYLLIFLKFVQAVIPTIEYDYTRHFTM----- 317
----------GVEPEVDKYLFLFLKFMASVIPTIEYDYTMDFDLGSSST 313
----------NDPIRVDQYMVLFLKFVSTMLPYFEIDYTIQA------- 275
ELDGVGDWEDLQDDIDDSLRVDQYLIVFLKFITSVTPSIQHDYTMEGW------ 310
B
WB α V5 (ATG3)
WB α V5 (ATG3)
ATG12-3
ATG3
mock
WTATG3
C264A
K271R
K271,272R
K272R
mock
WTATG3
C264A
K242R
K71R
K83R
C
WB α HA (ATG3)
WB α myc (ATG7)
ATG12-3
ATG3
ATG7
*
WB α ATG12
WB α V5 (ATG10)
ATG12
ATG10
YFP-ATG12
ATG7-myc
WTATG3-HA
ATG3 (C264A)-HA
WTATG10-V5
ATG10 (C165A)-V5

Figure 5: Auto-conjugation of ATG12 onto a single lysine of ATG3.

(A) HEK293T cells expressing YFP-ATG12, myc-tagged ATG7, and V5-tagged WTATG3 or the indicated ATG3 mutants.

(B) *atg3-/-* MEFs were stably reconstituted with empty vector (BABE), wild type ATG3, or the indicated mutants. Cells were then transduced with retrovirus encoding empty vector (MSCV) or FHA-ATG12, lysed and immunoblotted with α-HA to detect ATG12-conjugated proteins.

(C) Crystal structure of yeast ATG3 with α-helices labeled in blue and β-sheets in purple. Positions of the conserved catalytic cysteine (C264 in mouse ATG3, green) and the principal lysine conjugated with ATG12 (K243, yellow) are shown. Diagram prepared using PyMOL.

(D) 293T cells transfected with YFP-ATG12, myc-tagged ATG7 and mutants of either HA or V5-tagged ATG3, as indicated.

(E) HEK293T cells transfected with Myc-tagged ATG7, V5-tagged ATG10, YFP-ATG12 and either HA-tagged ATG5 or ATG3 C264A. For this assay, catalytically inactive ATG3 (C264A) was used to distinguish the E2 activity of ATG10 from ATG3 during ATG12-ATG3 formation.

Figure 5

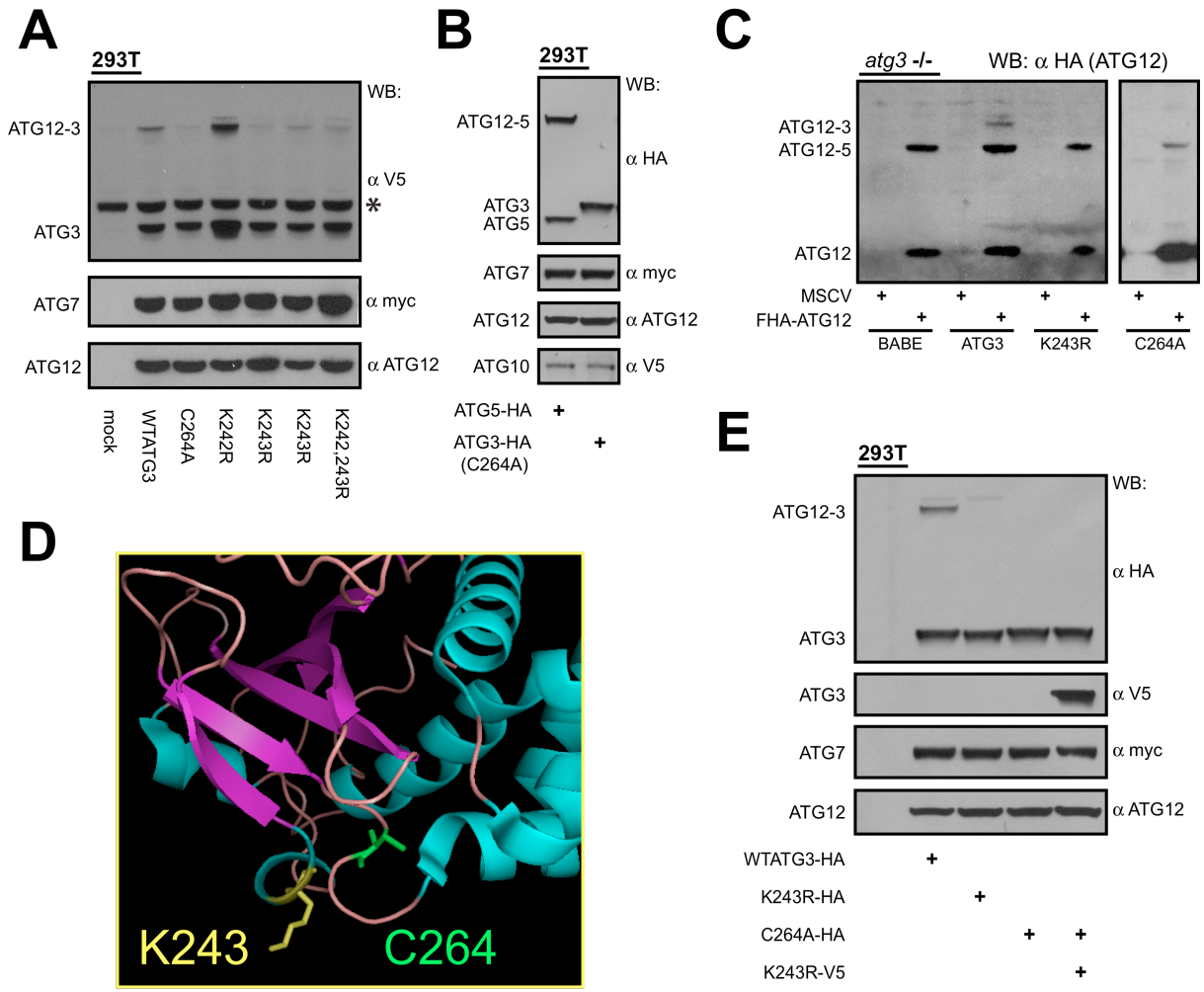
A
293T
WB:
ATG12-3
α V5
*
ATG3
ATG7
α myc
ATG12
α ATG12
mock
WTATG3
C264A
K242R
K243R
K243R
K242,243R
B
293T
WB:
ATG12-5
α HA
ATG3
ATG5
ATG7
α myc
ATG12
α ATG12
ATG10
α V5
ATG5-HA +
ATG3-HA (C264A) +
C
atg3 -/-
WB: α HA (ATG12)
ATG12-3
ATG12-5
ATG12
MSCV + + + +
FHA-ATG12 + + + +
BABE
ATG3
K243R
C264A
D
K243
C264
E
293T
WB:
ATG12-3
α HA
ATG3
ATG3
α V5
ATG7
α myc
ATG12
α ATG12
WTATG3-HA +
K243R-HA +
C264A-HA + +
K243R-V5 +

of this single lysine to arginine, complex formation was virtually eliminated. Remarkably, mutating an adjacent lysine at position 242 of ATG3 had no effect on ATG12 conjugation. In contrast, mutating the ATG3 catalytic cysteine to alanine (C264A) potently inhibited formation of the ATG12-ATG3 complex (Figure 5A) [62]. To corroborate these results, we stably complemented ATG3 deficient fibroblasts with epitope-tagged wild type (WT) ATG3, the non-conjugatable ATG3 mutant K243R and the catalytically inactive mutant C264A [74]. Unlike cells reconstituted with WTATG3, ATG12-ATG3 complex formation was not observed in cells co-expressing FHA-ATG12 and either K243R or C264A (Figure 5B).

Since ATG12-ATG3 formation required ATG3 catalytic activity, we hypothesized that an autocatalytic activity of ATG3 served as the E2 enzyme for this conjugation. Several E2 enzymes undergo self-ubiquitination [114-116]. Typically, these are cis-acting intramolecular reactions, in which the target lysine of the E2 enzyme lies in close proximity to the active site cysteine; upon inspection of its tertiary structure, this also appeared to be the case for ATG3 (Figure 5C) [112]. To test whether ATG12 conjugation to ATG3 could occur in trans, we co-expressed two differentially tagged versions of ATG3, along with ATG12 and ATG7, in 293T cells. This first was catalytically inactive ATG3 (C264A) possessing the target lysine, while the second was catalytically active ATG3 that lacked the target lysine (K243R). In contrast to WTATG3, no ATG12-ATG3 complex was formed upon co-expressing these two mutant forms of ATG3, supporting that ATG12 conjugation to ATG3 was a cis-acting reaction

(Figure 5D). Finally, we assessed if ATG10, the E2 enzyme responsible for ATG12 conjugation to ATG5, contributed to the formation of ATG12-ATG3. However, ATG10 was unable to mediate ATG12-ATG3 complex formation, and the expression of catalytically inactive ATG10 (C165A) was unable to dominantly inhibit the auto-conjugation of ATG12 onto ATG3 (Figure 5E and Figure 4C). Overall, these results indicate that ATG3 auto-catalyzes the conjugation of ATG12 onto a single conserved lysine residue (K243) of this E2-like enzyme required for autophagy.

Discussion:

Since the initial discovery of the ATG12 ubiquitin-like conjugation system, ATG5 remains the only known target of ATG12[97, 98]. Here, we provide evidence that multiple ATG12 substrates exist and identify ATG3, the E2-like enzyme that mediates ATG8/LC3 lipidation during autophagy, as a novel target for ATG12 conjugation[62]. Though ATG12 and ATG3 have been previously reported to physically interact, to our knowledge, we provide the first evidence for a covalent complex between these two essential components of the autophagy conjugation machinery. Similar to ATG12-ATG5, formation of the ATG12-ATG3 complex requires activation of ATG12 by the E1-like enzyme, ATG7. In contrast to ATG12-ATG5 formation, the E2-like protein ATG10 is not necessary for ATG12-ATG3 formation. Instead, ATG3 auto-catalyzes the conjugation of ATG12 onto lysine residue 243. Based on immunoprecipitation studies, only a subset of the

total pool of ATG3 (less than 50%) is in complex with ATG12. Furthermore, both free ATG3 and the ATG12-ATG3 complex are concomitantly present in mammalian cells. This also differs from ATG5, which appears to be completely conjugated to ATG12.

Among the ATG proteins responsible for early autophagosome formation in yeast and mammalian cells, ATG12 interacts with the broadest array of cellular proteins. As a result we expected that some of these proteins might be conjugates of ATG12 in addition to being interacting partners. The identification of ATG3 as a covalent conjugate of ATG12 affirmed this hypothesis, since the two proteins were previously known to physically interact. Since ATG7 is the only known E1-like enzyme required for autophagy, it is logical that it also mediates ATG12-ATG3 complex formation. Moreover, ATG7 is thus uniquely poised to act as a switch between its UBL substrates, ATG12 and LC3, and its E2-like conjugating enzymes, ATG10 and ATG3, as most E1 enzymes help to specify the trans-thiolation of their substrates. Measuring the affinity of ATG7 for each of these targets in addition to mapping binding domains between ATG7 and its interacting partners could shed light on how the specification process occurs. Manipulation of this molecular switch could also prove useful therapeutically to tip the cellular balance towards the activity of one UBL complex instead of the other.

Several studies have characterized instances of ubiquitin E2 enzymes autocatalyzing their own degradation on a lysine in close proximity to the catalytic cysteine. Gwozd and colleagues initially described this phenomenon in Baker's yeast for the stress-related ubiquitin E2, UBC4 [115]. However, unlike ATG3,

UBC4 mediates autoconjugation on two internal lysines in an intermolecular reaction *in trans*; furthermore, mutation of the targeted lysines lacks an obvious biological phenotype. Subsequently, Walter and colleagues made the observation that the E2 protein, UBC6p, is short lived and that this property depends on its catalytic site and its c-terminal region [114]. Ultimately, they demonstrate that UBC6p mediates its own degradation through auto-ubiquitination of the protein *in cis*. Finally, UBET2, an E2 for the Fanconi anemia pathway, is monoubiquitinated at a conserved lysine adjacent to its catalytic cysteine [116]. Though it is unclear whether this modification occurs *in cis* or *in trans*, monoubiquitination at this residue abrogates the E2's catalytic activity. The authors speculate that this could be a means of negative regulation of UBET2, if for example it cannot access its E3. Ultimately, these three papers are important precedents for autocatalysis of UBL modification by E2 enzymes both *in cis* and *in trans*.

Interestingly, the catalytically inactive mutant of ATG3 (C264A) also abrogates formation of the ATG12-ATG3 complex. Moreover the combination of the catalytically inactive mutant with the conjugation incompetent mutant (K243R) does not restore complex formation. Therefore it appears that one molecule of ATG3 passes an activated-ATG12 internally from catalytic cysteine to target lysine. The proximity of K243 in ATG3 to its catalytic cysteine may mean that modification by ATG12 at this residue blocks the catalytic function of the protein. We went on to interrogate this hypothesis by characterizing the biological function of the ATG12-ATG3 complex in Chapter III. In summary, in this chapter

we illustrate that ATG12 is a broader-based UBL than previously appreciated and that it can modify ATG3 in a process requiring ATG7 and an autocatalytic function of ATG3 *in cis*.

Experimental Procedures:

Materials: Dr. Noburu Mizushima (Tokyo Medical and Dental University) generously provided *atg5+/+* and *atg5-/-* MEFs and Dr. Masaaki Komatsu (Juntendo University) generously provided *atg7+/+*, *atg7-/-*, *atg3+/+* and *atg3-/-* MEFs. Fibroblasts and HeLa cells were cultured in DMEM (Invitrogen) supplemented with 10% FBS, penicillin and streptomycin.

Generation of stable pools: For retroviral transduction, VSV-G-pseudo typed retroviruses were generated, and cells were infected and selected as previously described [117]. Following infection and drug selection, early passage stable pools (maximum of 6-8 passages) were utilized for experiments to avoid clonal selection or drift.

Mass spectrometry: Lysates were sequentially immunoprecipitated with α-FLAG M2 affinity gel and monoclonal α-HA conjugated to agarose and eluted with 3X FLAG peptide or HA peptide, respectively (Sigma). The final eluate was separated by SDS-PAGE and visualized with Novex Colloidal Blue Stain Kit (Invitrogen). Bands of interest were in-gel tryptically digested following destain,

and sent for tandem mass spectrometry (MS/MS) using electrospray ionization (ESI) and a quadropole quadropole time-of-flight (QqTOF) mass spectrometer located in the UCSF Mass Spectroscopy Core (QStarXL).

Acknowledgements:

We thank the Fisher Lab Mass-Spectroscopy Core Facility at UCSF for help with the identification of ATG3. We are very grateful to Dr. Nan Chen for help with the cis/trans experiments during the paper revision. We thank Drs. Noboru Mizushima and Masaaki Komatsu for reagents, and Drs. Gerard Evan, Don Ganem, Abul Abbas and Feroz Papa for critically reading the manuscript. Grant support to JD includes the NIH (RO1CA126792, KO8CA098419), a Culpeper Medical Scholar Award (Partnership For Cures), an AACR-Genentech BioOncology Award, a HHMI Physician-Scientist Early Career Award, and a Stewart Family Trust Award. LR was a Genentech/Sandler Graduate Student Fellow and EF was an HHMI Summer Undergraduate Research Fellow.

CHAPTER III:

ATG12 CONJUGATION TO ATG3 REGULATES MITOCHONDRIAL HOMEOSTASIS AND CELL DEATH

Abstract:

We recently identified that ATG12 has a second novel conjugation target, another autophagy regulator called ATG3. The ATG12-ATG5 complex and ATG3 each modulate steps in early autophagosome expansion and closure. The close proximity of the target lysine on ATG3 to its catalytic cysteine suggests that while ATG12 is bound to ATG3, the catalytic function of ATG3 may be sterically inhibited. Therefore we initially hypothesized that the ATG12-ATG3 complex could negatively regulate early autophagosome formation. We complemented *atg3*-deficient cells with either wild type ATG3 or a lysine to arginine mutant of ATG3 that is conjugation incompetent. We then compared whether the cells expressing the mutant protein could induce and/or undergo autophagy as well as their wild type counterparts. Surprisingly, disrupting ATG12 conjugation to ATG3 does not affect starvation-induced autophagy. Rather, the lack of ATG12-ATG3 complex formation produces an expansion in mitochondrial mass with reduced mitochondrial degradation in response to chemical uncoupling and impaired targeting of mitochondria to autophagosomes. Finally, conjugation incompetent cells display resistance to cell death mediated by the intrinsic apoptotic pathway, which correlates with increased levels of the anti-apoptotic protein, Bcl-X_L.

Introduction:

Impaired autophagy has a plethora of cellular consequences, for which a subset can be compensated by other stress responses. For example, long-lived protein degradation that normally occurs through autophagy can be complemented by increased proteasomal degradation[118, 119]. In addition to being a cellular starvation response, autophagy is also the only means of degradation of bulk cargo in the cell. Therefore, organelle degradation and protein aggregate clearance, which exceeds the maximum volume of the proteasome, primarily occurs through autophagy. As a result, basal or homeostatic autophagy plays an essential role in cellular survival. Blocking autophagy results in an accumulation of damaged mitochondria and protein aggregates, for which there is no known compensatory pathway. Since the greatest quantifiable amount of cellular damage from autophagy deficiency appears to emanate from damaged mitochondria (which contribute to ROS accumulation and DNA damage[84]) a considerable effort has been made to explore the crosstalk between autophagy and mitochondria and to understand how specific mitochondrial degradation (mitophagy) works.

Mitochondria trapped in lysosomes were initially observed in early electron micrographs of rat hepatocytes, which had been supplemented with glucagon to increase cellular catabolism[120]. More recent work in yeast and reticulocytes (red blood cell precursor) suggest that under specific environmental or developmental conditions, cells can upregulate a program to clear most or all of their

mitochondria through mitophagy. Like most examples of specific autophagy, linker molecules are required to identify the damaged or surplus organelle and bring it to the expanding autophagosome. In yeast, ATG32 fulfills this role in concert with ATG11. ATG32 is an outer mitochondrial membrane protein with a WXXL domain that interacts with ATG8; it can also bind ATG11. If yeast switch from a carbon source that requires oxidative phosphorylation (like glycerol) to glucose or nitrogen deprivation, ATG32 targets surplus mitochondria for degradation in the vacuole to cull the unnecessary mitochondria or to complement the energy requirement of the cell. However, ATG32 does not seem to differentiate between damaged and healthy mitochondria during this process[121-123]. Similarly during reticulocyte maturation, NIX also known as BNIP3L, becomes upregulated through a developmental program that removes healthy mitochondria. NIX is also a mitochondrial outer membrane protein which has a WXXL motif that can bind to LC3[124-126]. Finally in most cells, damaged mitochondria are identified and targeted for mitophagy. This pathway requires PINK1 and Parkin, a kinase and a ubiquitin E3 ligase, respectively. In an unknown mechanism, depolarized mitochondria stabilize PINK1, which is otherwise rapidly degraded, this process leads to Parkin relocalization to the mitochondria, which subsequently ubiquitinates outer mitochondrial proteins such as VDAC1 and the mitofusins[127-129]. Many surface proteins are ubiquitinated with both K63 and K48 linkages, leading to their rapid proteasomal degradation[130, 131]. The ubiquitin signal also attracts the linker molecule p62, which clusters mitochondria and may potentially (conflicting reports exist) mediate engulfment of

the damaged mitochondrion by the canonical autophagy machinery[132, 133]. To date most studies of mitophagy have investigated and characterized specific linker proteins between the mitochondria and the autophagosome, however an as yet unexplored possibility is that the mediators of early autophagosome expansion could play a more proximal role in mitophagy as well.

Based on both proteins' well-characterized role in early autophagosome formation, we hypothesized that ATG12 modification of ATG3 would somehow alter ATG3 enzymatic function, the most obvious potential consequence being a sterically repressive effect on lipidation of ATG8/LC3 orthologues. On the other hand, since ATG3 is responsible for the final modification of PE by LC3, the enzyme could instead be uniquely positioned to mediate the extensive autophagosome expansion required for larger cargo, like mitochondria. As such, we also endeavored to test whether ATG12 conjugation to ATG3 had an effect on selective autophagy of organelles. Contrary to our initial hypothesis, disrupting ATG12-ATG3 complex formation has no discernable effect on nonselective autophagy. Instead, upon disrupting ATG12 conjugation to ATG3, cells display increased mitochondrial mass, decreased targeting of mitochondria to autophagosomes after chemical uncoupling and enhanced survival in response to agents that activate mitochondrial cell death pathways. Overall, these results demonstrate a newly discovered role for the ATG12-ATG3 complex in mitochondrial homeostasis and cell death. We propose that the ATG12-ATG3 complex alters cellular functions distinct from the early steps of autophagosome

formation and demonstrate that essential autophagy proteins may directly modulate mitophagy.

Results:

Starvation-induced autophagy remains intact upon disrupting ATG12 conjugation to ATG3. We next tested if ATG12-ATG3 modulates known ATG3 biological activities, namely PE-lipidation of ATG8/LC3 and autophagosome formation [74, 116]. For these experiments, we reconstituted *atg3-/-* fibroblasts with a control empty vector (BABE), wild type ATG3 (WTATG3), or the K243R mutant (KR) that was incapable of ATG12-ATG3 complex formation. In response to nutrient starvation using Hank's buffered saline (HBSS) or rapamycin-mediated mTORC1 inactivation, we found equivalent levels of LC3 lipidation (LC3-II) between WT and KR and efficient LC3-II turnover in the lysosome (Figure 1A-B). We also observed no significant differences in the number or morphology of GFP-LC3 puncta, a widely utilized marker for autophagosome formation, upon HBSS starvation, although we did note an increase in punctate GFP-LC3 in KR cells cultured in nutrient rich conditions (Figure 1C-D and Figure 2B) [109]. Furthermore, WTATG3 and KR cells exhibited no differences in the lipidation of other mammalian ATG8 orthologues, including GABARAP and GATE-16 (Figure 2C). To extend these results, we evaluated the accumulation of p62SQSTM, an ubiquitin-binding scaffold protein selectively degraded by autophagy, via immunofluorescence [134]. In both nutrient-rich and starvation conditions, p62

cytoplasmic bodies amassed in autophagy-deficient cells lacking ATG3; this accumulation was profoundly decreased in cells rescued with either WTATG3 or the KR mutant (Figure 1E). Finally, we assessed the processing of an ectopically-expressed autophagy cargo protein betaine homocysteine methyltransferase (BHMT) [135]. Efficient proteolytic cleavage of BHMT during HBSS starvation required both ATG3 and lysosomal function; this autophagy dependent cleavage was restored at equivalent levels upon rescue with either WTATG3 or KR (Figure 1F). Overall, these data support that disrupting ATG12 conjugation to ATG3 does not impair ATG8/LC3 lipidation, autophagosome formation or autophagic proteolysis in response to nutrient starvation**.**

Cells expressing non-conjugatable ATG3 (KR) exhibit increased mitochondrial mass and a fragmented mitochondrial morphology. Recent studies support that autophagy is required to maintain mitochondrial homeostasis [136, 137]. Flow cytometric analysis for Mitotracker® Green (MTG), a mitochondrial specific intravital dye, demonstrated that cells reconstituted with WTATG3 exhibit an approximately 15% reduction in total mitochondrial mass compared to *atg3-/-* (BABE) controls; similarly, *atg3+/+* possessed reduced MTG staining compared to *atg3-/-* cells. In contrast, the mitochondrial mass of cells reconstituted with KR was unchanged relative to *atg3-/-* (BABE) cells (Figure 3A). Protein levels of the mitochondrial inner membrane protein, cytochrome *c* oxidase subunit IV (COX IV) corroborated these differences in MTG staining (Figure 3B).

Figure 1: Starvation-induced autophagy remains intact upon disrupting ATG12 conjugation to ATG3. Stable pools of *atg3-/-* fibroblasts expressing an empty vector (BABE), wild type mouse ATG3 (WTATG3) or mutant ATG3 unable to be conjugated by ATG12 (KR) were used for experiments as indicated.
(A and B) Cells were grown in complete media, starved in Hank's buffered salt solution (HBSS) for 4h, or treated with 10nM rapamycin (B) for 6h. Cells were lysed and immunoblotted with indicated antibodies. Phosphorylated ribosomal S6 (P-S6) was used to verify rapamycin-mediated mTORC1 inhibition. When indicated, bafilomycin A (BafA, 10nM) was added to cells 1h prior to lysis.
(C) Indicated cells types expressing GFP-LC3 were grown in complete media (control) or HBSS-starved for 4h; boxed areas from center panels are enlarged in the bottom panels. Bars, 25μm.
(D) Quantification of punctate GFP-LC3 or GFP-LC3ΔG (mean +/-SEM puncta per cell).
(E) Indicated cell types grown in complete media (control) or HBSS-starved for 4h, and then fixed and immunostained with α-p62 antibody. Bar, 25μm.
(F) Indicated cell types were transfected with a GST-BHMT fusion construct, HBSS-starved for 6h, lysed and immunoblotted with α-GST. Asterisk (*) indicates full-length GST-BHMT protein and arrow indicates the cleaved BHMT produced in autolysosomes. When indicated, bafilomycin A (BafA, 10nM) was used to inhibit lysosomal function. α-myc was used to detect GFP-myc (expressed from an IRES sequence) to control for transfection efficiency [135].

Figure 1

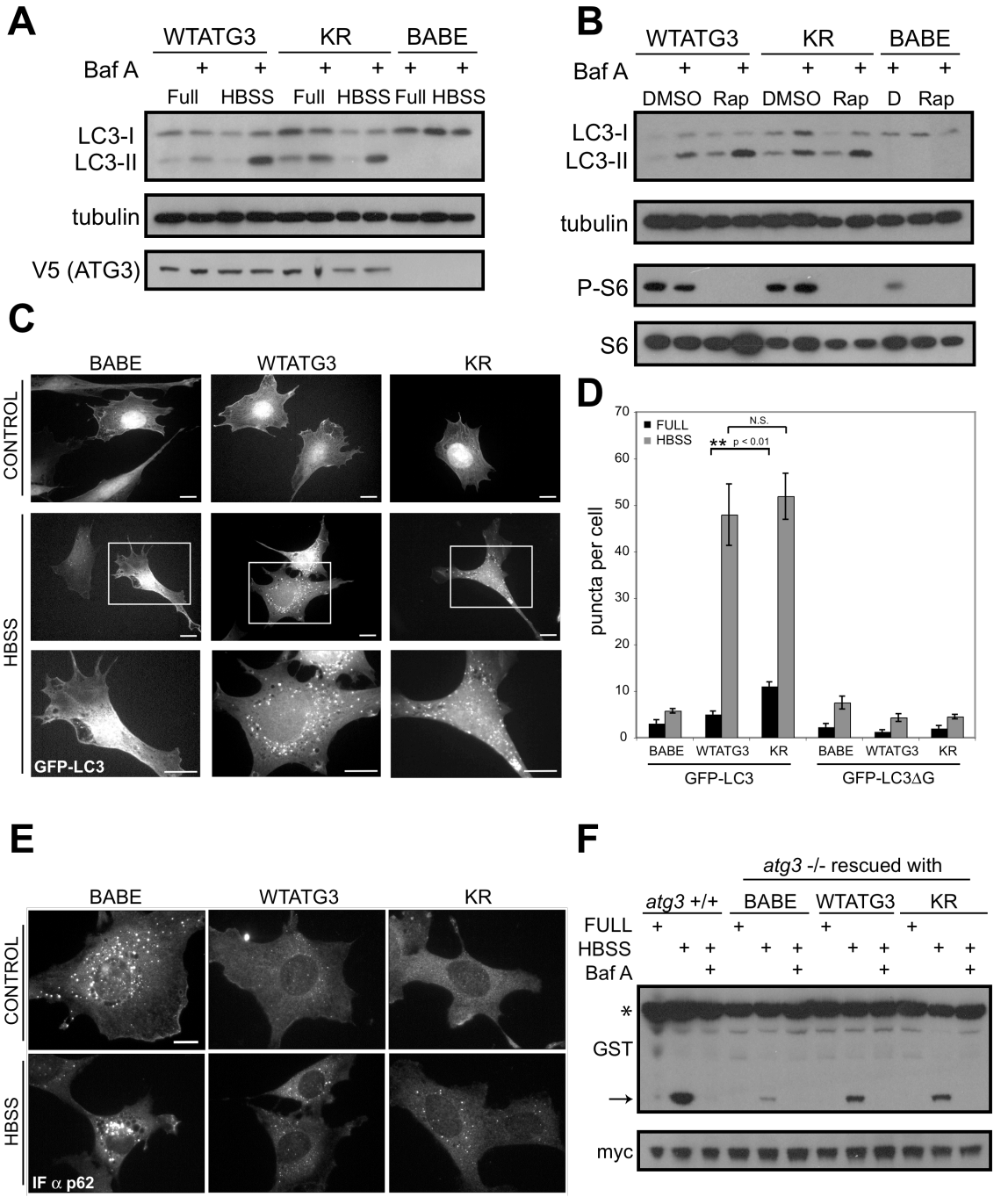
A
WTATG3
KR
BABE
Baf A
Full
HBSS
LC3-I
LC3-II
tubulin
V5 (ATG3)
B
DMSO
Rap
D
P-S6
S6
C
CONTROL
HBSS
GFP-LC3
D
FULL
HBSS
N.S.
** p < 0.01
puncta per cell
GFP-LC3
GFP-LC3ΔG
E
IF α p62
F
atg3 -/- rescued with
atg3 +/+
FULL
GST
myc

Figure 2: Effects of WTATG3 and KR on Lipidation of the mammalian ATG8 orthologues, GABARAP and GATE-16

(A) Comparison of relative levels of ATG3 protein in atg3+/+ MEFs, and atg3 −/− MEFs complemented with WTATG3 or the KR mutant.

(B) Cells were grown in complete media, starved in Hank's buffered salt solution (HBSS) for 4 hr and when indicated, bafilomycin A (BafA, 10 nM) was added to cells 1h prior to lysis.

(C) Indicated cells were starved as above in HBSS for 4 hr and subsequently fixed and stained with α-V5.

Figure 2

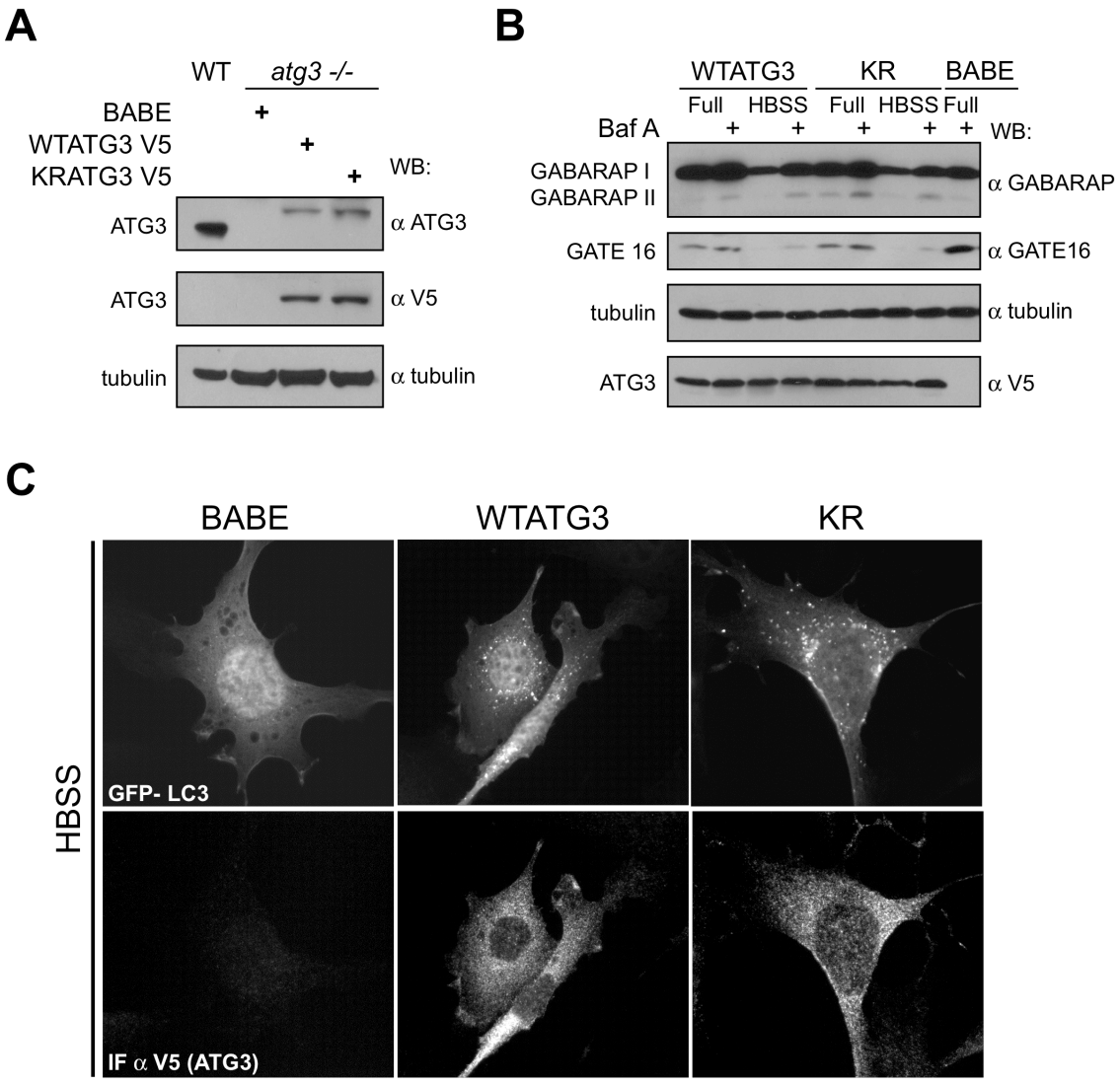
A
WT
atg3 -/-
BABE
WTATG3 V5
KRATG3 V5
WB:
ATG3
α ATG3
ATG3
α V5
tubulin
α tubulin
B
WTATG3
KR
BABE
Full
HBSS
Full
HBSS
Full
Baf A
WB:
GABARAP I
GABARAP II
α GABARAP
GATE 16
α GATE16
tubulin
α tubulin
ATG3
α V5
C
BABE
WTATG3
KR
HBSS
GFP- LC3
IF α V5 (ATG3)

Figure 3: Mitochondrial mass and morphology in cells expressing a non-conjugatable ATG3 mutant (KR).

(A) Left: Mitotracker Green (MTG) fluorescence intensity (mean+/-SEM from 5 independent experiments) for the indicated cell types relative to *atg3-/-* cells expressing empty vector (BABE). Statistical significance calculated using ANOVA, followed by Tukey's HSD test. Right: MTG fluorescence intensity (mean+/-SEM from 3 experiments) for *atg3+/+* cells relative to *atg3-/-* cells.

(B) Lysates from indicated cell types were immunoblotted with α-COX IV, α-tubulin and α-V5.

(C) Indicated cell types were immunostained with TOM20 (top and middle) or cytochrome c (bottom) antibodies.

(D) Percent of cells with purely fragmented/round morphology or purely tubular morphology was quantified in the indicated cell types from TOM20-immunostained images. Results are the mean +/-SEM from 5 independent experiments, where at least 250 cells were scored per condition for each individual experiment. Statistical significance calculated using ANOVA, followed by Tukey's HSD test.

(E) Differentially labeled cells expressing either mitochondria-targeted dsRed (mt-dsRed, red) or CFP (mt-CFP, green) were combined in a PEG fusion assay to assess mitochondrial fusion activity. Representative merged images of cell hybrids from each cell type are shown; the colocalization of these signals (yellow) within cell hybrids indicates mitochondrial fusion [138]. Each bottom panel is an enlargement of the boxed inset in the corresponding panel above. Bar, 25μm.

Figure 3

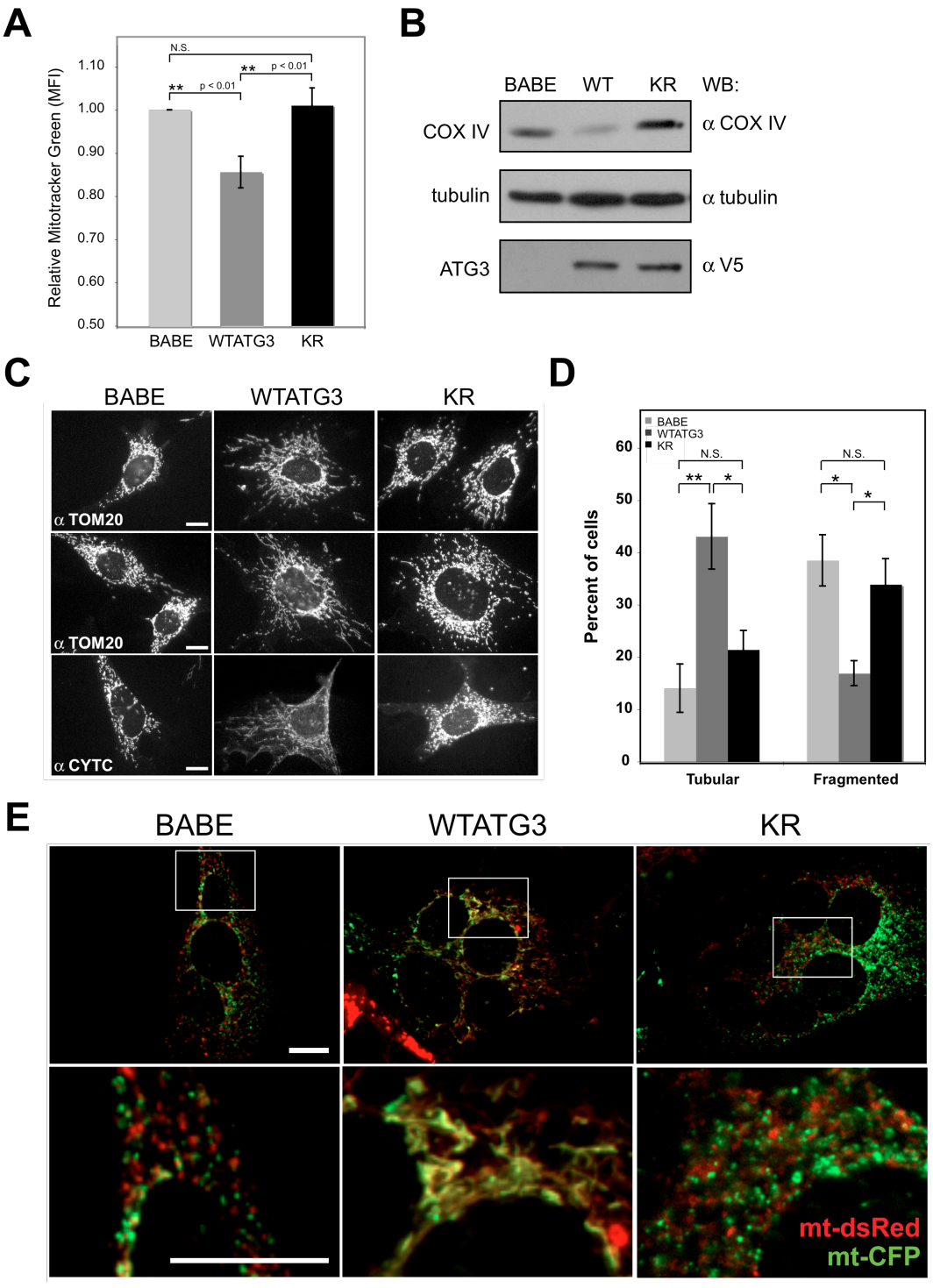
A
Relative Mitotracker Green (MFI)
1.10
1.00
0.90
0.80
0.70
0.60
0.50
N.S.
**
p < 0.01
**
p < 0.01
BABE
WTATG3
KR
B
BABE
WT
KR
WB:
COX IV
α COX IV
tubulin
α tubulin
ATG3
α V5
C
BABE
WTATG3
KR
α TOM20
α TOM20
α CYTC
D
BABE
WTATG3
KR
Percent of cells
60
50
40
30
20
10
0
N.S.
**
*
N.S.
*
*
Tubular
Fragmented
E
BABE
WTATG3
KR
mt-dsRed
mt-CFP

We next evaluated mitochondrial morphology in the various cell types by immunostaining for TOM20, a mitochondrial import receptor located in the outer membrane, and cytochrome c, located in the inner membrane. In both ATG3 null (BABE) and KR cultures, numerous cells possessed fragmented and round mitochondria, whereas in WTATG3 cells, the mitochondria predominantly formed tubular networks (Figure 3C). Because the mitochondria in individual cells in these cultures exhibited a range of morphologies (Figure 4A), we enumerated cells from each condition that showed purely fragmented/round versus purely tubular mitochondrial morphology. We confirmed a significant increase in cells possessing fragmented mitochondria in ATG3 null and KR cells compared to WTATG3 cells, as well as a corresponding decrease in cells with purely tubular mitochondria (Figure 3D). In contrast, we observed no obvious morphological differences in other organelles, such as the endoplasmic reticulum, peroxisomes, or Golgi apparatus (Figure 4B).

Fragmentation can arise as an early consequence of declining mitochondrial function or cell viability [139]. Hence, to determine whether the excess mitochondria in KR cells were depolarized, we co-stained cells with Mitotracker® Red (MTR), whose accumulation in mitochondria depends on intact membrane potential, and MTG, which labels the lipid membranes of all mitochondria [140]. A small population of depolarized mitochondria (MTR negative, MTG positive) was present in ATG3 null cells, which was not significantly reduced upon rescue with either WTATG3 or KR (Figure 4C). We also performed growth curves for the three cell types and found no overt differences in

Figure 4: Morphology of mitochondria and other organelles in ATG3 null (BABE). WTATG3, and KR cells.

(A) Range of mitochondrial morphologies observed in *atg3-/-* (BABE), WTATG3, and KR cells. Right graph delineates the percent of each cell type that exhibits a purely fragmented/round (yellow), purely tubular (red), or a mixed (blue) mitochondrial morphology. Results are the mean +/-SEM from 5 experiments, where at least 250 cells stained with TOM20 were scored per condition in each individual experiment. Note that these results (percent fragmented and percent tubular) are also reported in Figure 3D.

(B) Organelle morphology in ATG3 null (BABE), WTATG3, and KR cells. Indicated cells types were immunostained with α-calreticulin to detect endoplasmic reticulum, α-catalase to detect peroxisomes, and α-GM130 to detect the Golgi apparatus.

(C) Mitotracker Red (MTR) versus Mitotracker Green (MTG) flow cytometry profiles of the indicated cell types; the gate indicates the percentage of cells with depolarized mitochondria (mean +/-SEM).

(D) Proliferation curves (mean cell number +/-SEM) of cells grown in full media.

Figure 4

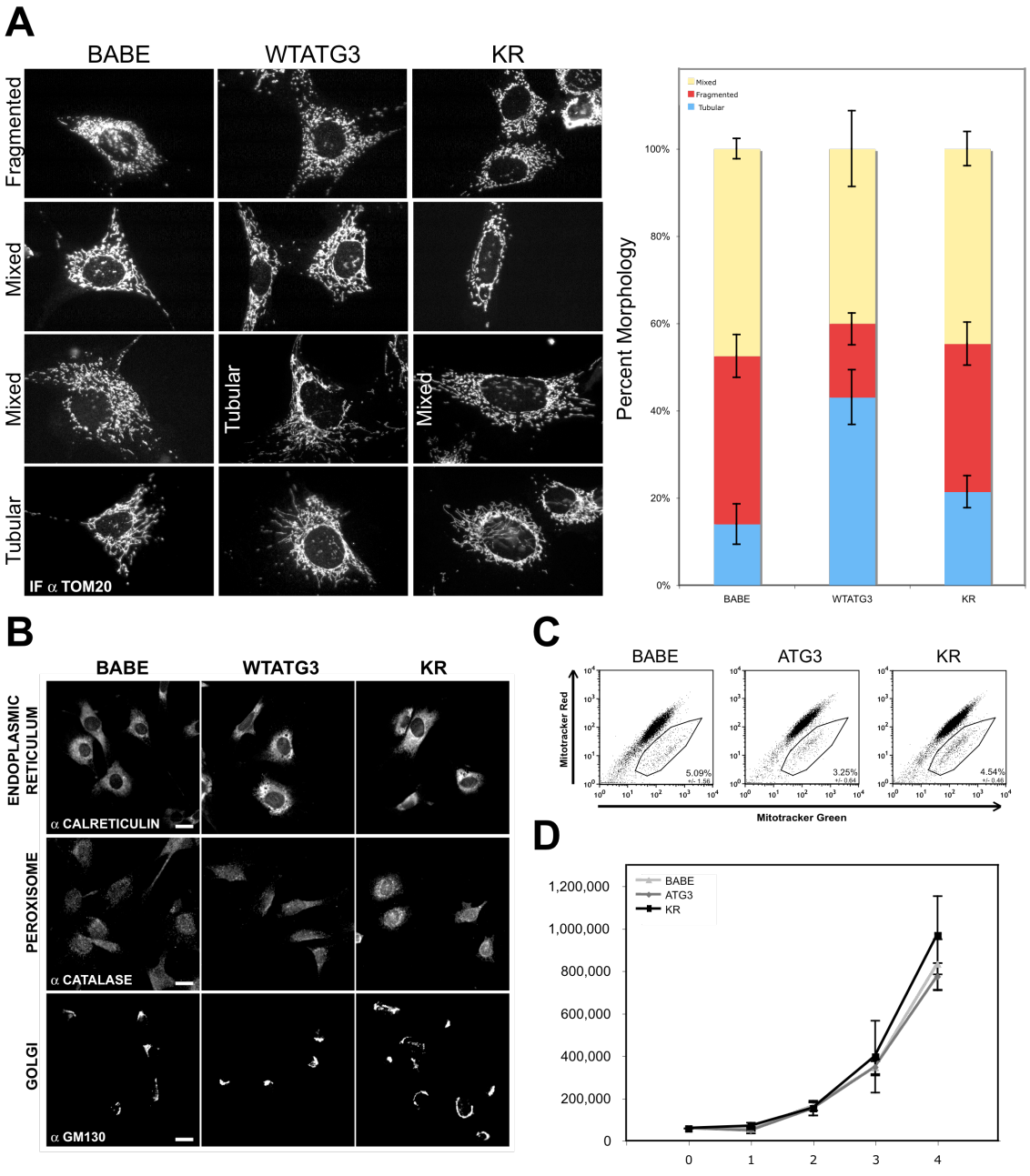
A
BABE
WTATG3
KR
Fragmented
Mixed
Mixed
Tubular
Tubular
Mixed
IF α TOM20
Mixed
Fragmented
Tubular
Percent Morphology
100%
80%
60%
40%
20%
0%
BABE
WTATG3
KR
B
BABE
WTATG3
KR
ENDOPLASMIC RETICULUM
α CALRETICULIN
PEROXISOME
α CATALASE
GOLGI
α GM130
C
BABE
ATG3
KR
Mitotracker Red
Mitotracker Green
5.09%
3.25%
4.54%
D
BABE
ATG3
KR
1,200,000
1,000,000
800,000
600,000
400,000
200,000
0
0
1
2
3
4

proliferation or viability (Figure 4D).

Alternatively, defects in mitochondrial fusion also promote fragmentation [136]. Accordingly, we evaluated mitochondrial fusion activity more directly using a polyethylene glycol (PEG) fusion assay [138]. For these assays, either mitochondria-targeted red (mt-dsRed) or cyan (mt-CFP) fluorescent proteins were ectopically expressed in each cell type; subsequently, hybrids between the differentially labeled populations were scored for mitochondrial fusion. While we observed robust mitochondrial fusion among hybrids derived from WTATG3 cells, such events were reduced in both ATG3 null and KR-expressing hybrids, indicating decreased fusion activity (Figure 3E and Figure 5A-B). Altogether, these results support that disrupting ATG12 conjugation to ATG3 produces a significant increase in mitochondrial mass and fragmentation, which correlates with a reduction in mitochondrial fusion activity. Most importantly, these phenotypes arise in cells capable of robust autophagy, indicating that the effects of the ATG12-ATG3 complex on mitochondria are separable from the well-established functions of ATG3 in ATG8/LC3 lipidation and autophagosome formation.

Effects of chemical uncoupling on mitochondria in cells expressing non-conjugatable ATG3 (KR). We next sought to clarify how the ATG12-ATG3 complex regulates mitochondrial homeostasis by stressing cells with carbonyl cyanide m-chlorophenylhydrazone (CCCP), a proton ionophore that uncouples

Figure 5: Quantification of mitochondrial fusion in polyethylene glycol (PEG) cell hybrids.

(A) Differentially labeled cells expressing either mitochondria-targeted dsRed (mt-dsRed, red) or CFP (mt-CFP, green) were combined in a PEG fusion assay to quantify fusion activity. For each cell type, 60-80 individual PEG cell hybrids from 5 independent fusion experiments were assessed for full, partial or no fusion, as illustrated in (B).

(B) Representative merged images of cell hybrids showing full, partial or no fusion of mitochondria. Each bottom panel is an enlargement of the boxed inset in the corresponding panel above. Bar, 25 μm.

Figure 5

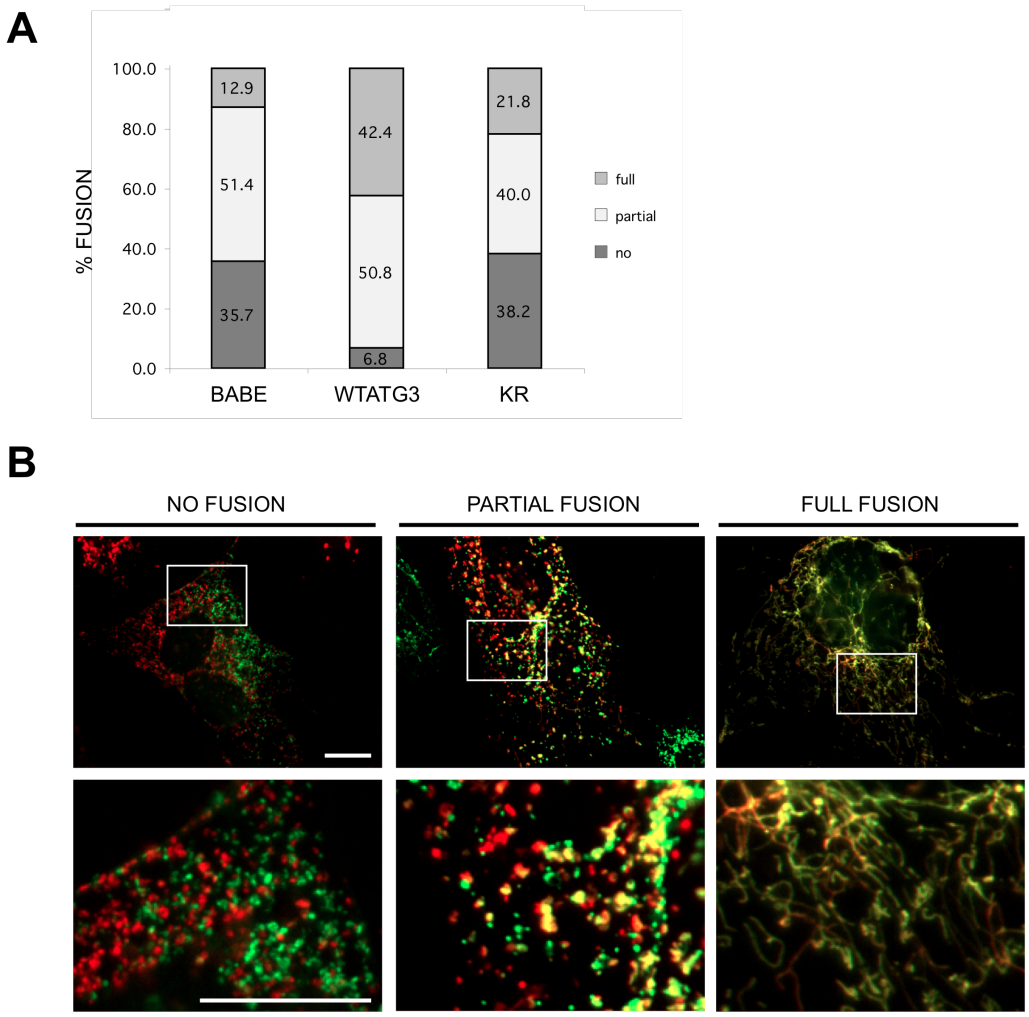
A
100.0
80.0
60.0
40.0
20.0
0.0
% FUSION
12.9
51.4
35.7
42.4
50.8
6.8
21.8
40.0
38.2
full
partial
no
BABE
WTATG3
KR
B
NO FUSION
PARTIAL FUSION
FULL FUSION

mitochondria. CCCP-induced depolarization elicits a multifaceted cellular response that includes an overall increase in mitochondrial biogenesis coupled to the autophagic degradation of damaged mitochondria, termed mitophagy. [127, 137, 141]. Indeed, CCCP treatment resulted in increased MTG intensity compared to DMSO-treated controls in all cell types, corroborating that overall mitochondrial mass increased during chemical uncoupling [141]. Notably, this CCCP-induced increase in MTG staining intensity was more pronounced in both ATG3 null (BABE, 27% increase) and KR cells (25% increase) in comparison to WTATG3 cells (14% increase) (Figure 6A). When directly compared to *atg3-/-* (BABE) cells, CCCP-treated WTATG3 cells displayed 20% lower MTG staining intensity; similar differences were observed between *atg3+/+* and *atg3-/-* cells. In contrast, KR cells possessed a 15% and 35% increase in mitochondria compared to BABE and WTATG3 cells, respectively (Figure 7A). TOM20 immunostaining of CCCP-treated cultures also supported that mitochondria were more abundant in ATG3 null and KR cells compared to WTATG3 cultures (Figure 6B). These results indicate that ATG12 conjugation to ATG3 restricts the expansion of mitochondrial mass during CCCP-induced depolarization.

We next assessed the protein levels of two mitochondrial resident proteins, COX IV and TOM40 and found that, compared to WTATG3, KR cells had higher levels of both proteins in control as well as CCCP-treated cultures. Interestingly, in WTATG3 cells, both proteins were slightly reduced during CCCP treatment, whereas in KR cells, these levels remained unchanged, suggesting

Figure 6: Effects of CCCP treatment on mitochondrial mass and autophagosome formation.

(A) Mean Fluorescence Intensity of Mitotracker Green staining in BABE, WTATG3 and KR cells with DMSO (carrier control) or 10μM CCCP treatment for 24h.

(B) Cells treated with 10 μM CCCP for 24h were immunostained with TOM20 to detect mitochondria. Bar, 25μm.

(C) Representative images of the indicated cell types expressing GFP-LC3 following 24h treatment with 10 μM CCCP. Bar, 20μm.

(D) Quantification of punctate GFP-LC3 (mean +/-SEM puncta per cell enumerated from at least 60 cells per cell type) following 24h CCCP treatment.

Figure 6

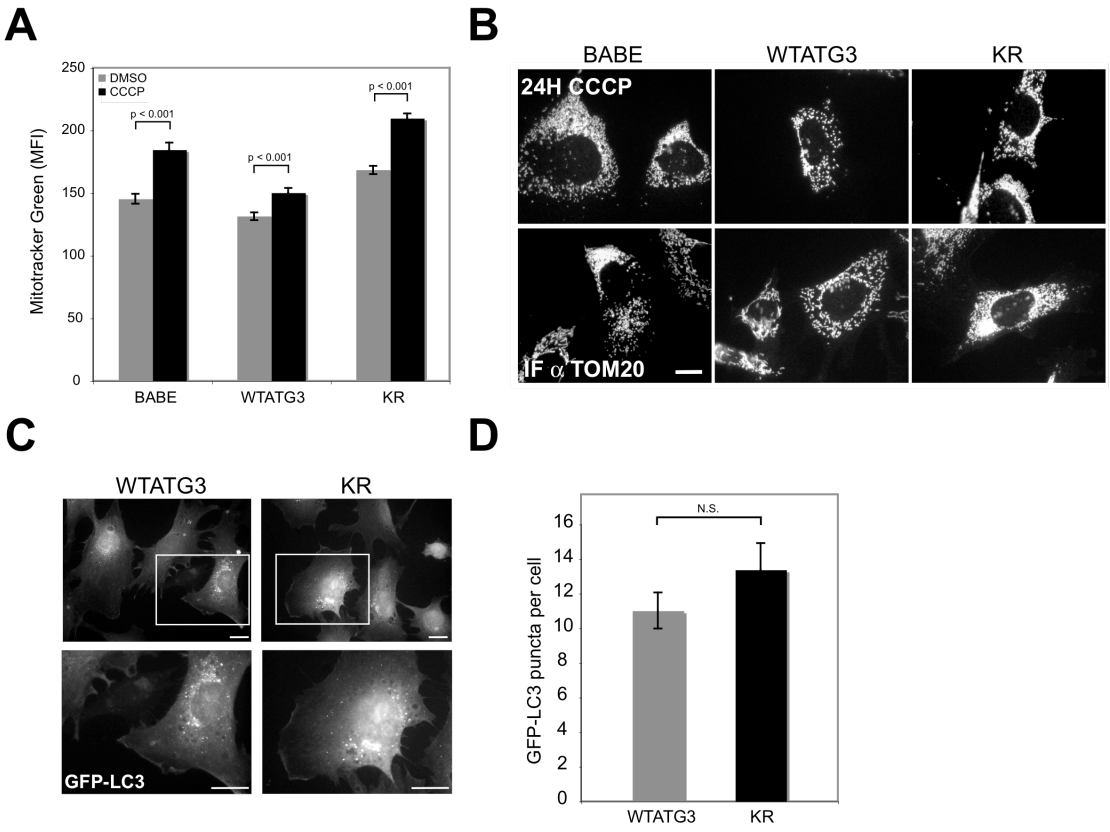
A
B
C
D
DMSO
CCCP
Mitotracker Green (MFI)
250
200
150
100
50
0
p < 0.001
p < 0.001
p < 0.001
BABE
WTATG3
KR
BABE
WTATG3
KR
24H CCCP
IF α TOM20
WTATG3
KR
GFP-LC3
GFP-LC3 puncta per cell
16
14
12
10
8
6
4
2
0
N.S.
WTATG3
KR

that the rate of mitochondrial degradation may be reduced in cells lacking the ATG12-ATG3 complex (Figure 7B). As a result, we sought to more closely analyze if KR cells exhibited decreased mitophagy. We first compared the rates of CCCP-induced autophagosome induction in WTATG3 and KR cells, but found no significant differences in punctate GFP-LC3 between these cells following CCCP treatment (Figure 6C-D). To measure mitochondrial targeting to autophagosomes during CCCP treatment, we assessed the level of colocalization between mito-dsRed and GFP-LC3 (Figure 7C). Importantly, the number of colocalizations was significantly higher in WTATG3 cells compared to KR cells (Figure 7C and D). Hence, upon loss of ATG12 conjugation to ATG3, mitochondrial targeting to autophagosomes is reduced.

To further assess if mitophagy was impaired in KR cells, we tested if 3-methyladenine (3MA), a pharmacological autophagy inhibitor, was able to augment mitochondrial mass during CCCP-treatment [142]. In WTATG3 cells, we observed a 27.5 % increase in mitochondrial mass upon treatment with CCCP+3MA compared to CCCP alone, which we attributed to 3MA-sensitive mitochondrial degradation. To control for the non-specific effects of 3MA, which can promote significant protein degradation in an autophagy-independent manner [25], we tested the effects of 3MA on *atg3-/-* (BABE) cells; 3MA-sensitive mitochondrial degradation in these autophagy-incompetent cells was reduced to 20% (Figure 7E). Similar to *atg3-/-* (BABE) cells, 3MA-sensitive mitochondrial degradation in KR cells was decreased to 22%. Overall, these results support that ATG12 conjugation to ATG3 facilitates mitochondrial degradation in the

Figure 7: Effects of CCCP treatment on mitochondria in cells expressing a non-conjugatable ATG3 mutant (KR).

(A) Left: Cells were treated with 10 μM CCCP for 24h and stained with MTG. MTG fluorescence intensity (mean+/-SEM from 8 experiments) relative to *atg3-/-* cells expressing empty vector (BABE) is shown. Statistical significance calculated using ANOVA, followed by Tukey's HSD test. Right: MTG fluorescence intensity (mean+/-SEM from 3 experiments) for CCCP-treated *atg3+/+* cells relative to *atg3-/-* cells.

(B) Cells were CCCP-treated as indicated, lysed and immunoblotted with antibodies against the resident mitochondrial proteins, TOM40 and COX IV, and tubulin as a loading control.

(C) Indicated cell types expressing GFP-LC3 were transfected with mito-dsRed and treated with 10μM CCCP for 24h. White arrows indicate colocalization of GFP-LC3 and mito-dsRed. Bar, 5μm

(D) Quantification of mito-dsRed and GFP-LC3 colocalizations per cell (mean +/-SEM).

(E) 3MA-sensitive mitochondrial degradation (mean+/-SEM from 5 independent experiments) during CCCP treatment. Cells were treated for 24h with 10 μM CCCP in the presence or absence of 5mM 3MA and stained with MTG. 3MA sensitive mitochondrial degradation was calculated as described in methods.

Figure 7

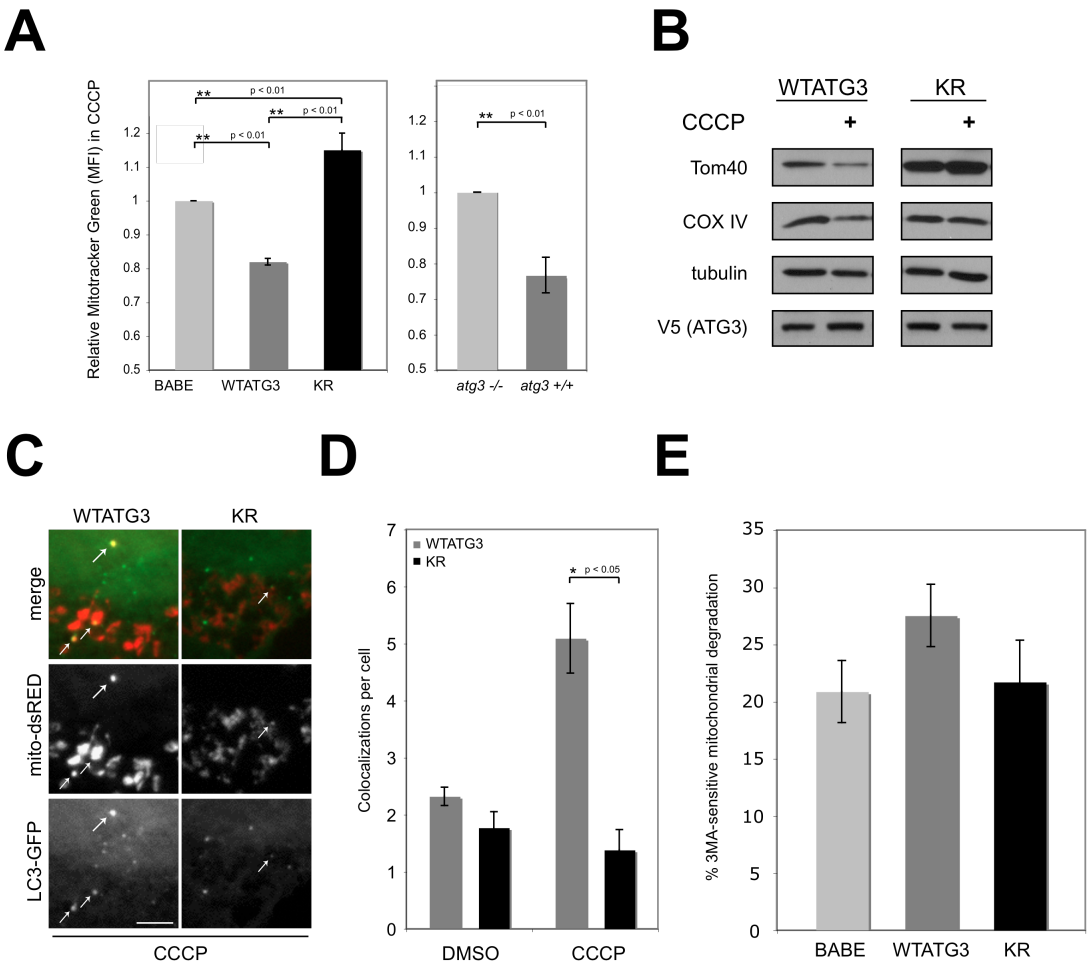
A
Relative Mitotracker Green (MFI) in CCCP
p < 0.01
p < 0.01
p < 0.01
BABE
WTATG3
KR
p < 0.01
atg3 -/-
atg3 +/+
B
WTATG3
KR
CCCP
+
+
Tom40
COX IV
tubulin
V5 (ATG3)
C
WTATG3
KR
merge
mito-dsRED
LC3-GFP
CCCP
D
WTATG3
KR
p < 0.05
Colocalizations per cell
DMSO
CCCP
E
% 3MA-sensitive mitochondrial degradation
BABE
WTATG3
KR

presence of CCCP. Importantly, this function of ATG12-ATG3 is entirely separable from the ability of ATG3 to induce autophagosome formation during mitochondrial depolarization.

Cells lacking ATG12-ATG3 exhibit reduced cell death mediated by mitochondrial pathways. Mitochondria play critical roles in many forms of cell death, including apoptosis mediated by the intrinsic pathway [143]. Accordingly, we determined how the ATG12-ATG3 complex influenced cell death. First, we compared the effects of CCCP on cell death in WTATG3 and KR cells; similar to other mitochondrial uncoupling agents, high doses of CCCP induce death that can be inhibited by anti-apoptotic Bcl-2 family members [144]. In response to CCCP treatment, KR cells exhibited a 2-fold reduction in death compared to WTATG3 controls (Figure 8A). Similarly, cell death was reduced in KR cells treated with staurosporine, a pan-kinase inhibitor that potently activates the intrinsic apoptosis pathway (Figure 8B). We also observed reduced cleavage of the executioner caspase, caspase-3, in KR cells in response to both agents, supporting that apoptosis was reduced compared to WTATG3 (data not shown). In contrast, both cell types exhibited robust and equivalent levels of cell death in response to Tumor Necrosis Factor-a (TNF-α). TNF-α induces apoptosis via the extrinsic pathway, in which death receptors directly activate executioner caspases independently of mitochondrial pathways (Figure 8C) [143]. Thus, ATG12 conjugation to ATG3 sensitizes cells to death downstream of mitochondrial pathways, but has no effect on death-receptor mediated apoptosis.

Figure 8: Cells lacking ATG12-ATG3 exhibit reduced cell death mediated by mitochondrial pathways. Stable pools of *atg3-/-* fibroblasts rescued with WTATG3 or mutant ATG3 unable to be conjugated by ATG12 (KR) were used as indicated. Cells were treated for 24h with the following agents:

(A) 100 μM CCCP;

(B) 100nM staurosporine; and

(C) 20ng/mL TNF-α + 2.5mg/mL cycloheximide. Percent cell death (mean+/-SEM) was assayed by propidium iodide uptake using flow cytometry.

(D) Cell lysates prepared from WTATG3 and KR cells were immunoblotted for the indicated markers.

(E) Cells were treated for 24h with 500 nM obatoclax. Cell death (mean +/-SEM) was quantified using trypan blue exclusion. Statistical significance was calculated using t test.

(F) Summary model of results.

Figure 8

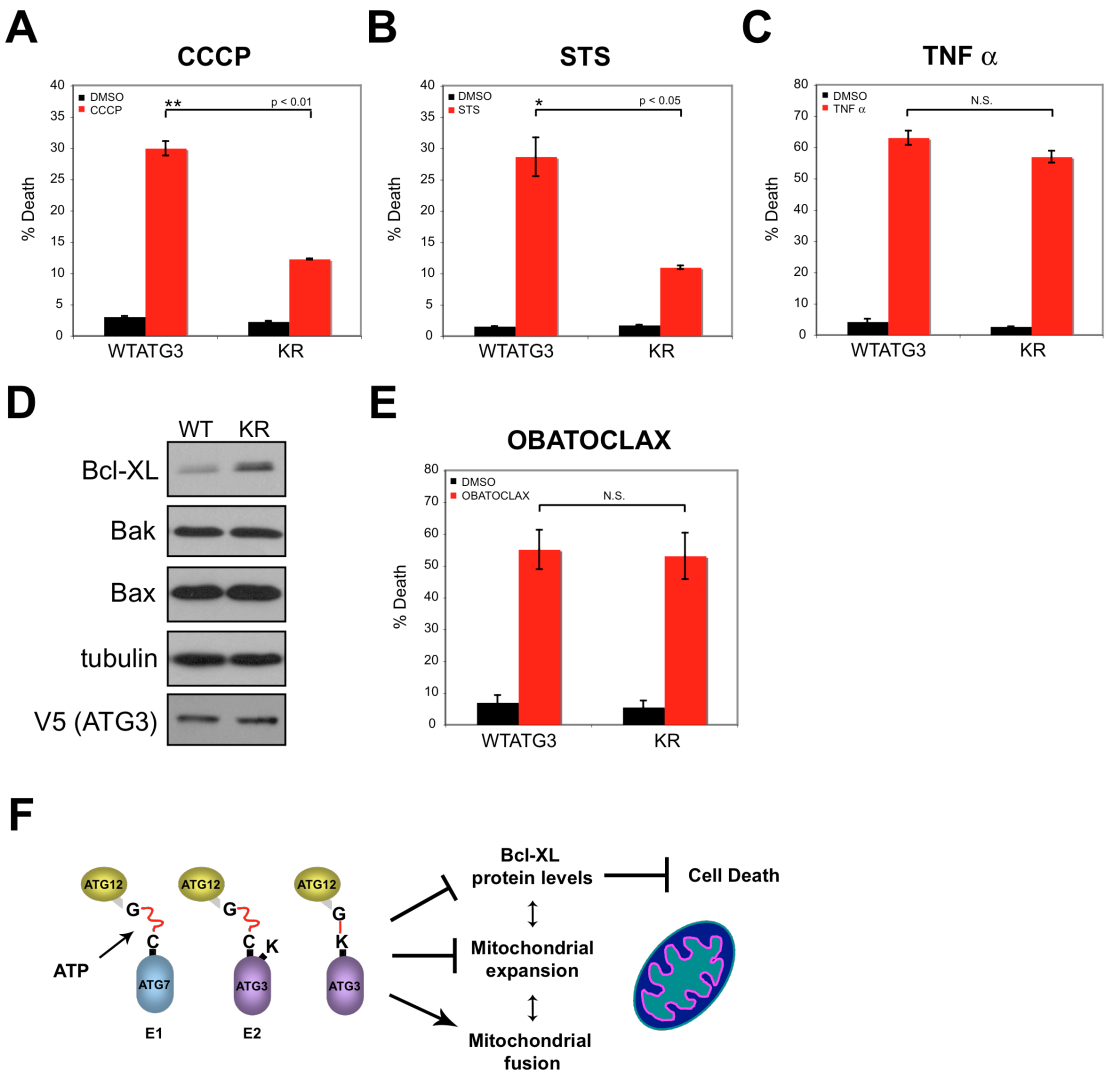
A
CCCP
DMSO
CCCP
**
p < 0.01
% Death
WTATG3
KR
B
STS
DMSO
STS
*
p < 0.05
% Death
WTATG3
KR
C
TNF α
DMSO
TNF α
N.S.
% Death
WTATG3
KR
D
WT
KR
Bcl-XL
Bak
Bax
tubulin
V5 (ATG3)
E
OBATOCLAX
DMSO
OBATOCLAX
N.S.
% Death
WTATG3
KR
F
ATG12
G
C
ATP
ATG7
E1
ATG12
G
C
K
ATG3
E2
ATG12
G
K
ATG3
Bcl-XL
protein levels
Cell Death
Mitochondrial
expansion
Mitochondrial
fusion

Anti-apoptotic members of the Bcl-2 family, such as Bcl-x_L, function as potent inhibitors of cell death; these proteins are mainly located on mitochondria, which is vital for their pro-survival functions [143]. Increased Bcl-x_L protein levels were present in KR cells compared to WTATG3, whereas no differences in the protein levels of the pro-apoptotic Bcl-2 family members, Bax and Bak, were observed (Figure 8D). Accordingly, we predicted that both WTATG3 and KR cells would be sensitive to the potent chemical inhibition of anti-apoptotic Bcl-2 family members. To test this hypothesis, we utilized obatoclax, a small molecule BH3 mimetic that antagonizes multiple anti-apoptotic Bcl-2 family proteins, including Bcl-x_L, Bcl-2 and Mcl-1 [145]. As a single agent, obatoclax was able to robustly induce cell death in both WTATG3 and KR cells; most importantly, we found no significant differences in obatoclax-mediated death between these two cell types (Figure 8E). In conclusion, cells lacking ATG12-ATG3 exhibit reduced cell death mediated by mitochondrial pathways; this protection correlates with an increase in anti-apoptotic Bcl-2 proteins secondary to the lack of ATG12 conjugation to ATG3.

Discussion:

Since the initial discovery of the ATG12 ubiquitin-like conjugation system, ATG5 remains as the only known target of ATG12 [97, 98]. Here, we provide evidence that multiple ATG12 substrates exist and identify ATG3, the E2-like enzyme that mediates ATG8/LC3 lipidation during autophagy, as a novel target for ATG12 conjugation [62]. ATG12 is covalently attached onto a single lysine of ATG3, which requires ATG7 as the E1 enzyme and an autocatalytic function of ATG3 as the E2 (Figure 7F). Since this novel complex links two components of the autophagy conjugation machinery, we reasoned that ATG12 modification of ATG3 would primarily regulate the early steps of autophagosome formation [105]. However, our results argue against this hypothesis. Disrupting ATG12 conjugation to ATG3 has no discernable effect on LC3/ATG8 lipidation or nonselective autophagy in response to three different stresses—nutrient starvation, rapamycin-mediated mTOR inhibition and CCCP-induced mitochondrial depolarization. Instead, the most obvious consequences of disrupting the ATG12-ATG3 complex are an increase in mitochondrial mass, fragmentation of the mitochondrial network, and resistance to cell death mediated by mitochondrial pathways (Figure 8F).

Mitochondrial homeostasis requires the careful balance and integration of numerous processes, namely fission, fusion, biogenesis and degradation [136]. Although we have observed decreased levels of mitophagy upon disrupting ATG12-ATG3 complex formation, we do not believe our results can be solely

explained by the defective autophagy of damaged mitochondria. First, the reduction in mitophagy in cells lacking ATG12-ATG3 is modest. Second, the increase in mitochondrial mass in KR cells is not accompanied by mitochondrial depolarization, suggesting that the excess mitochondria are functional. Third, during CCCP-induced uncoupling, we have uncovered that mitochondrial mass is actually higher in autophagy-competent KR cells than in ATG3 null cells, which are autophagy-deficient. Based on these results, we hypothesize that the ATG12-ATG3 complex may also restrict mitochondrial expansion using mitophagy-independent mechanisms. Notably, other proteins, like Parkin, have versatile effects on mitochondria. In addition to promoting mitophagy, Parkin has been demonstrated to control mitochondrial dynamics and to induce biogenesis; the precise interrelationships between these diverse biological outcomes remain unclear [127, 146-148]. Notably, we have uncovered increased basal levels of Bcl-X_L in KR cells, which may contribute to changes in both mitochondrial mass and morphology. Recent work in neurons demonstrates that Bcl-X_L plays a vital role in mitochondrial homeostasis, and is able to increase mitochondrial fission, fusion and biomass [149]. Future studies are required to more precisely dissect how this novel complex between two ATGs uniquely affects mitochondrial expansion and morphology, as well as to identify potential interconnections with the mitochondrial fission and fusion machinery.

Surprisingly, despite possessing fragmented mitochondrial morphology, cells lacking ATG12-ATG3 exhibit resistance to death mediated by mitochondrial pathways. Further studies in vivo are required to validate the physiological

significance of this phenotype. Overall, the effects of mitochondrial fission and fusion on cell death are variable and context dependent [150]. We hypothesize that the protection found in KR cells may result, at least in part, from increased basal levels of anti-apoptotic Bcl-2 family proteins. In support, specific and potent antagonism of anti-apoptotic Bcl-2 proteins causes equivalent amounts of cell death in WTATG3 and KR cells. A future challenge will be to discern which of these dramatic perturbations in mitochondrial morphology and function in KR cells is causal, since mitochondrial homeostasis, dynamics, and cell death are in delicate equilibrium (Figure 8F).

Importantly, our results indicate that the effects of the ATG12-ATG3 complex on mitochondrial homeostasis and cell death are unique functions that can be completely separated from the established roles of either ATG in autophagosome formation. Although this is a novel finding for ATG12 and ATG3, other studies demonstrate that pleiotropic roles for ATGs beyond autophagy do exist. For example, recent work delineates a macroautophagy-independent mechanism of LC3-recruitment to the mammalian phagosome, which is dependent on Beclin-1 and ATG5 [151]. Moreover, our studies indicate that ATG12, like ubiquitin and SUMO, serves as a broad-based ubiquitin-like protein conjugation with far-reaching implications in biology and human disease. Accordingly, we are actively pursuing the identification and validation of additional substrates subject to “12-ylation.”

Experimental Procedures:

Materials: Dr. Masaaki Komatsu (Juntendo University) generously provided *atg3+/+* and *atg3-/-* MEFs. Fibroblasts were cultured in DMEM (Invitrogen) supplemented with 10% FBS, penicillin and streptomycin. A peptide corresponding to the N-terminus common to human, mouse and rat MAP1LC3 was used to create α-LC3 rabbit polyclonal antibody [152].

Generation of stable pools: For retroviral transduction, VSV-G-pseudo typed retroviruses were generated, and cells were infected and selected as previously described [117]. Following infection and drug selection, early passage stable pools (maximum of 6-8 passages) were utilized for experiments to avoid clonal selection or drift.

Immunofluorescence: Immunofluorescent staining was carried out as previously described [117] with the following modifications during fixation and permeabilization. Fibroblasts were fixed with 2% paraformaldehyde at 4C for 10 min, followed by cold methanol (-20C) for 10 min and then permeabilized for 10 min at 20C with 0.5% Triton X-100 in PBS.

Microscopy: Widefield immunofluorescence imaging was performed at 20C using the 63x (1.4 NA) or 100x (1.3 NA) objectives of a Zeiss Axiovert 200 microscope equipped with a Spot RT camera (Diagnostics Instruments) and

mercury lamp; images were acquired using Metamorph (v6.0) software (Molecular Devices). Confocal analysis was performed at 20C using the 60x (1.4 NA) objective of a Nikon C1si Spectral Confocal System equipped with an argon laser (488 line) and two solid-state diodes (405 and 546 lines). Images were color-combined in Metamorph (v6.0) and arranged in Adobe Photoshop (v7.0).

Analysis of punctate GFP-LC3: Fibroblasts expressing GFP-LC3 were grown overnight on fibronectin-coated coverslips prior to HBSS starvation. Cells were fixed with 4% paraformaldehyde, washed with PBS, mounted using Immunomount (Thermo), and analyzed by widefield immunofluorescent microscopy as described above; images were acquired and punctate GFP-LC3 was quantified using Metamorph (v6.0) software. At least 250 cells from 4 independent experiments were enumerated. For analysis of GFP-LC3 colocation with mitochondria**,** cells expressing GFP-LC3 were transiently transfected with mito-dsRed, plated onto fibronectin-coated coverslips, and treated with 10 μM CCCP treatment for 24h. Cells were fixed, washed and imaged as above and colocalization, defined as the complete overlap of a GFP-LC3 puncta with mito-dsRed, was quantified per cell; at least 50 cells from 3 independent experiments were enumerated.

Flow cytometry for mitochondrial mass: As indicated, cells were grown in full media or subject to the indicated treatments for 24h. Cells were stained with 100 nM Mitotracker® Green (MTG) for 25 min at 37C. Cells were trypsinized,

collected by centrifugation, washed twice in PBS and analyzed using a FACSCalibur (BD) and CellQuest Pro software. When indicated, cells were co-stained with 100 nM Mitotracker® Red CMXRos (MTR). For assays of 3MA-sensitive mitochondrial degradation during CCCP treatment, cells were treated for 24h with 10 μM CCCP in the presence or absence of 5mM 3MA and then stained with MTG as described. 3MA sensitive degradation was calculated as follows:

$$\frac{\text{(MFI (Mean MTG fluorescence intensity) for CCCP+3MA treated cells - MFI for CCCP alone)}}{\text{(MFI for CCCP alone)}}$$

Cell death assays: Cells grown overnight in six well dishes were treated with death agents for 24h. Cells were then trypsinized, pooled with detached cells (floaters), pelleted by centrifugation, PBS washed, and stained with propidium iodide (0.5 mg/mL) in PBS for 10 min at 20C. Cells were analyzed using a FACSCalibur (BD) and CellQuest Pro software. Cells treated with obatoclax were analyzed using trypan blue exclusion because nonspecific fluorescence associated with drug treatment technically interfered with PI detection by flow cytometry.

Statistics: Experimental groups were compared using t test for pair wise comparisons or ANOVA (followed by Tukey's HSD test). For all experiments, statistical significance was indicated as follows: N.S., nonsignificant; * $p<0.05$; ** $p<0.01$; *** $p<0.001$.

Acknowledgements:

We thank Drs. Noboru Mizushima, Masaaki Komatsu and Patrick Dennis for reagents, and Drs. Gerard Evan, Don Ganem, Abul Abbas and Feroz Papa for critically reading the manuscript. Confocal microscopy was performed in the Nikon Biological Imaging Development Center at UCSF. Grant support to JD includes the NIH (RO1CA126792, KO8CA098419), a Culpeper Medical Scholar Award (Partnership For Cures), an AACR-Genentech BioOncology Award, a HHMI Physician-Scientist Early Career Award, and a Stewart Family Trust Award. LR was a Genentech/Sandler Graduate Student Fellow and EF was an HHMI Summer Undergraduate Research Fellow.

CHAPTER IV:

CONCLUDING REMARKS AND FUTURE DIRECTIONS

Summary

In the past five years, autophagy has progressed from what was perceived as an obscure proteolytic process to what is in fact a critical modulator of many hard to treat diseases. Moreover, in the years to come basic science discoveries will hopefully lead to the possibility of specifically activating or repressing autophagy in the context of neurodegenerative and autoimmune diseases and in cancer, respectively. As with any nascent field, certain paradigms established by early experiments became entrenched as dogma, because all of the initial evidence suggested a certain functional model. As time goes on, more and more of these early certainties will likely be overturned or at least more complex than initially appreciated. During the course of my thesis, we challenged the paradigm that ATG12 solely modifies ATG5. We were able to show that ATG12 did indeed bind to a number of covalent conjugates, independent of ATG5. We identified the predominant target of ATG12 modification as ATG3, which is the E2 enzyme responsible for ATG8/LC3 lipidation. We also found that ATG12-ATG3 complex formation requires ATG7 as an E1 and autocatalytic activity of ATG3 as an E2 *in cis*. Furthermore, the C-terminal glycine of ATG12 binds a single lysine on ATG3, lysine K243, which is in close proximity to the catalytic cysteine, C264. To dissect the biological function of the complex we complemented *atg3* deficient fibroblasts with either WTATG3 or ATG3 K243R (KR). The KR mutant was able to complement ATG3's function in starvation or rapamycin induced-autophagy but the mutant had a striking fragmentation of the mitochondrial network relative

to WTATG3 cells. This defect was present in *atg3* deficient cells, rescued in WTATG3 cells but not rescued in KR cells. Further investigation revealed that KR cells also have increased mitochondrial mass that is at least partially due to defects in mitophagy. The fragmented mitochondrial phenotype arises from or causes a functional defect in mitochondrial fusion. Additionally, the increased mitochondrial mass correlates with an increase in Bcl-X_L protein levels and resistance to inducers of mitochondrial cell death. Much remains to be determined about the exact molecular mechanism of ATG12-ATG3's effect on the mitochondria, however taken together, we have demonstrated that ATG12 can conjugate to multiple additional cellular proteins and that the ATG12-ATG3 complex profoundly alters mitochondrial morphology and cell death.

Future Directions and Significance

By preventing ATG12 conjugation to ATG3, we uncovered a novel effect of the ATG12-ATG3 complex on mitochondrial homeostasis that is distinct from each protein's known individual role in early autophagosome function. The mitochondrial network is in delicate equilibrium between fusion, fission, biogenesis and destruction. Altering any one of these processes can directly or indirectly impinge upon the others. A future challenge will be to identify how the ATG12-ATG3 complex mechanistically exerts its influence on mitochondrial homeostasis. ATG12 could relocalize ATG3 to a different cellular compartment or potentially change its substrate specificity, repress its activity or vary its

interacting partners. An important next step will be gathering more information about the complex through both biochemistry and dynamic imaging. Much may be gleaned by simple localization of fluorescently tagged ATG12 and ATG3. Because the ATG12-ATG3 complex is less abundant than ATG12-ATG5 and ATG3, colocalization of the two proteins in reference to organelles or basal colocalization in comparison to during mitochondrial uncoupling could indicate how the complex exerts its effects. In a similar vein, forced conjugation of ATG12 and ATG3 through molecular cloning could lead to hyper activity of the complex, thereby elucidating its primary function. While none of the autophagy inducers we attempted have any different effect on WT versus KR function, it is possible that testing a more extensive panel could reveal a difference at the level of LC3/ATG8 homologue conversion (and therefore indicate ATG12-ATG3 function). In addition, testing via western blotting whether ATG12-ATG3 conjugation is induced by a variety of chemicals, which target mitochondrial function, is an essential future direction.

Though we understand much more about how the ATG12-ATG3 complex is formed than how it exerts its biological effects, in depth biochemical analysis of the conjugation will likely provide key insight into whether ATG12 can sterically inhibit ATG3 function when bound to K243. Establishing an *in vitro* system of conjugation could also furnish critical information about ATG12 affinity for ATG5 or ATG3, or additionally for ATG7 affinity for its various substrates and E2 conjugating enzymes. It is possible that ATG12-ATG3 complex formation is regulated by ATG7's proximity to ATG10 or other permutations of cellular

interactions and this would be more efficiently determined *in vitro*. We were also curious whether ATG12-ATG3 modification was conserved in other model organisms. Preliminary unpublished experiments suggest that the conserved lysine of ATG3, which is the conjugation target of ATG12, is important to the survival of yeast. When the non-conjugatable mutant of ATG3 was introduced into wild type or Δatg3 strains, there were no viable transformants. Transforming the yeast with an inducible form of the KR mutant yielded transformants, however more work would be necessary to determine whether ATG12-ATG3 forms in yeast and if abrogation of its cellular function has similar consequences to the analogous experiment in mammalian cells or if the lysine is instead important for another unrelated function of the protein.

Since we observed a small but significant difference in mitochondrial targeting to lysosomes and a dramatic difference in mitochondrial mass, it would be interesting to follow up these observations in more established models of mitophagy. It would be particularly appealing to assess the mutant's effect on reticulocyte mitophagy or at the very least to determine if the mutant functions in Parkin-dependent mitophagy in a cell line that has higher basal Parkin levels than do fibroblasts. In the same vein, further elucidation of the bioenergetic profile of the KR cells and response of the of the KR cells to apoptosis could be informative in a non-transformed cell line or *in vivo* to better assess the effects of the ATG12-ATG3 complex on cell death in cells with intact p53 status. Moreover, because ATG12 conjugation to ATG3 is entirely separable from its function in autophagy, it would be particularly compelling to knock in the K243R

mutant to an *atg3*-deficient mouse because the animal would presumably survive beyond its first perinatal day (since its ability to induce autophagy would be intact) and any phenotype emanating from the KR mutant would be indicative of the tissues in which ATG12-ATG3 complex formation plays a role *in vivo*. Ultimately this body of work suggests that ATG12 fulfills at least two distinct cellular roles based on alternate substrates. It is likely that further exploration of the other ATG proteins in new and different cellular contexts will contribute more evidence for the emerging notion in autophagy research that many of the ATG proteins may play pleiotropic roles in cell biology beyond canonical autophagy. Finally, it seems that ATG12 may be more similar to ubiquitin and SUMO than previously appreciated, in that it is probable that additional cellular targets of "12ylation" with broader cell biological roles remain to be discovered.

References:

1. Klionsky, D.J. Autophagy revisited: a conversation with Christian de Duve. *Autophagy* **4**, 740-3 (2008).
2. Tsukada, M. & Ohsumi, Y. Isolation and characterization of autophagy-defective mutants of Saccharomyces cerevisiae. *FEBS Lett* **333**, 169-74 (1993).
3. Thumm, M., Egner, R., Koch, B., Schlumpberger, M., Straub, M., Veenhuis, M. & Wolf, D.H. Isolation of autophagocytosis mutants of Saccharomyces cerevisiae. *FEBS Lett* **349**, 275-80 (1994).
4. Harding, T.M., Hefner-Gravink, A., Thumm, M. & Klionsky, D.J. Genetic and phenotypic overlap between autophagy and the cytoplasm to vacuole protein targeting pathway. *J Biol Chem* **271**, 17621-4 (1996).
5. Nakatogawa, H., Ichimura, Y. & Ohsumi, Y. Atg8, a ubiquitin-like protein required for autophagosome formation, mediates membrane tethering and hemifusion. *Cell* **130**, 165-78 (2007).
6. Arias, E. & Cuervo, A.M. Chaperone-mediated autophagy in protein quality control. *Curr Opin Cell Biol* (2010).
7. Kraft, C., Peter, M. & Hofmann, K. Selective autophagy: ubiquitin-mediated recognition and beyond. *Nat Cell Biol* **12**, 836-41 (2010).
8. Takeshige, K., Baba, M., Tsuboi, S., Noda, T. & Ohsumi, Y. Autophagy in yeast demonstrated with proteinase-deficient mutants and conditions for its induction. *J Cell Biol* **119**, 301-11 (1992).

9. Scott, S.V. & Klionsky, D.J. In vitro reconstitution of cytoplasm to vacuole protein targeting in yeast. *J Cell Biol* **131**, 1727-35 (1995).

10. Scott, S.V., Baba, M., Ohsumi, Y. & Klionsky, D.J. Aminopeptidase I is targeted to the vacuole by a nonclassical vesicular mechanism. *J Cell Biol* **138**, 37-44 (1997).

11. Baba, M., Osumi, M., Scott, S.V., Klionsky, D.J. & Ohsumi, Y. Two distinct pathways for targeting proteins from the cytoplasm to the vacuole/lysosome. *J Cell Biol* **139**, 1687-95 (1997).

12. Wang, C.W. & Klionsky, D.J. The molecular mechanism of autophagy. *Mol Med* **9**, 65-76 (2003).

13. Kamada, Y., Funakoshi, T., Shintani, T., Nagano, K., Ohsumi, M. & Ohsumi, Y. Tor-mediated induction of autophagy via an Apg1 protein kinase complex. *J Cell Biol* **150**, 1507-13 (2000).

14. Kabeya, Y., Kamada, Y., Baba, M., Takikawa, H., Sasaki, M. & Ohsumi, Y. Atg17 functions in cooperation with Atg1 and Atg13 in yeast autophagy. *Mol Biol Cell* **16**, 2544-53 (2005).

15. Cheong, H., Yorimitsu, T., Reggiori, F., Legakis, J.E., Wang, C.W. & Klionsky, D.J. Atg17 regulates the magnitude of the autophagic response. *Mol Biol Cell* **16**, 3438-53 (2005).

16. Kihara, A., Noda, T., Ishihara, N. & Ohsumi, Y. Two distinct Vps34 phosphatidylinositol 3-kinase complexes function in autophagy and carboxypeptidase Y sorting in Saccharomyces cerevisiae. *J Cell Biol* **152**, 519-30 (2001).

17. Nice, D.C., Sato, T.K., Stromhaug, P.E., Emr, S.D. & Klionsky, D.J. Cooperative binding of the cytoplasm to vacuole targeting pathway proteins, Cvt13 and Cvt20, to phosphatidylinositol 3-phosphate at the pre-autophagosomal structure is required for selective autophagy. *J Biol Chem* **277**, 30198-207 (2002).

18. Wurmser, A.E. & Emr, S.D. Novel PtdIns(3)P-binding protein Etf1 functions as an effector of the Vps34 PtdIns 3-kinase in autophagy. *J Cell Biol* **158**, 761-72 (2002).

19. Stromhaug, P.E., Reggiori, F., Guan, J., Wang, C.W. & Klionsky, D.J. Atg21 is a phosphoinositide binding protein required for efficient lipidation and localization of Atg8 during uptake of aminopeptidase I by selective autophagy. *Mol Biol Cell* **15**, 3553-66 (2004).

20. Sekito, T., Kawamata, T., Ichikawa, R., Suzuki, K. & Ohsumi, Y. Atg17 recruits Atg9 to organize the pre-autophagosomal structure. *Genes Cells* **14**, 525-38 (2009).

21. Suzuki, K., Kirisako, T., Kamada, Y., Mizushima, N., Noda, T. & Ohsumi, Y. The pre-autophagosomal structure organized by concerted functions of APG genes is essential for autophagosome formation. *Embo J* **20**, 5971-81 (2001).

22. Mizushima, N., Noda, T. & Ohsumi, Y. Apg16p is required for the function of the Apg12p-Apg5p conjugate in the yeast autophagy pathway. *EMBO J* **18**, 3888-96 (1999).

23. Kuma, A., Mizushima, N., Ishihara, N. & Ohsumi, Y. Formation of the approximately 350-kDa Apg12-Apg5.Apg16 multimeric complex, mediated by Apg16 oligomerization, is essential for autophagy in yeast. *J Biol Chem* **277**, 18619-25 (2002).

24. Fujioka, Y., Noda, N.N., Nakatogawa, H., Ohsumi, Y. & Inagaki, F. Dimeric coiled-coil structure of Saccharomyces cerevisiae Atg16 and its functional significance in autophagy. *J Biol Chem* **285**, 1508-15 (2010).

25. Mizushima, N., Yamamoto, A., Hatano, M., Kobayashi, Y., Kabeya, Y., Suzuki, K., Tokuhisa, T., Ohsumi, Y. & Yoshimori, T. Dissection of autophagosome formation using Apg5-deficient mouse embryonic stem cells. *J Cell Biol* **152**, 657-68 (2001).

26. Ichimura, Y., Kirisako, T., Takao, T., Satomi, Y., Shimonishi, Y., Ishihara, N., Mizushima, N., Tanida, I., Kominami, E., Ohsumi, M., Noda, T. & Ohsumi, Y. A ubiquitin-like system mediates protein lipidation. *Nature* **408**, 488-92 (2000).

27. Mizushima, N., Yoshimori, T. & Levine, B. Methods in mammalian autophagy research. *Cell* **140**, 313-26 (2010).

28. Hanada, T., Noda, N.N., Satomi, Y., Ichimura, Y., Fujioka, Y., Takao, T., Inagaki, F. & Ohsumi, Y. The Atg12-Atg5 conjugate has a novel E3-like activity for protein lipidation in autophagy. *J Biol Chem* **282**, 37298-302 (2007).

29. Klionsky, D.J. The molecular machinery of autophagy: unanswered questions. *J Cell Sci* **118**, 7-18 (2005).

30. Yang, Z., Huang, J., Geng, J., Nair, U. & Klionsky, D.J. Atg22 recycles amino acids to link the degradative and recycling functions of autophagy. *Mol Biol Cell* **17**, 5094-104 (2006).

31. Yang, Z. & Klionsky, D.J. Permeases recycle amino acids resulting from autophagy. *Autophagy* **3**, 149-50 (2007).

32. Yang, Z. & Klionsky, D.J. Mammalian autophagy: core molecular machinery and signaling regulation. *Curr Opin Cell Biol* **22**, 124-31.

33. Stipanuk, M.H. Macroautophagy and its role in nutrient homeostasis. *Nutr Rev* **67**, 677-89 (2009).

34. Kroemer, G., Marino, G. & Levine, B. Autophagy and the integrated stress response. *Mol Cell* **40**, 280-93 (2010).

35. Neufeld, T.P. Contribution of Atg1-dependent autophagy to TOR-mediated cell growth and survival. *Autophagy* **3**, 477-9 (2007).

36. Egan, D.F., Shackelford, D.B., Mihaylova, M.M., Gelino, S., Kohnz, R.A., Mair, W., Vasquez, D.S., Joshi, A., Gwinn, D.M., Taylor, R., Asara, J.M., Fitzpatrick, J., Dillin, A., Viollet, B., Kundu, M., Hansen, M. & Shaw, R.J. Phosphorylation of ULK1 (hATG1) by AMP-activated protein kinase connects energy sensing to mitophagy. *Science* **331**, 456-61 (2010).

37. Yan, J., Kuroyanagi, H., Kuroiwa, A., Matsuda, Y., Tokumitsu, H., Tomoda, T., Shirasawa, T. & Muramatsu, M. Identification of mouse ULK1, a novel protein kinase structurally related to C. elegans UNC-51. *Biochem Biophys Res Commun* **246**, 222-7 (1998).

38. Kundu, M., Lindsten, T., Yang, C.Y., Wu, J., Zhao, F., Zhang, J., Selak, M.A., Ney, P.A. & Thompson, C.B. Ulk1 plays a critical role in the autophagic clearance of mitochondria and ribosomes during reticulocyte maturation. *Blood* **112**, 1493-502 (2008).

39. Hara, T., Takamura, A., Kishi, C., Iemura, S., Natsume, T., Guan, J.L. & Mizushima, N. FIP200, a ULK-interacting protein, is required for autophagosome formation in mammalian cells. *J Cell Biol* **181**, 497-510 (2008).

40. Ganley, I.G., Lam du, H., Wang, J., Ding, X., Chen, S. & Jiang, X. ULK1.ATG13.FIP200 complex mediates mTOR signaling and is essential for autophagy. *J Biol Chem* **284**, 12297-305 (2009).

41. Jung, C.H., Jun, C.B., Ro, S.H., Kim, Y.M., Otto, N.M., Cao, J., Kundu, M. & Kim, D.H. ULK-Atg13-FIP200 complexes mediate mTOR signaling to the autophagy machinery. *Mol Biol Cell* **20**, 1992-2003 (2009).

42. Hosokawa, N., Hara, T., Kaizuka, T., Kishi, C., Takamura, A., Miura, Y., Iemura, S., Natsume, T., Takehana, K., Yamada, N., Guan, J.L., Oshiro, N. & Mizushima, N. Nutrient-dependent mTORC1 association with the ULK1-Atg13-FIP200 complex required for autophagy. *Mol Biol Cell* **20**, 1981-91 (2009).

43. Itakura, E., Kishi, C., Inoue, K. & Mizushima, N. Beclin 1 forms two distinct phosphatidylinositol 3-kinase complexes with mammalian Atg14 and UVRAG. *Mol Biol Cell* **19**, 5360-72 (2008).

44. Sun, Q., Fan, W., Chen, K., Ding, X., Chen, S. & Zhong, Q. Identification of Barkor as a mammalian autophagy-specific factor for Beclin 1 and class III phosphatidylinositol 3-kinase. *Proc Natl Acad Sci U S A* **105**, 19211-6 (2008).

45. Liang, C., Feng, P., Ku, B., Dotan, I., Canaani, D., Oh, B.H. & Jung, J.U. Autophagic and tumour suppressor activity of a novel Beclin1-binding protein UVRAG. *Nat Cell Biol* **8**, 688-99 (2006).

46. Fimia, G.M., Stoykova, A., Romagnoli, A., Giunta, L., Di Bartolomeo, S., Nardacci, R., Corazzari, M., Fuoco, C., Ucar, A., Schwartz, P., Gruss, P., Piacentini, M., Chowdhury, K. & Cecconi, F. Ambra1 regulates autophagy and development of the nervous system. *Nature* **447**, 1121-5 (2007).

47. Pattingre, S., Tassa, A., Qu, X., Garuti, R., Liang, X.H., Mizushima, N., Packer, M., Schneider, M.D. & Levine, B. Bcl-2 antiapoptotic proteins inhibit Beclin 1-dependent autophagy. *Cell* **122**, 927-39 (2005).

48. Matsunaga, K., Saitoh, T., Tabata, K., Omori, H., Satoh, T., Kurotori, N., Maejima, I., Shirahama-Noda, K., Ichimura, T., Isobe, T., Akira, S., Noda, T. & Yoshimori, T. Two Beclin 1-binding proteins, Atg14L and Rubicon, reciprocally regulate autophagy at different stages. *Nat Cell Biol* **11**, 385-96 (2009).

49. Itakura, E. & Mizushima, N. Atg14 and UVRAG: mutually exclusive subunits of mammalian Beclin 1-PI3K complexes. *Autophagy* **5**, 534-6 (2009).

50. Takahashi, Y., Coppola, D., Matsushita, N., Cualing, H.D., Sun, M., Sato, Y., Liang, C., Jung, J.U., Cheng, J.Q., Mule, J.J., Pledger, W.J. & Wang, H.G. Bif-1 interacts with Beclin 1 through UVRAG and regulates autophagy and tumorigenesis. *Nat Cell Biol* **9**, 1142-51 (2007).

51. Liang, C., Lee, J.S., Inn, K.S., Gack, M.U., Li, Q., Roberts, E.A., Vergne, I., Deretic, V., Feng, P., Akazawa, C. & Jung, J.U. Beclin1-binding UVRAG targets the class C Vps complex to coordinate autophagosome maturation and endocytic trafficking. *Nat Cell Biol* **10**, 776-87 (2008).

52. Zhong, Y., Wang, Q.J., Li, X., Yan, Y., Backer, J.M., Chait, B.T., Heintz, N. & Yue, Z. Distinct regulation of autophagic activity by Atg14L and Rubicon associated with Beclin 1-phosphatidylinositol-3-kinase complex. *Nat Cell Biol* **11**, 468-76 (2009).

53. Fujita, N., Hayashi-Nishino, M., Fukumoto, H., Omori, H., Yamamoto, A., Noda, T. & Yoshimori, T. An Atg4B mutant hampers the lipidation of LC3 paralogues and causes defects in autophagosome closure. *Mol Biol Cell* **19**, 4651-9 (2008).

54. Axe, E.L., Walker, S.A., Manifava, M., Chandra, P., Roderick, H.L., Habermann, A., Griffiths, G. & Ktistakis, N.T. Autophagosome formation from membrane compartments enriched in phosphatidylinositol 3-phosphate and dynamically connected to the endoplasmic reticulum. *J Cell Biol* **182**, 685-701 (2008).

55. Walker, S., Chandra, P., Manifava, M., Axe, E. & Ktistakis, N.T. Making autophagosomes: localized synthesis of phosphatidylinositol 3-phosphate holds the clue. *Autophagy* **4**, 1093-6 (2008).

56. Matsunaga, K., Morita, E., Saitoh, T., Akira, S., Ktistakis, N.T., Izumi, T., Noda, T. & Yoshimori, T. Autophagy requires endoplasmic reticulum targeting of the PI3-kinase complex via Atg14L. *J Cell Biol* **190**, 511-21 (2010).

57. Hayashi-Nishino, M., Fujita, N., Noda, T., Yamaguchi, A., Yoshimori, T. & Yamamoto, A. A subdomain of the endoplasmic reticulum forms a cradle for autophagosome formation. *Nat Cell Biol* **11**, 1433-7 (2009).

58. Polson, H.E., de Lartigue, J., Rigden, D.J., Reedijk, M., Urbe, S., Clague, M.J. & Tooze, S.A. Mammalian Atg18 (WIPI2) localizes to omegasome-anchored phagophores and positively regulates LC3 lipidation. *Autophagy* **6** (2010).

59. Hailey, D.W., Rambold, A.S., Satpute-Krishnan, P., Mitra, K., Sougrat, R., Kim, P.K. & Lippincott-Schwartz, J. Mitochondria supply membranes for autophagosome biogenesis during starvation. *Cell* **141**, 656-67 (2010).

60. Tanida, I., Nishitani, T., Nemoto, T., Ueno, T. & Kominami, E. Mammalian Apg12p, but not the Apg12p.Apg5p conjugate, facilitates LC3 processing. *Biochem Biophys Res Commun* **296**, 1164-70 (2002).

61. Tanida, I., Tanida-Miyake, E., Ueno, T. & Kominami, E. The human homolog of Saccharomyces cerevisiae Apg7p is a Protein-activating

enzyme for multiple substrates including human Apg12p, GATE-16, GABARAP, and MAP-LC3. *J Biol Chem* **276**, 1701-6 (2001).

62. Tanida, I., Tanida-Miyake, E., Komatsu, M., Ueno, T. & Kominami, E. Human Apg3p/Aut1p homologue is an authentic E2 enzyme for multiple substrates, GATE-16, GABARAP, and MAP-LC3, and facilitates the conjugation of hApg12p to hApg5p. *J Biol Chem* **277**, 13739-44 (2002).

63. Tanida, I., Komatsu, M., Ueno, T. & Kominami, E. GATE-16 and GABARAP are authentic modifiers mediated by Apg7 and Apg3. *Biochem Biophys Res Commun* **300**, 637-44 (2003).

64. Tanida, I., Sou, Y.S., Minematsu-Ikeguchi, N., Ueno, T. & Kominami, E. Atg8L/Apg8L is the fourth mammalian modifier of mammalian Atg8 conjugation mediated by human Atg4B, Atg7 and Atg3. *FEBS J* **273**, 2553-62 (2006).

65. Kabeya, Y., Mizushima, N., Yamamoto, A., Oshitani-Okamoto, S., Ohsumi, Y. & Yoshimori, T. LC3, GABARAP and GATE16 localize to autophagosomal membrane depending on form-II formation. *J Cell Sci* **117**, 2805-12 (2004).

66. Tanida, I., Ueno, T. & Kominami, E. LC3 conjugation system in mammalian autophagy. *Int J Biochem Cell Biol* **36**, 2503-18 (2004).

67. Scherz-Shouval, R., Sagiv, Y., Shorer, H. & Elazar, Z. The COOH terminus of GATE-16, an intra-Golgi transport modulator, is cleaved by the human cysteine protease HsApg4A. *J Biol Chem* **278**, 14053-8 (2003).

68. Weidberg, H., Shvets, E., Shpilka, T., Shimron, F., Shinder, V. & Elazar, Z. LC3 and GATE-16/GABARAP subfamilies are both essential yet act differently in autophagosome biogenesis. *EMBO J* **29**, 1792-802 (2010).

69. Gutierrez, M.G., Munafo, D.B., Beron, W. & Colombo, M.I. Rab7 is required for the normal progression of the autophagic pathway in mammalian cells. *J Cell Sci* **117**, 2687-97 (2004).

70. Jager, S., Bucci, C., Tanida, I., Ueno, T., Kominami, E., Saftig, P. & Eskelinen, E.L. Role for Rab7 in maturation of late autophagic vacuoles. *J Cell Sci* **117**, 4837-48 (2004).

71. Pankiv, S., Alemu, E.A., Brech, A., Bruun, J.A., Lamark, T., Overvatn, A., Bjorkoy, G. & Johansen, T. FYCO1 is a Rab7 effector that binds to LC3 and PI3P to mediate microtubule plus end-directed vesicle transport. *J Cell Biol* **188**, 253-69 (2010).

72. Kuma, A., Hatano, M., Matsui, M., Yamamoto, A., Nakaya, H., Yoshimori, T., Ohsumi, Y., Tokuhisa, T. & Mizushima, N. The role of autophagy during the early neonatal starvation period. *Nature* **432**, 1032-6 (2004).

73. Komatsu, M., Waguri, S., Ueno, T., Iwata, J., Murata, S., Tanida, I., Ezaki, J., Mizushima, N., Ohsumi, Y., Uchiyama, Y., Kominami, E., Tanaka, K. & Chiba, T. Impairment of starvation-induced and constitutive autophagy in Atg7-deficient mice. *J Cell Biol* **169**, 425-34 (2005).

74. Sou, Y.S., Waguri, S., Iwata, J., Ueno, T., Fujimura, T., Hara, T., Sawada, N., Yamada, A., Mizushima, N., Uchiyama, Y., Kominami, E., Tanaka, K. & Komatsu, M. The Atg8 conjugation system is indispensable for proper

development of autophagic isolation membranes in mice. *Mol Biol Cell* **19**, 4762-75 (2008).

75. Yue, Z., Jin, S., Yang, C., Levine, A.J. & Heintz, N. Beclin 1, an autophagy gene essential for early embryonic development, is a haploinsufficient tumor suppressor. *Proc Natl Acad Sci U S A* **100**, 15077-82 (2003).

76. Qu, X., Yu, J., Bhagat, G., Furuya, N., Hibshoosh, H., Troxel, A., Rosen, J., Eskelinen, E.L., Mizushima, N., Ohsumi, Y., Cattoretti, G. & Levine, B. Promotion of tumorigenesis by heterozygous disruption of the beclin 1 autophagy gene. *J Clin Invest* **112**, 1809-20 (2003).

77. Komatsu, M., Waguri, S., Chiba, T., Murata, S., Iwata, J., Tanida, I., Ueno, T., Koike, M., Uchiyama, Y., Kominami, E. & Tanaka, K. Loss of autophagy in the central nervous system causes neurodegeneration in mice. *Nature* **441**, 880-4 (2006).

78. Jung, H.S., Chung, K.W., Won Kim, J., Kim, J., Komatsu, M., Tanaka, K., Nguyen, Y.H., Kang, T.M., Yoon, K.H., Kim, J.W., Jeong, Y.T., Han, M.S., Lee, M.K., Kim, K.W., Shin, J. & Lee, M.S. Loss of autophagy diminishes pancreatic beta cell mass and function with resultant hyperglycemia. *Cell Metab* **8**, 318-24 (2008).

79. Levine, B., Mizushima, N. & Virgin, H.W. Autophagy in immunity and inflammation. *Nature* **469**, 323-35 (2011).

80. Massey, D.C. & Parkes, M. Genome-wide association scanning highlights two autophagy genes, ATG16L1 and IRGM, as being significantly associated with Crohn's disease. *Autophagy* **3**, 649-51 (2007).

81. Cadwell, K., Liu, J.Y., Brown, S.L., Miyoshi, H., Loh, J., Lennerz, J.K., Kishi, C., Kc, W., Carrero, J.A., Hunt, S., Stone, C.D., Brunt, E.M., Xavier, R.J., Sleckman, B.P., Li, E., Mizushima, N., Stappenbeck, T.S. & Virgin, H.W.t. A key role for autophagy and the autophagy gene Atg16l1 in mouse and human intestinal Paneth cells. *Nature* **456**, 259-63 (2008).

82. Cadwell, K., Patel, K.K., Maloney, N.S., Liu, T.C., Ng, A.C., Storer, C.E., Head, R.D., Xavier, R., Stappenbeck, T.S. & Virgin, H.W. Virus-plus-susceptibility gene interaction determines Crohn's disease gene Atg16L1 phenotypes in intestine. *Cell* **141**, 1135-45 (2010).

83. Saitoh, T., Fujita, N., Jang, M.H., Uematsu, S., Yang, B.G., Satoh, T., Omori, H., Noda, T., Yamamoto, N., Komatsu, M., Tanaka, K., Kawai, T., Tsujimura, T., Takeuchi, O., Yoshimori, T. & Akira, S. Loss of the autophagy protein Atg16L1 enhances endotoxin-induced IL-1beta production. *Nature* **456**, 264-8 (2008).

84. Karantza-Wadsworth, V., Patel, S., Kravchuk, O., Chen, G., Mathew, R., Jin, S. & White, E. Autophagy mitigates metabolic stress and genome damage in mammary tumorigenesis. *Genes Dev* **21**, 1621-35 (2007).

85. Mathew, R., Kongara, S., Beaudoin, B., Karp, C.M., Bray, K., Degenhardt, K., Chen, G., Jin, S. & White, E. Autophagy suppresses tumor progression by limiting chromosomal instability. *Genes Dev* **21**, 1367-81 (2007).

86. Fung, C., Lock, R., Gao, S., Salas, E. & Debnath, J. Induction of autophagy during extracellular matrix detachment promotes cell survival. *Mol Biol Cell* **19**, 797-806 (2008).

87. Lock, R. & Debnath, J. Extracellular matrix regulation of autophagy. *Curr Opin Cell Biol* **20**, 583-8 (2008).

88. Lock, R., Roy, S., Kenific, C.M., Su, J.S., Salas, E., Ronen, S.M. & Debnath, J. Autophagy facilitates glycolysis during Ras-mediated oncogenic transformation. *Mol Biol Cell* **22**, 165-78 (2011).

89. Guo, J.Y., Chen, H.Y., Mathew, R., Fan, J., Strohecker, A.M., Karsli-Uzunbas, G., Kamphorst, J.J., Chen, G., Lemmons, J.M., Karantza, V., Coller, H.A., Dipaola, R.S., Gelinas, C., Rabinowitz, J.D. & White, E. Activated Ras requires autophagy to maintain oxidative metabolism and tumorigenesis. *Genes Dev* (2011).

90. Kerscher, O., Felberbaum, R. & Hochstrasser, M. Modification of proteins by ubiquitin and ubiquitin-like proteins. *Annu Rev Cell Dev Biol* **22**, 159-80 (2006).

91. Hochstrasser, M. Origin and function of ubiquitin-like proteins. *Nature* **458**, 422-9 (2009).

92. Amerik, A.Y. & Hochstrasser, M. Mechanism and function of deubiquitinating enzymes. *Biochim Biophys Acta* **1695**, 189-207 (2004).

93. Huang, D.T., Walden, H., Duda, D. & Schulman, B.A. Ubiquitin-like protein activation. *Oncogene* **23**, 1958-71 (2004).

94. van Wijk, S.J. & Timmers, H.T. The family of ubiquitin-conjugating enzymes (E2s): deciding between life and death of proteins. *FASEB J* **24**, 981-93 (2010).

95. Seeler, J.S. & Dejean, A. Nuclear and unclear functions of SUMO. *Nat Rev Mol Cell Biol* **4**, 690-9 (2003).

96. Suzuki, N.N., Yoshimoto, K., Fujioka, Y., Ohsumi, Y. & Inagaki, F. The crystal structure of plant ATG12 and its biological implication in autophagy. *Autophagy* **1**, 119-26 (2005).

97. Mizushima, N., Noda, T., Yoshimori, T., Tanaka, Y., Ishii, T., George, M.D., Klionsky, D.J., Ohsumi, M. & Ohsumi, Y. A protein conjugation system essential for autophagy. *Nature* **395**, 395-8 (1998).

98. Mizushima, N., Sugita, H., Yoshimori, T. & Ohsumi, Y. A new protein conjugation system in human. The counterpart of the yeast Apg12p conjugation system essential for autophagy. *J Biol Chem* **273**, 33889-92 (1998).

99. Colell, A., Ricci, J.E., Tait, S., Milasta, S., Maurer, U., Bouchier-Hayes, L., Fitzgerald, P., Guio-Carrion, A., Waterhouse, N.J., Li, C.W., Mari, B., Barbry, P., Newmeyer, D.D., Beere, H.M. & Green, D.R. GAPDH and autophagy preserve survival after apoptotic cytochrome c release in the absence of caspase activation. *Cell* **129**, 983-97 (2007).

100. Prigione, A. & Cortopassi, G. Mitochondrial DNA Deletions and Chloramphenicol Treatment Stimulate the Autophagic Transcript ATG12. *Autophagy* **3**, 377-80 (2007).

101. Kouroku, Y., Fujita, E., Tanida, I., Ueno, T., Isoai, A., Kumagai, H., Ogawa, S., Kaufman, R.J., Kominami, E. & Momoi, T. ER stress (PERK/eIF2alpha phosphorylation) mediates the polyglutamine-induced

LC3 conversion, an essential step for autophagy formation. *Cell Death Differ* **14**, 230-9 (2007).

102. Brown, V.M., Krynetski, E.Y., Krynetskaia, N.F., Grieger, D., Mukatira, S.T., Murti, K.G., Slaughter, C.A., Park, H.W. & Evans, W.E. A novel CRM1-mediated nuclear export signal governs nuclear accumulation of glyceraldehyde-3-phosphate dehydrogenase following genotoxic stress. *J Biol Chem* **279**, 5984-92 (2004).
103. Mazzola, J.L. & Sirover, M.A. Subcellular localization of human glyceraldehyde-3-phosphate dehydrogenase is independent of its glycolytic function. *Biochim Biophys Acta* **1622**, 50-6 (2003).
104. Welchman, R.L., Gordon, C. & Mayer, R.J. Ubiquitin and ubiquitin-like proteins as multifunctional signals. *Nat Rev Mol Cell Biol* **6**, 599-609 (2005).
105. Ohsumi, Y. Molecular dissection of autophagy: two ubiquitin-like systems. *Nat Rev Mol Cell Biol* **2**, 211-6 (2001).
106. Levine, B. & Kroemer, G. Autophagy in the pathogenesis of disease. *Cell* **132**, 27-42 (2008).
107. Hanada, T. & Ohsumi, Y. Structure-function relationship of Atg12, a ubiquitin-like modifier essential for autophagy. *Autophagy* **1**, 110-8 (2005).
108. Sugawara, K., Suzuki, N.N., Fujioka, Y., Mizushima, N., Ohsumi, Y. & Inagaki, F. The crystal structure of microtubule-associated protein light chain 3, a mammalian homologue of Saccharomyces cerevisiae Atg8. *Genes Cells* **9**, 611-8 (2004).

109. Kabeya, Y., Mizushima, N., Ueno, T., Yamamoto, A., Kirisako, T., Noda, T., Kominami, E., Ohsumi, Y. & Yoshimori, T. LC3, a mammalian homologue of yeast Apg8p, is localized in autophagosome membranes after processing. *Embo J* **19**, 5720-8 (2000).

110. Tanida, I., Mizushima, N., Kiyooka, M., Ohsumi, M., Ueno, T., Ohsumi, Y. & Kominami, E. Apg7p/Cvt2p: A novel protein-activating enzyme essential for autophagy. *Mol Biol Cell* **10**, 1367-79 (1999).

111. Nemoto, T., Tanida, I., Tanida-Miyake, E., Minematsu-Ikeguchi, N., Yokota, M., Ohsumi, M., Ueno, T. & Kominami, E. The mouse APG10 homologue, an E2-like enzyme for Apg12p conjugation, facilitates MAP-LC3 modification. *J Biol Chem* **278**, 39517-26 (2003).

112. Yamada, Y., Suzuki, N.N., Hanada, T., Ichimura, Y., Kumeta, H., Fujioka, Y., Ohsumi, Y. & Inagaki, F. The crystal structure of Atg3, an autophagy-related ubiquitin carrier protein (E2) enzyme that mediates Atg8 lipidation. *J Biol Chem* **282**, 8036-43 (2007).

113. Fujita, N., Itoh, T., Omori, H., Fukuda, M., Noda, T. & Yoshimori, T. The Atg16L complex specifies the site of LC3 lipidation for membrane biogenesis in autophagy. *Mol Biol Cell* **19**, 2092-100 (2008).

114. Walter, J., Urban, J., Volkwein, C. & Sommer, T. Sec61p-independent degradation of the tail-anchored ER membrane protein Ubc6p. *EMBO J* **20**, 3124-31 (2001).

115. Gwozd, C.S., Arnason, T.G., Cook, W.J., Chau, V. & Ellison, M.J. The yeast UBC4 ubiquitin conjugating enzyme monoubiquitinates itself in vivo:

evidence for an E2-E2 homointeraction. *Biochemistry* **34**, 6296-302 (1995).

116. Machida, Y.J., Machida, Y., Chen, Y., Gurtan, A.M., Kupfer, G.M., D'Andrea, A.D. & Dutta, A. UBE2T is the E2 in the Fanconi anemia pathway and undergoes negative autoregulation. *Mol Cell* **23**, 589-96 (2006).

117. Debnath, J., Muthuswamy, S.K. & Brugge, J.S. Morphogenesis and oncogenesis of MCF-10A mammary epithelial acini grown in three-dimensional basement membrane cultures. *Methods* **30**, 256-68 (2003).

118. Pandey, U.B., Batlevi, Y., Baehrecke, E.H. & Taylor, J.P. HDAC6 at the intersection of autophagy, the ubiquitin-proteasome system and neurodegeneration. *Autophagy* **3**, 643-5 (2007).

119. Pandey, U.B., Nie, Z., Batlevi, Y., McCray, B.A., Ritson, G.P., Nedelsky, N.B., Schwartz, S.L., DiProspero, N.A., Knight, M.A., Schuldiner, O., Padmanabhan, R., Hild, M., Berry, D.L., Garza, D., Hubbert, C.C., Yao, T.P., Baehrecke, E.H. & Taylor, J.P. HDAC6 rescues neurodegeneration and provides an essential link between autophagy and the UPS. *Nature* **447**, 859-63 (2007).

120. Youle, R.J. & Narendra, D.P. Mechanisms of mitophagy. *Nat Rev Mol Cell Biol* **12**, 9-14 (2011).

121. Okamoto, K., Kondo-Okamoto, N. & Ohsumi, Y. Mitochondria-anchored receptor Atg32 mediates degradation of mitochondria via selective autophagy. *Dev Cell* **17**, 87-97 (2009).

122. Kanki, T., Wang, K., Cao, Y., Baba, M. & Klionsky, D.J. Atg32 is a mitochondrial protein that confers selectivity during mitophagy. *Dev Cell* **17**, 98-109 (2009).

123. Ishihara, N. & Mizushima, N. A receptor for eating mitochondria. *Dev Cell* **17**, 1-2 (2009).

124. Schweers, R.L., Zhang, J., Randall, M.S., Loyd, M.R., Li, W., Dorsey, F.C., Kundu, M., Opferman, J.T., Cleveland, J.L., Miller, J.L. & Ney, P.A. NIX is required for programmed mitochondrial clearance during reticulocyte maturation. *Proc Natl Acad Sci U S A* **104**, 19500-5 (2007).

125. Sandoval, H., Thiagarajan, P., Dasgupta, S.K., Schumacher, A., Prchal, J.T., Chen, M. & Wang, J. Essential role for Nix in autophagic maturation of erythroid cells. *Nature* **454**, 232-5 (2008).

126. Zhang, J., Randall, M.S., Loyd, M.R., Dorsey, F.C., Kundu, M., Cleveland, J.L. & Ney, P.A. Mitochondrial clearance is regulated by Atg7-dependent and -independent mechanisms during reticulocyte maturation. *Blood* **114**, 157-64 (2009).

127. Narendra, D., Tanaka, A., Suen, D.F. & Youle, R.J. Parkin is recruited selectively to impaired mitochondria and promotes their autophagy. *J Cell Biol* **183**, 795-803 (2008).

128. Narendra, D.P., Jin, S.M., Tanaka, A., Suen, D.F., Gautier, C.A., Shen, J., Cookson, M.R. & Youle, R.J. PINK1 is selectively stabilized on impaired mitochondria to activate Parkin. *PLoS Biol* **8**, e1000298 (2010).

129. Geisler, S., Holmstrom, K.M., Skujat, D., Fiesel, F.C., Rothfuss, O.C., Kahle, P.J. & Springer, W. PINK1/Parkin-mediated mitophagy is dependent on VDAC1 and p62/SQSTM1. *Nat Cell Biol* **12**, 119-31 (2010).

130. Chan, N.C., Salazar, A.M., Pham, A.H., Sweredoski, M.J., Kolawa, N.J., Graham, R.L., Hess, S. & Chan, D.C. Broad activation of the ubiquitin-proteasome system by Parkin is critical for mitophagy. *Hum Mol Genet* (2011).

131. Gegg, M.E., Cooper, J.M., Chau, K.Y., Rojo, M., Schapira, A.H. & Taanman, J.W. Mitofusin 1 and mitofusin 2 are ubiquitinated in a PINK1/parkin-dependent manner upon induction of mitophagy. *Hum Mol Genet* **19**, 4861-70 (2010).

132. Narendra, D., Kane, L.A., Hauser, D.N., Fearnley, I.M. & Youle, R.J. p62/SQSTM1 is required for Parkin-induced mitochondrial clustering but not mitophagy; VDAC1 is dispensable for both. *Autophagy* **6**, 1090-106 (2010).

133. Okatsu, K., Saisho, K., Shimanuki, M., Nakada, K., Shitara, H., Sou, Y.S., Kimura, M., Sato, S., Hattori, N., Komatsu, M., Tanaka, K. & Matsuda, N. p62/SQSTM1 cooperates with Parkin for perinuclear clustering of depolarized mitochondria. *Genes Cells* **15**, 887-900 (2010).

134. Bjorkoy, G., Lamark, T., Brech, A., Outzen, H., Perander, M., Overvatn, A., Stenmark, H. & Johansen, T. p62/SQSTM1 forms protein aggregates degraded by autophagy and has a protective effect on huntingtin-induced cell death. *J Cell Biol* **171**, 603-14 (2005).

135. Dennis, P.B. & Mercer, C.A. The GST-BHMT assay and related assays for autophagy. *Methods Enzymol* **452**, 97-118 (2009).

136. Chen, H. & Chan, D.C. Mitochondrial dynamics--fusion, fission, movement, and mitophagy--in neurodegenerative diseases. *Hum Mol Genet* **18**, R169-76 (2009).

137. Lemasters, J.J. Selective mitochondrial autophagy, or mitophagy, as a targeted defense against oxidative stress, mitochondrial dysfunction, and aging. *Rejuvenation Res* **8**, 3-5 (2005).

138. Chen, H., Detmer, S.A., Ewald, A.J., Griffin, E.E., Fraser, S.E. & Chan, D.C. Mitofusins Mfn1 and Mfn2 coordinately regulate mitochondrial fusion and are essential for embryonic development. *J Cell Biol* **160**, 189-200 (2003).

139. Youle, R.J. & Karbowski, M. Mitochondrial fission in apoptosis. *Nat Rev Mol Cell Biol* **6**, 657-63 (2005).

140. Tal, M.C., Sasai, M., Lee, H.K., Yordy, B., Shadel, G.S. & Iwasaki, A. Absence of autophagy results in reactive oxygen species-dependent amplification of RLR signaling. *Proc Natl Acad Sci U S A* **106**, 2770-5 (2009).

141. Rohas, L.M., St-Pierre, J., Uldry, M., Jager, S., Handschin, C. & Spiegelman, B.M. A fundamental system of cellular energy homeostasis regulated by PGC-1alpha. *Proc Natl Acad Sci U S A* **104**, 7933-8 (2007).

142. Seglen, P.O. & Gordon, P.B. 3-Methyladenine: specific inhibitor of autophagic/lysosomal protein degradation in isolated rat hepatocytes. *Proc Natl Acad Sci U S A* **79**, 1889-92 (1982).

143. Brenner, D. & Mak, T.W. Mitochondrial cell death effectors. *Curr Opin Cell Biol* (2009).

144. de Graaf, A.O., van den Heuvel, L.P., Dijkman, H.B., de Abreu, R.A., Birkenkamp, K.U., de Witte, T., van der Reijden, B.A., Smeitink, J.A. & Jansen, J.H. Bcl-2 prevents loss of mitochondria in CCCP-induced apoptosis. *Exp Cell Res* **299**, 533-40 (2004).

145. Nguyen, M., Marcellus, R.C., Roulston, A., Watson, M., Serfass, L., Murthy Madiraju, S.R., Goulet, D., Viallet, J., Belec, L., Billot, X., Acoca, S., Purisima, E., Wiegmans, A., Cluse, L., Johnstone, R.W., Beauparlant, P. & Shore, G.C. Small molecule obatoclax (GX15-070) antagonizes MCL-1 and overcomes MCL-1-mediated resistance to apoptosis. *Proc Natl Acad Sci U S A* **104**, 19512-7 (2007).

146. Kuroda, Y., Mitsui, T., Kunishige, M., Shono, M., Akaike, M., Azuma, H. & Matsumoto, T. Parkin enhances mitochondrial biogenesis in proliferating cells. *Hum Mol Genet* **15**, 883-95 (2006).

147. Deng, H., Dodson, M.W., Huang, H. & Guo, M. The Parkinson's disease genes pink1 and parkin promote mitochondrial fission and/or inhibit fusion in Drosophila. *Proc Natl Acad Sci U S A* **105**, 14503-8 (2008).

148. Lutz, A.K., Exner, N., Fett, M.E., Schlehe, J.S., Kloos, K., Lammermann, K., Brunner, B., Kurz-Drexler, A., Vogel, F., Reichert, A.S., Bouman, L.,

Vogt-Weisenhorn, D., Wurst, W., Tatzelt, J., Haass, C. & Winklhofer, K.F. Loss of parkin or PINK1 function increases Drp1-dependent mitochondrial fragmentation. *J Biol Chem* **284**, 22938-51 (2009).

149. Berman, S.B., Chen, Y.B., Qi, B., McCaffery, J.M., Rucker, E.B., 3rd, Goebbels, S., Nave, K.A., Arnold, B.A., Jonas, E.A., Pineda, F.J. & Hardwick, J.M. Bcl-x L increases mitochondrial fission, fusion, and biomass in neurons. *J Cell Biol* **184**, 707-19 (2009).

150. Suen, D.F., Norris, K.L. & Youle, R.J. Mitochondrial dynamics and apoptosis. *Genes Dev* **22**, 1577-90 (2008).

151. Sanjuan, M.A., Dillon, C.P., Tait, S.W., Moshiach, S., Dorsey, F., Connell, S., Komatsu, M., Tanaka, K., Cleveland, J.L., Withoff, S. & Green, D.R. Toll-like receptor signalling in macrophages links the autophagy pathway to phagocytosis. *Nature* **450**, 1253-7 (2007).

152. Fung, C., Lock, R., Gao, S., Salas, E. & Debnath, J. Induction of Autophagy during Extracellular Matrix Detachment Promotes Cell Survival. *Mol. Biol. Cell* **19**, 797-806 (2008).

Publishing Agreement

It is the policy of the University to encourage the distribution of all theses, dissertations, and manuscripts. Copies of all UCSF theses, dissertations, and manuscripts will be routed to the library via the Graduate Division. The library will make all theses, dissertations, and manuscripts accessible to the public and will preserve these to the best of their abilities, in perpetuity.

Please sign the following statement:

I hereby grant permission to the Graduate Division of the University of California, San Francisco to release copies of my thesis, dissertation, or manuscript to the Campus Library to provide access and preservation, in whole or in part, in perpetuity.

Lillian C. Barbosa — 3·21·2011

Author Signature — Date